YURI SILVESTRE BARBOSA

# MÉTODOS COMPUTACIONAIS NO CÂNCER DE CABEÇA E PESCOÇO

BRASÍLIA, 2026

**UNIVERSIDADE DE BRASÍLIA**
**FACULDADE DE CIÊNCIAS DA SAÚDE**
**PROGRAMA DE PÓS-GRADUAÇÃO EM CIÊNCIAS DA SAÚDE**

YURI SILVESTRE BARBOSA

# MÉTODOS COMPUTACIONAIS NO CÂNCER DE CABEÇA E PESCOÇO

Dissertação apresentada como requisito parcial para a obtenção do título de Mestre em Ciências da Saúde pelo programa de Pós-Graduação em Ciências da Saúde da Universidade de Brasília.

Orientadora: Profa. Dra. Eliete Neves da Silva Guerra

BRASÍLIA, 2026

YURI SILVESTRE BARBOSA

**MÉTODOS COMPUTACIONAIS NO CÂNCER DE CABEÇA E PESCOÇO**

Dissertação apresentada como requisito parcial para a obtenção do título de Mestre em Ciências da Saúde pelo programa de Pós-Graduação em Ciências da Saúde da Universidade de Brasília.

Aprovada em 30 de janeiro de 2026

BANCA EXAMINADORA

_____

Profa. Dra. Eliete Neves da Silva Guerra (Presidente)
Universidade de Brasília

_____

Profa. Dra. Camila Pacheco de Oliveira Pereira
Universidade de Alberta

_____

Prof. Dr. João Vitor dos Santos Canellas
Universidade de Brasília

_____

Profa. Dra. Juliana Amorim dos Santos (Suplente)
Universidade de Michigan

*Ao meu avô João Silvestre*

**AGRADECIMENTOS**

Ao “bom Deus”, que nunca permitiu que me faltasse aquilo de que precisei para realizar meus sonhos;

Aos meus pais, Juciê e Elba, ao meu irmão, Haldane, e à minha cunhada, Mare, pelo apoio incondicional e pela base familiar que me sustenta e me fortalece diante dos desafios da vida;

A todos os meus amigos que torcem por mim, com quem compartilho momentos, alegrias e angústias, e que estiveram sempre presentes para apoiar e incentivar;

À minha amiga e companheira de pós-graduação, Vitória, pela valiosa contribuição à execução deste trabalho e pela constante disposição em ajudar no que fosse necessário;

Às professoras Paula Elaine Diniz Reis e Elaine Barros Ferreira, e ao Ricardo Gomes dos Reis, físico médico do Hospital Universitário de Brasília, pelo apoio e pelas importantes contribuições a este estudo;

Aos membros da minha banca examinadora, Prof. João Vitor Canellas, Profa. Camila Pacheco-Pereira e Dra. Juliana Amorim, pelo tempo, dedicação e valiosas contribuições à avaliação deste trabalho. À Juliana, em especial, além do reconhecimento acadêmico, agradeço pela amizade sincera, pelo apoio constante, mesmo à distância, e pelos momentos compartilhados ao longo dos anos;

Ao querido professor André Leite, coorientador deste trabalho, pela estima que nutro, pela inspiração profissional e humana, e por me acompanhar desde os primeiros passos na vida acadêmica;

À professora Eliete Guerra, mulher extraordinária, orientadora exemplar, companheira de luta, referência como docente, cientista e cidadã, cuja atuação incansável é inspiração constante;

Ao grupo de pesquisa “Resistência”, pelas contribuições e discussões ao longo deste período, essenciais para o meu crescimento acadêmico;

À Coordenação de Aperfeiçoamento de Pessoal de Nível Superior (CAPES) e ao Conselho Nacional de Desenvolvimento Científico e Tecnológico (CNPq) pelo

contínuo incentivo à formação de pesquisadores no Brasil e ao desenvolvimento científico do país;

Ao Programa de Pós-Graduação em Ciências da Saúde (PPGCS), pela excelência da formação oferecida aos seus discentes;

Ao Decanato de Pós-Graduação (DPG), pelo apoio institucional e pela dedicação contínua à promoção da pesquisa e da formação acadêmica;

E, finalmente, à Universidade de Brasília (UnB), por todas as portas que me abriu ao longo desses anos e por sua importância para a sociedade brasileira, enquanto instituição pública que oferece ensino gratuito e de qualidade, sendo, com orgulho, minha Alma Mater.

*“Seus medos você já conhece. Experimente suas coragens.”*

**RESUMO**

O câncer de cabeça e pescoço (CCP) é um grupo heterogêneo de neoplasias, predominantemente constituídas por carcinomas de células escamosas, com alta incidência e mortalidade mundial e no Brasil. Fatores de risco incluem tabagismo, etilismo, radiação, infecções virais e hábitos culturais, sendo o diagnóstico precoce crucial para sobrevida, embora a maioria dos casos seja identificada tardiamente. O tratamento envolve radioterapia (RT), quimioterapia e cirurgia, entretanto, está associado a efeitos adversos significativos, como osteorradionecrose (ORN), caracterizada por necrose óssea em regiões irradiadas. Avanços computacionais, especialmente inteligência artificial (IA), machine learning e deep learning, têm potencial para aprimorar diagnóstico, estadiamento, prognóstico e suporte à decisão clínica. Abordagens complementares, como índices radiomorfométricos e dimensão fractal (DF), permitem avaliação quantitativa da microarquitetura óssea, sendo úteis para detecção precoce de alterações em pacientes irradiados. O trabalho está dividido em dois capítulos, sendo eles: (1) O Capítulo 1, que consiste em uma análise bibliométrica que incluiu 1.019 publicações sobre IA e CCP entre 1995 e 2024, utilizando Web of Science como base de busca e as ferramentas VosViewer e Biblioshiny/Bibliometrix. A maioria dos estudos identificados e incluídos (71,6%) são artigos originais, com aumento expressivo de publicações a partir de 2016, atingindo pico em 2023. Predominaram países de alta renda, evidenciando disparidade global na produção científica. Palavras-chave de destaque incluem machine learning, deep learning, radiomics e radioterapia, com foco recente em diagnóstico, predição de sobrevida e histopatologia. Conclui-se que há crescimento do uso de IA em CCP, mas são necessários mais ensaios clínicos e revisões para ampliar sua aplicação clínica global. (2) O Capítulo 2, que apresenta um estudo primário observacional transversal que avaliou os ossos mandibulares cortical e trabecular em pacientes após a RT comparando-os a controles não irradiados, utilizando tomografia computadorizada de feixe cônico (TCFC) para calcular o Índice Mentual por Tomografia Computadorizada (CTMI), o Índice Cortical por Tomografia Computadorizada (CTCI) e a DF. Não foram observadas diferenças significativas entre grupos para CTMI, CTCI ou DF. Subanálises mostraram DF trabecular maior em tumores de laringe comparado aos demias e CTMI mais elevado em pacientes avaliados com mais de 30 meses pós-RT, enquanto a DF na cortical e o CTCI não exibiram diferenças significativas na comparação do intervalo de tempo entre a RT e a execução da TCFC. Os resultados sugerem respostas ósseas heterogêneas, destacando a utilidade da TCFC para detecção precoce de alterações ósseas induzidas por RT e a necessidade de manejo individualizado dos pacientes. No geral, os métodos computacionais investigados nesse trabalho mostram potencial para uso no contexto do CCP, mas são necessários mais estudos e padronização para aplicação clínica efetiva.

**Palavras-chave**: Câncer de Cabeça e Pescoço; Radioterapia; Inteligência Artificial; Dimensão Fractal; Índices Radiomorfométricos.

## ABSTRACT

Head and neck cancer (HNC) is a heterogeneous group of neoplasms, predominantly represented by squamous cell carcinomas, with high incidence and mortality worldwide and in Brazil. Risk factors include smoking, alcohol consumption, radiation, viral infections, and cultural habits, with early diagnosis being crucial for survival, although most cases are identified at advanced stages. Treatment involves radiotherapy (RT), chemotherapy, and surgery, but it is associated with significant adverse effects, such as osteoradionecrosis (ORN), characterized by bone necrosis in irradiated regions. Computational advances, particularly artificial intelligence (AI), machine learning, and deep learning, have the potential to improve diagnosis, staging, prognosis, and clinical decision support. Complementary approaches, such as radiomorphometric indices and fractal dimension (FD), allow quantitative assessment of bone microarchitecture, being useful for early detection of changes in irradiated patients. This work is divided into two chapters: (1) Chapter 1 consists of a bibliometric analysis of 1,019 publications on AI and HNC between 1995 and 2024, using the Web of Science as the search database and VosViewer and Biblioshiny/Bibliometrix as analysis tools. Most studies included were original articles (71.6%), with a marked increase in publications from 2016 onward, peaking in 2023. High-income countries predominated, highlighting global disparities in scientific production. Key terms included machine learning, deep learning, radiomics, and radiotherapy, with recent focus on diagnosis, survival prediction, and histopathology. It was concluded that the use of AI in HNC is growing, but more clinical trials and reviews are needed to expand its global clinical application. (2) Chapter 2 reports a study that evaluated mandibular cortical and trabecular bone in patients after RT, compared to non-irradiated controls, using cone-beam computed tomography (CBCT) to calculate the Computed Tomography Mental Index (CTMI), Computed Tomography Cortical Index (CTCI), and FD. No significant differences were observed between groups for CTMI, CTCI or FD. Sub-analyses showed higher trabecular FD in larynx tumors compared to other tumors and higher CTMI in patients evaluated more than 30 months post-RT, while cortical FD and CTCI did not exhibit significant differences when comparing the time interval between RT and CBCT acquisition. The results suggest heterogeneous bone responses, highlighting the utility of CBCT for early detection of RT-induced bone changes and the need for individualized patient management. Overall, the computational methods investigated in this work show potential for use in the HNC context, but further studies and standardization are required for effective clinical application.

**Key words:** Head and Neck Cancer; Radiotherapy; Artificial Intelligence; Fractal Dimension; Radiomorphometric Indices.

## LISTA DE FIGURAS

### Capítulo 1.

**Figura 1:** (A) Informações gerais das publicações. Visão geral das 1.019 publicações incluídas no estudo, categorizadas em artigos de pesquisa original, revisões e outros tipos (cartas, anais de congressos, editoriais). (B) Produção científica anual. Número anual de publicações de 1995 a 2024, mostrando aumento significativo após 2016, com 94,4% dos artigos publicados após 2016 e 2023 como o ano mais produtivo.

**Figura 2:** (A) Mapa de colaboração entre países. O mapa mostra a produção científica e o impacto dos 20 principais países nos campos de câncer de cabeça e pescoço (HNC) e inteligência artificial (IA), destacando contribuições de economias emergentes como China e Índia, que ocupam o segundo e terceiro lugar, respectivamente. (B) Países mais produtivos. O gráfico ilustra as parcerias internacionais de pesquisa em HNC e IA. Cerca de 32% das publicações resultam de colaborações entre países, com parcerias frequentes incluindo EUA/China, EUA/Países Baixos, EUA/Reino Unido, entre outras. Abreviações: Publicações de País Único (SCP); Publicações de Múltiplos Países (MCP).

**Figura 3:** (A) Análise das palavras-chave dos autores. O gráfico exibe as palavras-chave mais frequentemente usadas entre os 46 termos que atingiram o limite de dez ocorrências. Termos comuns incluem “machine learning”, “deep learning”, “inteligência artificial”, “câncer de cabeça e pescoço” e “câncer oral”, além de termos mais específicos como “radiomics”, “radioterapia” e “convolutional neural network”. (B) Co-ocorrência das palavras-chave dos autores. A figura ilustra a clusterização das palavras-chave em grupos temáticos. O cluster verde representa termos relacionados à radiômica e suas aplicações em HNC, incluindo radioterapia e técnicas de imagem. O cluster azul foca nas aplicações de machine learning em HNC, abrangendo termos como prognóstico e diagnóstico. O cluster vermelho inclui termos específicos de IA, como deep learning e CNN. Abreviações: Inteligência Artificial (IA); Convolutional Neural Network (CNN); Câncer de Cabeça e Pescoço (HNC); Carcinoma de Células Escamosas de Cabeça e Pescoço (HNSCC); Carcinoma de Células Escamosas Oral (OSCC).

**Figura 4:** (A) Ilustração das palavras-chave mais importantes ao longo dos anos. Em 2023, os termos mais usados foram “diagnóstico” (21 ocorrências), “sobrevida global” (10 ocorrências) e “histopatologia” (10 ocorrências). (B) Tendências temporais das palavras-chave comuns. Demonstração da evolução das palavras-chave utilizadas pelos autores em três períodos distintos: 1995-2015 (antes do crescimento significativo das publicações), 2016-2019 (pré-COVID-19) e 2020-presente (pandemia e período atual). A figura destaca as mudanças de foco ao longo do tempo.

**Capítulo 2.**

**Figura 1:** Distribuição da dose em heat-map e histograma dose–volume representativo. (A) vista coronal da tomografia computadorizada (CT); (B) vista axial da CT; (C) vista sagital da CT; (D) reconstrução tridimensional; (E) histograma dose–volume.

**Figura 2:** Análise da dimensão fractal (FD). (A) análise do lado direito com ROI 1 (trabecular) e ROI 3 (cortical); (B) análise do lado esquerdo com ROI 2 (trabecular) e ROI 4 (cortical); (C) recorte (crop); (D) desfoque gaussiano (Gaussian Blur); (E) operação matemática (math); (F) limiarização (threshold); (G) binarização (binary).

**Figura 3:** Procedimento de medição do CTMI – distância entre as bordas cortical interna e externa na região do forame mental.

**Figura 4:** Análise do CTCI. Tipo 1: a margem endostal é uniforme e nítida em ambos os lados; Tipo 2: presença de defeitos semilunares, reabsorção lacunar e resíduos endostais em um ou ambos os lados; Tipo 3: margem endostal fina e porosa, com grande quantidade de resíduos endostais.

**Figura 5:** Fluxograma da amostra do estudo.

**Figura 6:** Resultados da FD entre grupos. (A) valores de FD para cada ROI nos Grupos 1 (triângulo com ápice para cima) e 2 (triângulo com ápice para baixo). ROI 1: trabeculado direito; ROI 2: trabeculado esquerdo; ROI 3: cortical direita; ROI 4: cortical esquerda. (B) valores de FD agrupados para análise do trabeculado (ROI 1 + ROI 2) e da cortical (ROI 3 + ROI 4), mantendo a notação dos triângulos para os grupos. Não foram observadas diferenças estatisticamente significativas entre os grupos em nenhuma análise ($p > 0,05$).

**Figura 7:** Resultados dos índices radiomorfométricos entre os grupos. (A) valores de CTMI para os Grupos 1 e 2; (B) valores de CTCI para os Grupos 1 e 2. Não foram observadas diferenças estatisticamente significativas entre os grupos para nenhum dos índices ($p > 0,05$).

## LISTA DE TABELAS

**Capítulo 1.**

**Tabela 1:** Top 10 países, afiliações, fontes e autores segundo o número de publicações.

**Tabela 2:** Os 10 documentos mais citados.

**Capítulo 2.**

**Tabela 1:** Análise de acordo com o sítio do tumor, agrupados como cabeça ou pescoço.

**Tabela 2:** CTCI de acordo com o sítio do tumor, agrupados como cabeça ou pescoço.

**Tabela 3:** Médias de FD nos dois grupos.

**Tabela 4:** CTMI nos dois grupos.

**Tabela 5:** CTCI nos dois grupos.

## LISTA DE ABREVIATURAS E SIGLAS

**3D-CRT** – Three-Dimensional Conformal Radiotherapy (Radioterapia Conformal Tridimensional)

**AI / IA**– Artificial Intelligence (Inteligência Artificial)

**ANN** – Artificial Neural Networks (Redes Neurais Artificiais)

**BA** – Bibliometric Analysis (Análise Bibliométrica)

**BIBLIO** – Guideline for reporting bibliometric reviews of biomedical literature (Diretriz para relatos de revisões bibliométricas da literatura biomédica)

**CBCT / TCFC** – Cone-Beam Computed Tomography (Tomografia Computadorizada de Feixe Cônico)

**CNN** – Convolutional Neural Networks (Redes Neurais Convolucionais)

**CT / TC** – Computed Tomography (Tomografia Computadorizada)

**CTCI** – Computed Tomography Cortical Index (Índice Cortical por Tomografia Computadorizada)

**CTMI** – Computed Tomography Mental Index (Índice Mentual por Tomografia Computadorizada)

**CTP** – Clinical Trials Processor (Processador de Ensaios Clínicos)

**EQUATOR** – Enhancing the Quality and Transparency of Health Research (Aprimorando a qualidade e a transparência da pesquisa em saúde)

**FD / DF** – Fractal Dimension (Dimensão Fractal)

**GPU** – Graphics Processing Unit (Unidade de Processamento Gráfico)

**Gy** – Gray (Gray – unidade de dose de radiação)

**HNC / CCP** – Head and Neck Cancer (Câncer de Cabeça e Pescoço)

**HPV** – Human Papilloma Virus (Papilomavírus Humano)

**ICC** – Intraclass Correlation Coefficient (Coeficiente de Correlação Intraclasse)

**IF** – Impact Factor (Fator de Impacto)

**IGRT** – Image-Guided Radiotherapy (Radioterapia Guiada por Imagem)

**IMRT** – Intensity-Modulated Radiotherapy (Radioterapia com Intensidade Modulada)

**INCA** – Instituto Nacional de Câncer

**MARS** – Multiple Adaptive Regression Splines (Splines de Regressão Adaptativa Multivariada)

**MPR** – Multiplanar Reconstruction (Reconstrução Multiplanar)

**MRI** – Magnetic Resonance Imaging (Imagem por Ressonância Magnética)

**NLP** – Natural Language Processing (Processamento de Linguagem Natural)

**OAR** – Organs at Risk (Órgãos em Risco)

**ORN** – Osteoradionecrosis (Osteorradionecrose)

**OSCC** – Oral Squamous Cell Carcinoma (Carcinoma de Células Escamosas Oral)

**OSF** – Open Science Framework

**PENTO** – Pentoxifylline + Tocopherol (Pentoxifilina + Tocoferol)

**PET** – Positron Emission Tomography (Tomografia por Emissão de Pósitrons)

**PRISMA** – Preferred Reporting Items for Systematic Reviews and Meta-Analyses (Itens preferenciais para relato de revisões sistemáticas e meta-análises)

**ROI** – Region of Interest (Região de Interesse)

**RSNA** – Radiological Society of North America (Sociedade Radiológica da América do Norte)

**RT** – Radiotherapy (Radioterapia)

**SVM** – Support Vector Machine (Máquina de Vetores de Suporte)

**SD** – Standard Deviation (Desvio Padrão)

**SPECT** – Single-Photon Emission Computed Tomography (Tomografia Computadorizada por Emissão de Fóton Único)

**TPU** – Tensor Processing Unit (Unidade de Processamento Tensorial)

**WoSCC** – Web of Science Core Collection (Coleção Principal da Web of Science)

## LISTA DE APÊNDICES

**Capítulo 1.**

**Figura Suplementar 1:** Fontes principais segundo a Lei de Bradford.

**Figura Suplementar 2:** Acoplamento bibliográfico das fontes. Um mínimo de cinco documentos publicados foi estabelecido. De 387 termos, 40 atingiram o limiar.

**Figura Suplementar 3:** Autores mais citados.

**Figura Suplementar 4:** Coautoria das afiliações. De 1.505 afiliações, 51 publicaram pelo menos 20 artigos.

**Figura Suplementar 5:** Análise de cocitação das referências citadas. De 24.285 referências, 25 foram citadas pelo menos 35 vezes.

**Tabela Suplementar 1:** Os 50 estudos mais citados.

**Tabela Suplementar 2:** Classificação dos estudos que relataram acurácia nos 50 trabalhos mais citados para diagnóstico de câncer (N=9 estudos) e desfechos de metástase (N=4 estudos).

**Tabela Suplementar 3:** Classificação do desempenho dos algoritmos relatado pela acurácia nos 50 trabalhos mais citados.

**Capítulo 2.**

**Figura Suplementar S1:** Foram observadas diferenças significativas para dose máxima ($p = 0,024$), dose média ($p = 0,015$) e DF trabecular ($p = 0,003$). Não foram encontradas diferenças significativas para DF cortical ($p = 0,412$) ou CTMI ($p = 0,573$).

**Figura Suplementar S2:** DF e índices radiomorfométricos de acordo com a dose máxima. Não foram observadas diferenças significativas entre pacientes que receberam <30 Gy ou >30 Gy na região anterior da mandíbula em relação à DF trabecular ($p = 0,310$), DF cortical ($p = 1,000$), CTMI ($p = 0,598$) ou CTCI ($p = 0,708$).

**Figura Suplementar S3:** DF e índices radiomorfométricos de acordo com o tempo entre RT e TCFC. Valores mais elevados de CTMI foram observados no grupo

avaliado após 30 meses (p = 0,034). Não foram observadas diferenças entre os grupos para DF ou CTCI.

**Tabela Suplementar S1:** Características descritivas da amostra.

**Tabela Suplementar S2:** Comparação dos valores de DF e CTMI de acordo com o sítio tumoral.

**Tabela Suplementar S3:** DF e índices radiomorfométricos de acordo com a dose máxima.

**Tabela Suplementar S4:** DF e CTMI de acordo com a dose média.

**Tabela Suplementar S5:** DF e índices radiomorfométricos de acordo com o tempo entre RT e TCFC.

**Anexos.**

Parecer Consubstanciado do Conselho de Ética em Pesquisa – Faculdade de Ciências da Saude da Universidade de Brasília.

**SUMÁRIO**

**PREFÁCIO** ..... **19**
**INTRODUÇÃO** ..... **21**
**OBJETIVOS** ..... **27**
Objetivo Geral ..... 27
Objetivos Específicos ..... 27
**CAPÍTULO 1** ..... **28**
INTRODUCTION ..... 29
MATERIAL AND METHODS ..... 30
RESULTS ..... 33
DISCUSSION ..... 41
CONCLUSION ..... 48
REFERENCES ..... 49
TABLES ..... 56
APPENDIX ..... 59
**CAPÍTULO 2** ..... **81**
INTRODUCTION ..... 82
METHODS ..... 84
RESULTS ..... 90
DISCUSSION ..... 95
CONCLUSION ..... 99
REFERENCES ..... 100
TABLES ..... 105
APPENDIX ..... 107
**CONSIDERAÇÕES FINAIS** ..... **111**
**REFERÊNCIAS** ..... **112**
**ANEXOS** ..... **117**

## PREFÁCIO

O presente trabalho integra o projeto intitulado “Estudo dos efeitos adversos da radioterapia em cabeça e pescoço”, que busca compreender as alterações induzidas pela radioterapia na região craniofacial. A radioterapia é amplamente utilizada no tratamento de neoplasias malignas de cabeça e pescoço, porém seus efeitos adversos a longo prazo ainda não estão completamente elucidados. Alterações ósseas, inevitavelmente impactadas pelo tratamento, podem comprometer significativamente a qualidade de vida do paciente. Esse projeto possibilita o desenvolvimento de estratégias clínicas específicas, contribui para a formação de recursos humanos e favorece intervenções médicas e odontológicas mais eficazes.

Inserido nesse contexto, métodos computacionais têm se consolidado como ferramentas promissoras na investigação do câncer de cabeça e pescoço e de seus tratamentos, especialmente no contexto da radioterapia. A inteligência artificial tem ampliado a capacidade de análise de grandes volumes de dados, permitindo a identificação de padrões complexos e a extração de informações relevantes para o diagnóstico, predição de risco, prognóstico e acompanhamento de diversas condições de saúde. De forma complementar, a análise da dimensão fractal e de índices radiomorfométricos podem possibilitar uma avaliação quantitativa e objetiva de exames de imagem, contribuindo para a compreensão da complexidade de estruturas o e potencial de observar alterações induzidas, por exemplo, pela radiação. Esses métodos oferecem potencial para a detecção precoce de efeitos adversos e para o aprimoramento da tomada de decisão clínica.

Esta dissertação reflete esse contexto de investigação dividindo-se em dois capítulos, reunindo estudos complementares: o primeiro, uma análise bibliométrica publicada no periódico *“Oral Surgery, Oral Medicine, Oral Pathology and Oral Radiology”*, que descreve tendências do o uso da inteligência artificial no câncer de cabeça e pescoço; o segundo, um estudo aplicado que utiliza os métodos como os índices radiomorfométricos e a dimensão fractal em tomografias computadorizadas de feixe cônico de pacientes irradiados na região de cabeça e pescoço. Ambos visam compreender melhor o uso de métodos computacionais e apoiar a prática clínica voltada à melhoria da saúde e bem-estar dos pacientes oncológicos.

Minha trajetória acadêmica e científica se entrelaça profundamente com o desenvolvimento deste trabalho. Desde a graduação na Universidade de Brasília (UnB), fui inspirado pela pesquisa e pelas oportunidades de aprendizado proporcionadas pelos programas de iniciação científica. Durante três projetos de iniciação científica, dediquei-me à análise de exames de imagem em diferentes contextos clínicos: avaliação de alterações da densidade mineral óssea em pacientes na pós-menopausa, condições periodontais e índices radiomorfométricos e dimensão fractal em pacientes com polipose adenomatosa familial. Além disso, participei como extensionista em um projeto de atendimento odontológico a pacientes oncológicos, experiência que reforçou meu desejo de contribuir para a saúde desses indivíduos.

Após três anos de residência em Cirurgia Bucomaxilofacial fora da UnB, retornei ao ambiente acadêmico para realizar o mestrado em Ciências da Saúde, integrando minha experiência clínica e meu interesse pela pesquisa científica no grupo do CNPq “Pesquisa translacional em câncer de cabeça e pescoço” liderado pela Profa Eliete Guerra. Este trabalho, portanto, representa não apenas a consolidação de minha trajetória científica, mas também meu compromisso com a produção de conhecimento que possa gerar impacto direto na prática clínica, beneficiando pacientes oncológicos e a sociedade como um todo.

## INTRODUÇÃO

O câncer de cabeça e pescoço (CCP) constitui um grupo heterogêneo de neoplasias que acomete o trato aerodigestivo superior, sendo representado principalmente pelo carcinoma de células escamosas (Mahmood *et al.*, 2021; Mäkitie *et al.*, 2023). Pode envolver lábio, cavidade oral, laringe, nasofaringe, orofaringe, hipofaringe e glândulas salivares. Mundialmente, é responsável por aproximadamente 950.000 casos novos e mais de 480.000 óbitos anualmente (Bray *et al.*, 2024). No Brasil, segundo estimativas do Instituto Nacional do Câncer (INCA) para o período de 2023 a 2025, o câncer oral está entre os dez mais incidentes, enquanto o câncer de laringe também figura entre os vinte mais frequentes. Somados, são responsáveis por mais de 22 mil casos e posicionam-se conjuntamente entre os cinco tipos de câncer mais incidentes no período (Santos *et al.,* 2023).

Quando detectado precocemente, o CCP apresenta taxa de sobrevida estimada de até 75% em cinco anos (Adoga *et al.*, 2018). Entretanto, frequentemente a doença é diagnosticada tardiamente, em estágios avançados, o que compromete o prognóstico e reduz significativamente a sobrevida (Mahmood *et al.*, 2021). No Brasil, cerca de 80% dos casos são identificados nos estágios III ou IV, percentual semelhante ao observado em países asiáticos, sem evidência de melhora nos últimos vinte anos. Adicionalmente, fatores socioeconômicos, especialmente o nível de escolaridade, estão diretamente associados ao diagnóstico tardio, representando um desafio significativo para o Sistema Único de Saúde, sobretudo na gestão de referências e contrarreferências nas redes de atenção (Nascimento de Carvalho *et al.*, 2025).

A exposição crônica ao álcool e ao tabaco constitui o principal fator de risco para o CCP, estando também associada ao diagnóstico tardio e, consequentemente, a pior prognóstico. Observa-se efeito independente e multiplicativo quando há consumo concomitante (Lins *et al.*, 2019). Radiação, imunodeficiência, mastigação misturas com folha de bétele (*betel-quid*), consumo de noz de areca e infecções pelos vírus HPV e Epstein-Barr também são considerados fatores etiológicos (Lander, Kallogjeri e Piccirillo, 2024; Mahmood *et al.*, 2020). No Brasil, etilismo e tabagismo permanecem entre as principais causas de CCP, especialmente em tumores de

cavidade oral, hipofaringe e laringe. Entre países com maior IDH, a infecção pelo HPV em tumores de orofaringe tem se destacado em pacientes mais jovens (Nascimento de Carvalho *et al.*, 2025). Além disso, embora não sejam fatores etiológicos prevalentes no Brasil, estima-se que aproximadamente um em cada três casos de câncer oral no mundo esteja associado ao consumo de noz de areca e tabaco não fumado, sendo Bangladesh, Índia, Paquistão e Papua Nova Guiné os países com maior incidência (Rumgay *et al.*, 2024).

O padrão de referência para o diagnóstico do CCP é a biópsia tecidual seguida de exame histopatológico (Yang *et al.*, 2022). Nesse processo, patologistas avaliam a morfologia celular e nuclear para determinar a presença e o grau de invasão tumoral, baseando-se majoritariamente em experiência empírica para o diagnóstico (Yang *et al.*, 2022). Adicionalmente, modalidades de imagem médica, como tomografia por emissão de pósitrons (PET), tomografia computadorizada por emissão de fóton único (SPECT), ressonância magnética (RM) e tomografia computadorizada (TC), fornecem informações importantes sobre morfologia, tamanho, localização e metabolismo do tumor (Salmanpour *et al.*, 2023).

Embora avanços tenham sido alcançados, o tratamento do CCP continua desafiador, envolvendo tipicamente radioterapia (RT) e quimioterapia (Bang *et al.*, 2023). A RT desempenha papel central, sendo empregada em aproximadamente 75% dos casos, isoladamente ou associada a quimioterapia e procedimentos cirúrgicos (Atun et al., 2015; Bang et al., 2023). Seu objetivo é destruir células em rápida divisão, promovendo redução tumoral, podendo ser utilizada com finalidade curativa ou paliativa (Chaput e Regnier, 2021). Paralelamente ao desenvolvimento de técnicas de imagem mais precisas para localização e delineamento tumoral, a RT evoluiu significativamente nos últimos anos, permitindo tratamentos mais individualizados e maior precisão na irradiação da região tumoral por meio de tecnologias como radioterapia guiada por imagem (IGRT) e radioterapia modulada por intensidade (IMRT) (Ahervo *et al.*, 2023; Bang *et al.*, 2023). Entretanto, devido à anatomia pequena e irregular da região de cabeça e pescoço e à presença de múltiplos órgãos críticos, o tratamento ainda está associado a diversos efeitos adversos, incluindo xerostomia, disfagia, mucosite, radiodermatite, candidíase, cáries extensas, trismo, fadiga, entre outros (Ahervo *et al.*, 2023; Araújo *et al.*, 2023; Leong *et al.*, 2024; Li *et al.*, 2023).

No tecido ósseo, a radiação atua principalmente sobre o suprimento vascular, ocasionando redução rápida de osteoblastos e aumento da atividade osteoclástica, resultando em diminuição da densidade óssea, remodelamento trabecular e substituição da medula vermelha ativa por medula amarela (Pacheco e Stock, 2013; Soares *et al.*, 2019). Consequentemente, a morfologia, a resistência e a microarquitetura óssea são alteradas nas regiões irradiadas (Bakar *et al.*, 2022). O principal desfecho clínico indesejável a nível ósseo após RT é a osteorradionecrose (ORN), condição iatrogênica observada em pacientes com câncer submetidos à RT de cabeça e pescoço, acometendo entre 5% e 15% desses pacientes (Moreno *et al.*, 2025).

A ORN é uma complicação tardia e potencialmente grave da RT para tumores de cabeça e pescoço, caracterizada por necrose óssea decorrente de dano vascular induzido pela radiação, manifestando-se por exposição óssea e/ou alterações radiográficas compatíveis, como esclerose, lise ou fratura patológica, na ausência de recorrência tumoral local. A ORN está associada a fatores de risco, incluindo higiene oral deficiente e extrações dentárias após RT, podendo evoluir para estados mórbidos caracterizados por alta carga de sintomas e comprometimento da qualidade de vida devido à perda dentária, disfunção orofacial e dor (Moreno *et al.*, 2025; Peterson *et al.*, 2024). Segundo a diretriz de Peterson e colaboradores (2024), a ORN ocorre tipicamente em regiões que receberam doses ≥50 Grays (Gy), podendo se apresentar de forma exposta ou não exposta, exigindo avaliação clínica e radiográfica combinada para diagnóstico. Em 2025, um consenso internacional de especialistas reforçou essa definição, destacando a necessidade de padronização global, estabelecendo uma nova definição internacional e propondo elementos mínimos de dados para uniformizar o diagnóstico, a comunicação científica e o monitoramento da ORN. Essas publicações evidenciam uma evolução conceitual importante, com ênfase na precisão diagnóstica, padronização e integração entre achados clínicos e radiográficos, fundamentais para o avanço da pesquisa e do manejo clínico da ORN (Moreno *et al.*, 2025).

Nos últimos anos, a rápida expansão do volume de dados digitais, aliada aos avanços computacionais, impulsionou o desenvolvimento de tecnologias capazes de auxiliar na execução de tarefas complexas, destacando-se a inteligência artificial (IA) e seus principais subcampos: machine learning (ML) e deep learning (DL). A IA refere-

se à capacidade não biológica de realizar tarefas complexas, enquanto o ML permite que sistemas aprendam padrões a partir de grandes conjuntos de dados, e o DL, como subcampo avançado do ML, extrai automaticamente representações de alto nível por meio de redes neurais profundas (Leite *et al.*, 2020). O avanço das pesquisas em IA e seus subcampos, como ML, DL, visão computacional e redes neurais convolucionais, tem se destacado em diversas áreas, incluindo as ciências médicas, especialmente no desenvolvimento de modelos que podem aprimorar a tomada de decisão clínica (Alabi *et al.*, 2024). Entre os progressos recentes, destaca-se a utilização do processamento de linguagem natural para diagnóstico diferencial, auto-triagem e automanejo, por meio de sistemas de verificação de sinais e sintomas clínicos (Meyer *et al.*, 2020).

No contexto do câncer, a IA pode ser útil para alcançar diagnóstico precoce, elucidar o impacto de fatores de risco, identificar novos biomarcadores ou alvos terapêuticos, realizar estadiamento tumoral, individualizar tratamentos, estimar taxas de sobrevida, prevenir recidivas e prever riscos e toxicidades (Alabi *et al.*, 2024; Araújo *et al.*, 2023; Kourou *et al.*, 2015; Mahmood *et al.*, 2021; Wu, Li e Tu, 2024). Para isso, é necessário um conjunto de dados oncológicos em larga escala, capaz de reconhecer padrões e estruturas a partir de informações previamente fornecidas (Wu, Li e Tu, 2024).

Especialmente no manejo do CCP, a aplicação da IA tem crescido de forma expressiva desde 2016, com destaque para abordagens em radiômica, RT e diagnóstico por imagem (Silvestre-Barbosa *et al*., 2025). Modelos de ML e DL vêm sendo amplamente utilizados para segmentação de estruturas, predição de sobrevida e apoio à tomada de decisão clínica, embora persistam desafios relacionados à validação clínica, padronização metodológica e desigualdade na produção científica entre países (Silvestre-Barbosa *et al*., 2025).

Esses modelos também têm sido aplicados a múltiplas modalidades de dados, incluindo imagens radiológicas e histopatológicas, exames endoscópicos, dados clínicos e genômicos, demonstrando potencial para aprimorar detecção precoce, caracterização tumoral, prognóstico e suporte à tomada de decisão clínica (Mäkitie *et al*., 2023). Uma recente revisão de revisões (*umbrella review*) indicou que as aplicações de IA em CCP se organizam em cinco eixos principais: identificação de lesões pré-cancerosas e cancerosas, predição da natureza histopatológica por

imagens, prognóstico, extração de achados patológicos e aplicações em RT. Entretanto, ainda existem limitações significativas relacionadas à ausência de padronização na coleta de dados, heterogeneidade metodológica, baixa qualidade de evidências e escassez de validação externa, o que impede a implementação plena desses modelos na prática clínica (Mäkitie *et al.*, 2023).

Paralelamente ao desenvolvimento recente do uso da IA, a radiômica emergiu como uma abordagem voltada à extração quantitativa de centenas de características matemáticas de imagens médicas, fornecendo parâmetros objetivos para apoiar diagnósticos, classificações e previsões clínicas. No campo da saúde, especialmente na radiologia e na odontologia, essas tecnologias têm mostrado resultados promissores, trazendo novas perspectivas para a detecção de doenças, planejamento terapêutico e suporte à tomada de decisão, com potencial para transformar a prática clínica ao reduzir a subjetividade e aumentar a precisão diagnóstica (Leite *et al.*, 2020).

Outro método computacional utilizado no contexto da saúde, especialmente em imaginologia, são os índices radiomorfométricos, que consistem em métodos de análise de imagens qualitativos e quantitativos amplamente empregados na avaliação de exames de imagem, como radiografias panorâmicas (Ersu *et al.*, 2023). Alguns desses índices foram adaptados para avaliação por tomografia computadorizada de feixe cônico (TCFC) e mostraram-se ferramentas úteis para identificar alterações ósseas (Koh e Kim, 2011), particularmente na região cortical mandibular, sítio potencialmente acometido pela RT (Borges *et al.*, 2021).

Adicionalmente, a dimensão fractal (DF), método matemático que permite a avaliação de estruturas corporais irregulares e complexas, pode ser aplicada em imagens radiograficas e tomograficas para quantificar a complexidade da microarquitetura óssea e detectar alterações precocemente nessa estrutura (Kato *et al.*, 2020). Esses métodos são frequentemente utilizados para identificar alterações ósseas em pacientes com distúrbios sistêmicos, constituindo ferramentas importantes para triagem e diagnóstico precoce de condições que afetam a morfologia óssea (Ersu *et al.*, 2023; Pacheco-Pereira *et al.*, 2021; Sindeaux *et al.*, 2014) e demonstram utilidade na avaliação de pacientes irradiados (Tepe *et al.*, 2025; Tomazelli *et al.*, 2025).

Dessa forma, a presente dissertação é estruturada em dois capítulos, abordando o uso de métodos computacionais no contexto do CCP. O primeiro capítulo apresenta uma análise bibliométrica sobre as tendências da literatura referentes à aplicação da IA nesse tipo de câncer. O segundo capítulo consiste em um estudo primário que avalia índices radiomorfométricos e DF em TCFC de pacientes irradiados na região de cabeça e pescoço, comparando-os com um grupo controle pareado.

# OBJETIVOS

## Objetivo Geral

Investigar o potencial de métodos computacionais, avaliando de que forma a IA tem sido aplicada no contexto do CCP e avaliar os índices radiomorfométricos e dimensão fractal em pacientes irradiados. Assim, poderemos aprimorar o diagnóstico e o monitoramento das alterações ósseas pós-RT, fornecendo subsídios para o manejo clínico individualizado e a detecção precoce de complicações por meio das ferramentas computacionais.

## Objetivos Específicos

- Responder à seguinte pergunta de pesquisa: “Quais são as tendências no uso da IA em CCP?”;
- Identificar e analisar, por meio de uma análise bibliométrica, o uso da IA em CCP, incluindo tópicos predominantes, lacunas de conhecimento e padrões de publicação, visando orientar futuros desenvolvimentos e aplicações clínicas da IA;
- Investigar as características das estruturas ósseas mandibulares cortical e trabecular em pacientes irradiados na região de cabeça e pescoço, por meio de TCFC, utilizando índices radiomorfométricos e análise de DF;
- Comparar os achados dos pacientes irradiados com um grupo controle pareado não irradiado, avaliando diferenças e padrões nas medidas obtidas.

## CAPÍTULO 1

Published: Oral Surgery, Oral Medicine, Oral Pathology and Oral Radiology (IF:1.9)

DOI: 10.1016/j.oooo.2025.02.014

### Worldwide Research Trends on Artificial Intelligence in Head and Neck Cancer: A Bibliometric Analysis

### ABSTRACT

**Objective:** This review aimed to explore scientific data on Artificial Intelligence (AI) and Head and Neck Cancer (HNC) through a bibliometric analysis focusing on identifying trends the research landscape on this topic. **Material and Methods:** a bibliometric analysis of AI-related HNC articles from the Web of Science Core Collection up to January 5th, 2024, was conducted. VosViewer and Biblioshiny/Bibiometrix for R Studio were used for data synthesis. This analysis covered key characteristics such as sources, authors, affiliations, countries, citations, references, and publications, as well as keyword analysis and trending topics. **Results:** A total of 1,019 papers from 1995 to 2024 were included in this review. Among them, 729 (71.6%) were original research articles and 78 (7.6%) were reviews. The 10 most cited documents were published from 2003 to 2019. The number of publications has been increasing with an annual growth rate by 94.4% after 2016, peaking in 2023. Among the 20 most productive countries, 14 are high-income economies. The keywords of strong citation revealed two main clusters: radiomics and radiotherapy. The most frequently occurring keywords include machine learning, deep learning, artificial intelligence, and head and neck cancer, with recent emphasis on diagnosis, survival prediction, and histopathology. **Conclusion:** This bibliometric analysis identified an increase in the use of AI in HNC research since 2016 and indicated a notable disparity in publication quantity between high-income and low/middle-income countries. Although most studies are original, further clinical trials and reviews are needed to enhance the accessibility of AI tools in HNC for healthcare professionals worldwide.

### KEYWORDS

Artificial Intelligence; Machine Learning; Deep Learning; Head and Neck Cancer; Bibliometrics Analysis.

## INTRODUCTION

Head and Neck Cancer (HNC) is a heterogeneous group of cancers represented mainly by squamous cell carcinoma [1,2]. It may affect the lip, oral cavity, larynx, nasopharynx, oropharynx, hypopharynx, and salivary glands, being responsible for approximately 930,000 new cases and more than 460,000 deaths each year worldwide [3,4]. Chronic exposure to alcohol and tobacco is the primary risk factor, while radiation, immunodeficiency, betel nut chewing, and infections by Human Papillomavirus (HPV) and Epstein-Barr virus are also considered etiological factors [5,6]. The reference standard for HNC diagnosis is tissue biopsy followed by histopathological examination [7]. Additionally, medical imaging modalities such as Positron Emission Tomography (PET), Single-Photon Emission Computed Tomography (SPECT), Magnetic Resonance Imaging (MRI), and Computed Tomography (CT) can provide key information on tumor morphology and size [8].

Although advances have been made in therapy, treatment remains challenging, typically involving radiotherapy and chemotherapy, which yield heterogeneous responses and can result in undesired outcomes and toxicities [9]. High death rates persist, with low improvement observed over the past decades [10]. Half of newly diagnosed individuals will survive five years after diagnosis, with significant disparities among transitioning and transitioned countries [3,10]. Moreover, the COVID-19 pandemic has led to delays in diagnoses and treatment in recent years and the full impact of this remains uncertain and will be gradually observed in the coming years [11].

Despite the negative impact of the scenario in recent years, there has been an increased reliance on technology to accomplish tasks that have become impossible to be executed by humans. Consequently, the advancement of research in the field of Artificial Intelligence (AI) and its subsets such as machine learning, deep learning, computer vision, and Convolutional Neural Networks has gained prominence across various domains, including medical sciences, especially for models that may improve clinical decision-making [12]. For instance, recent advancements include the utilization of Natural Language Processing (NLP) for differential diagnosis, self-triage, or self-treatment in the form of clinical sign and symptom checkers [13].

In the context of cancer, AI can be beneficial for achieving early diagnosis, elucidating the impact of risk factors, identifying novel biomarkers or drug targets, tumor staging, tailoring specific treatments, estimating survival rates, preventing recurrence, and predicting risks and toxicities [1,12,14–16]. This requires a large-scale cancer dataset to recognize patterns and structures within previously given information [16].

Specifically, for HNC, a recent overview summarized AI and its subfields' applications in five distinct fundamental areas: detection of precancerous and cancerous lesions in histopathologic slides; prediction of the histopathologic nature of a given lesion from imaging; prognostication; extraction of pathological findings from imaging; and applications in radiation oncology. The status, quality of available evidence, and challenges vary across these areas [2].

An efficient approach to gathering information on the use of AI in HNC is through Bibliometric Analysis (BA), a methodology developed to explore database sources and synthesize a large quantity of available data. It enables high-impact research, as it can identify trends, gaps, literature clusters, and guide future research by deriving novel ideas for investigation and intended contributions [17]. Moreover, in an era marked by the exponential growth of scientific production, BA has become an essential tool for grasping the dynamics of research areas [18].

Despite the rapid expansion of AI research in oncology, no systematic mapping of global research trends in HNC has been conducted. Understanding publication trends, dominant topics, and gaps in research can inform future AI developments and clinical applications. To fill this gap, our study investigated bibliometric data and aimed to answer the following question: What are the trends in the use of AI in HNC?

## MATERIAL AND METHODS

The methodology of this BA was described based on preliminary guideline for reporting bibliometric reviews of biomedical literature (BIBLIO) [19], and its registered protocol is available on the Open Science Framework (OSF) platform (DOI: 10.17605/OSF.IO/45CKW).

**Search engines (data sources)**

The Web of Science Core Collection (WoSCC) is a globally recognized database encompassing over 21,000 high-quality journals and various knowledge domains, routinely employed in BA for its reliability and consistent bibliographic information. Therefore, we leveraged WoSCC to extract pertinent bibliometric data.

**Search strategy and period**

The following search strategy was adapted for the WoSCC search: Topic = **(**"Head And Neck Squamous Cell Carcinomas" OR "Squamous Cell Carcinoma of the Head and Neck" OR "Head and Neck Squamous Cell Carcinoma" OR "HNSCC" OR "Squamous Cell Carcinoma of the Larynx" OR "Laryngeal Squamous Cell Carcinoma" OR "Squamous Cell Carcinoma of Larynx" OR "Squamous Cell Carcinoma of the Nasal Cavity" OR "Oral Tongue Squamous Cell Carcinoma" OR "Hypopharyngeal Squamous Cell Carcinoma" OR "Oral Squamous Cell Carcinoma" OR "Oral Cavity Squamous Cell Carcinoma" OR "Oral Squamous Cell Carcinomas" OR "Squamous Cell Carcinoma of the Mouth" OR "Oropharyngeal Squamous Cell Carcinoma" OR "Head And Neck Cancer" OR "Cancer of the Head and Neck" OR "Cancer of the Larynx" OR "Laryngeal Cancer" OR "Cancer of Larynx" OR "Cancer of the Nasal Cavity" OR "Oral Tongue Cancer" OR "Hypopharyngeal Cancer" OR "Oral Cancer" OR "Oral Cavity Cancer" OR "Cancer of the Mouth" OR "Oropharyngeal Cancer") AND ("AI" OR "Artificial Intelligence" OR "Machine Learning" OR "Deep Learning" OR "Supervised Learning" OR "Unsupervised Learning" OR "Computational Intelligence" OR "Machine Intelligence" OR "Computer Reasoning" OR "Computer Vision Systems" OR "Computer Vision System" OR "Knowledge Acquisition" OR "Knowledge Representation" OR "Knowledge Representations"). We collected data on January 5$^{th}$**,** 2024, and no time or language restriction was applied.

**Eligibility criteria**

Papers addressing any aspect of the use of AI in HNC met the eligibility criteria, including reviews, editorials, proceedings, conference papers, book chapters, and letters. Studies were excluded if they: 1) did not consider AI tools or protocols; 2) assessed benign or potentially malignant disorders; and 3) assessed malignant lesions

outside the head and neck region. It is important to note that if a study aimed to evaluate potentially malignant disorders to prevent HNC, it was included for analysis.

**Data refinement (data selection procedure)**

After removing duplicates with EndNote Web (Thompson Reuters, Philadelphia, PA), two independent authors selected the included papers. Initially, the two authors reviewed titles and abstracts, selecting articles based on eligibility criteria using Rayyan [20]. Subsequently, they cross-checked all the information found. In disagreements, a third author was involved before reaching a final decision. Finally, one author collected all the metadata from the selected articles directly from WoSCC.

**Data synthesis**

Analyses were conducted, including performance evaluations, where a general view of the field is presented through an assessment of various scientific data. Co-authorship was analyzed to uncover social interactions among authors and their affiliations. Bibliographic coupling, which involves analyzing the citing publications among included articles, was performed to identify the development of periodic knowledge or trends. Co-citation analysis, focusing on cited publications and authors, and retrospective knowledge and co-occurrence were also utilized to explore the most important keywords periodically and their existing or future relationships [21]. Furthermore, data were collected from the 50 most cited articles in the field, including details on the specialty of each article, the use of any EQUATOR (Enhancing the Quality and Transparency of Health Research) reporting guidelines (https://www.equator-network.org/reporting-guidelines/), the algorithms tested, the primary application of the algorithms and the performance outcomes of these algorithms.

The techniques for BA were reported and illustrated with the aid of the bibliometric software VOSviewer [22] and the Bibliometrix/Biblioshiny package for RStudio [23]. From the data synthesis of the bibliometric software, some graphs were generated using the Flourish data visualization tool (Flourish, URL: https://flourish.studio).

## RESULTS

### General information and temporal distribution

A total of 1,161 publications were identified in the WoSCC database. After data refinement (removing duplicates and applying eligibility criteria), 1,019 papers from 1995 to 2024 published in 387 sources were finally included. Among them, 729 (71.6%) are original research articles, 78 (7.6%) are reviews, and 212 (20.8%) take other forms, including letters, proceedings papers, and editorials. A total of 4,823 authors were identified with a mean of 8.28 co-authors per document, and almost 32% of international co-authorship. In all the included documents, a total of 1,772 authors' keywords and 24,885 references were found. Additionally, the number of publications has been increasing at a rate of 1.41% annually. This growth is particularly notable after 2016, with 962 articles out of the 1,019 (94.4%) published after this year. The growth rate averaged 95.8% from 2016 until 2023. The last and most productive complete year included when 267 (26.2%) documents were published. The main information and annual scientific production are presented in Figure 1A and Figure 1B, respectively.

### Sources

The ten most relevant sources, based on the number of documents, are ranked in Table I. In this BA, 387 sources published at least one paper. Among these, 13 were classified as core sources, falling within Zone 1 of Bradford's Law and accounting for 34% of all publications (Supplementary Figure 1). Bibliographic coupling reveals that some of these core sources frequently share common references and could be divided into clusters, suggesting they usually cover similar content. For this analysis, a minimum of five published documents were established. Of 387 terms, 40 met the threshold. Cluster 1 includes Cancers, Scientific Reports, Head and Neck-Journal for the Sciences and Specialties of the Head and Neck, Clinical Cancer Research, and Computers in Biology and Medicine. Cluster 2 includes Medical Physics, Radiotherapy and Oncology, Frontiers in Oncology, International Journal of Radiation Oncology Biology Physics, and Physics in Medicine and Biology. Finally, cluster 3 includes Oral Oncology and Diagnostics (Supplementary Figure 2).

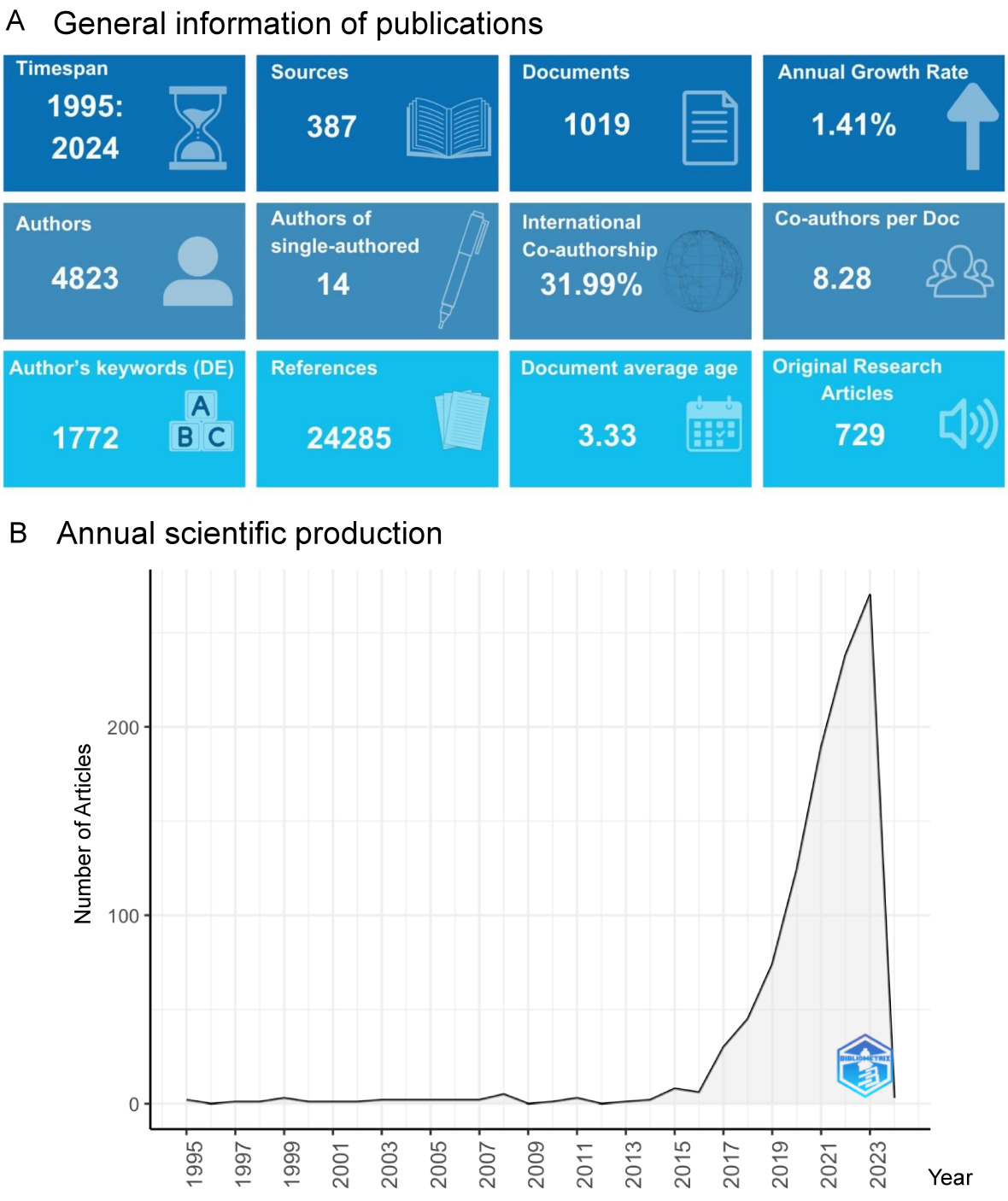


Figure 1. (A) General information of publications. Overview of the 1,019 publications included in the study, categorized into original research articles, reviews, and other types (letters, proceedings papers, editorials). (B) Annual scientific production. Annual number of publications from 1995 to 2024, showing a notable increase after 2016, with 94.4% of the articles published post-2016 and 2023 as the most productive year.

### Authors and affiliations

In total, 4,823 authors were identified across all years, with an average of 8.28 authors per document. Table I ranks the most productive authors by the number of

papers. Almangush A, from the University of Helsinki, emerged as the most cited author, with 124 citations, followed by Wang X (Hospital of Hainan Medical University) with 118 citations, and Alabi R (University of Helsinki) with 114 citations (Supplementary Figure 3). The most prominent collaborators were Fuller C (MD Anderson Cancer Center, University of Texas), Mohamed A (MD Anderson Cancer Center, University of Texas), and Suresh A (Mazumdar Shaw Medical Center), with total link strengths of 227, 206, and 180 in co-authorship analysis, respectively.

Out of 1,505 affiliations, 51 published at least 20 articles. Among the ten most productive institutions listed in Table I, it is noteworthy that all are from developed countries, confirming the hegemony of the USA, which accounts for five of the top 10 positions in the affiliation's rank. In terms of collaboration, the University of Helsinki (Finland), the German Cancer Research Center (Germany), and the Karolinska Institute (Sweden) stand out, with total link strengths of 99, 76, and 75 in co-authorship analysis, respectively. The University of Helsinki and the Karolinska Institute frequently collaborate, and both are often associated with the University of Turku (Finland) and the University of Vaasa (Finland). The German Cancer Research Center collaborates strongly with the Dresden University of Technology, also from Germany. Another notable collaboration is between Emory University (USA) and the Georgia Institute of Technology (USA), with a link strength of 12 between them (Supplementary Figure 4).

**Countries**

The influence of countries' production in the HNC and AI field, as well as their collaborations, is illustrated in Figure 2A. Out of the 20 most productive countries, six are emerging economies, including China and India, which hold the second and third positions, respectively (Figure 2A). Approximately 32% of included documents have more than one country co-authorship and the most frequent international partnerships are USA/China (48), USA/Netherlands (25), USA/UK (21), USA/Canada (18), USA/India (15), Finland/Sweden (13), USA/Finland (12), USA/Australia (11), Italy/Netherlands (10), and Netherlands/Denmark (10) (Figure 2B).

**Citations and publications**

The ten most cited documents, presented in Table II, ranged from 2003 to 2019, with six of them published after 2016, highlighting the notable growth of publications initiated in this year. Only one of the top 10 most cited articles was not an original research article; it was classified as a systematic review, assessing risk prediction models [24]. The most cited article proposed a deep learning tool for fast segmentation of head and neck anatomy [25], and another highly ranked study assessed Convolutional Neural Network (CNN) in organ segmentation for radiotherapy [26]. Radiomics associated with machine learning was the topic in two of the ten articles [27,28]. Additionally, the top 10 documents reported on dose prediction models and treatment planning for radiotherapy [29,30], survival prediction [10,27,28], analysis of a prognostic plasma biomarker [31], and generation of a diagnostic RNA signature [32].

Recently, two studies on fusion-based radiomic reproducible features for survival prediction have received significant attention, with both having the highest citation rates since their publication [8,33].

Supplementary Table 1 provides details on specialty, guidelines followed, algorithms used, and performance of 50 most cited articles. Of these, 24 investigated AI applications in radiology. Pathology was also a frequent subject, featured in 19 studies. Genomics, oncology, and epidemiology were among the other topics covered. Only five articles adhered to any EQUATOR guidelines, two of which were systematic reviews that followed PRISMA (Preferred Reporting Items for Systematic Reviews and Meta-Analyses).

The data on algorithms used, their applications, and performance are highly diverse, with a notable emphasis on deep learning models for segmentation, such as U-Net variants, as well as traditional machine learning techniques, including Support Vector Machines (SVM), decision trees, discriminant analysis, and Multiple Adaptive Regression Splines (MARS). Overall, performance varied depending on the methodology and dataset characteristics.

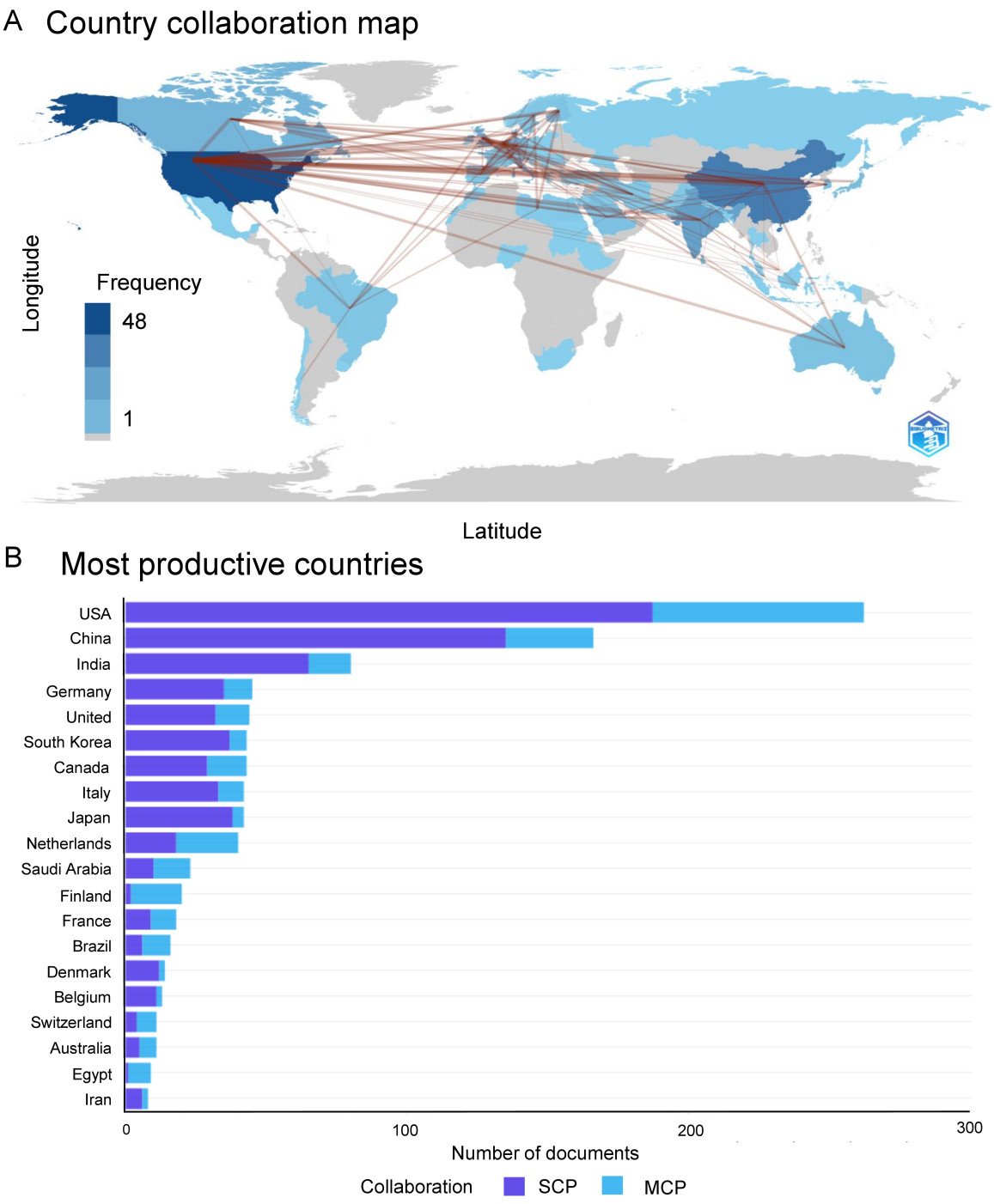


Figure 2. (A) Countries collaboration map. The map shows the research output and impact of the top 20 countries in the fields of HNC and AI, highlighting contributions from emerging economies such as China and India, which rank second and third, respectively. (B) Most productive countries. The graphic illustrates the international research partnerships in HNC and AI. Around 32% of the publications result from collaborations between countries, with frequent partnerships including USA/China, USA/Netherlands, USA/UK, and others. Abbreviations: Single Country Publications (SCP); Multiple Country Publications (MCP).

There were overlaps among the AI applications included in the 50 most cited studies, particularly in tumor diagnosis and organ segmentation. For the differentiation

between healthy and tumorous tissue, 5 out of 10 studies employed CNNs, highlighting a preference for computer vision techniques in this diagnostic task. In contrast, for metastasis assessment, there was no overlap, as different algorithms were used across studies. Regarding the segmentation of organs at risk, 3 out of 4 studies consistently utilized U-Net architectures, indicating a common approach for this application. For treatment outcome prediction, 2 out of 4 studies relied on SVMs, demonstrating a frequent choice of algorithm in this context.

The ranking of studies by performance in diagnosis and metastasis prediction among the 50 most cited studies is presented by Supplementary Table 2. Accuracy was chosen as the ranking criterion since it was the most frequently reported performance measure. SVM, CNN, and ensemble learning approaches achieved high accuracy across multiple applications. The highest accuracy for cancer diagnosis was 96% [34], while 93.5% was achieved for metastasis prediction [35].

Across different applications, the highest accuracy (98%) was achieved using an artificial neural network (ANN) for distinguishing pulmonary metastases from primary lung cancers [36]. Other top-performing models include a custom CNN for multi-class grading of OSCC (97.5%) [37] and MobileNet CNN for quantifying tumor-infiltrating lymphocytes (96.31%) [38]. SVM, CNN, and ensemble learning approaches demonstrated high accuracy across multiple applications. Overall, CNN-based models, including ResNet34, AlexNet, and MobileNet, showed strong predictive capabilities, with several studies reporting accuracies exceeding 90% (Supplementary Table 3).

**Co-cited references**

Co-citation analysis identifies studies that are frequently cited together in the reference lists of the included documents, suggesting a potential relationship between these studies. Out of 24,285 references, 25 were cited at least 35 times. The most frequently cited reference is a global cancer statistics study from 2011, with 86 citations across the included articles [39]. The second most cited reference pertains to convolutional networks for biomedical image segmentation, with 72 citations [40]. Lastly, ranking third among the most cited references is a study utilizing a radiomics approach to quantify tumor image intensity, shape, and texture in CT scans, which garnered 70

citations [41]. Data on the top cited references and network visualization of co-citation analysis are presented in Supplementary Figure 5.

**Keyword analysis and trend topics**

For co-occurrence analysis of the author's keywords, a minimum of ten occurrences were established. Out of 1,772 terms, 46 met the threshold. General terms for this topic, such as "machine learning", "deep learning", "artificial intelligence", "head and neck cancer", and "oral cancer", are among the most frequent (Figure 3A). Additionally, some more specific terms like "radiomics", "radiotherapy", and "convolutional neural network" are included in this list.

The author's keywords were also clustered in a thematic network, as shown in Figure 3B. The green cluster shows frequent terms related to radiomics and its applications in the context of HNC. Terms related to radiotherapy, image segmentation, organs at risk, CT, MRI, and PET are included in this cluster. The blue cluster exhibits terms related to the use of machine learning in HNC. It includes prognosis, diagnosis, prediction, early detection, biomarker, and screening. The red cluster encompasses specific terms of AI, such as deep learning and CNN.

Trending topics are illustrated in Figure 4A. In 2023, the last complete year analyzed, terms such as "diagnosis", "overall survival", and "histopathology" were particularly prominent, with 21, 10, and 10 mentions, respectively. Figure 4B shows the evolution of common keywords used by authors. The first column encompasses terms from 1995 to 2015, the period before the notable growth in the number of publications. The second column covers the period from 2016 to 2019, the years preceding the COVID-19 pandemic. The last column provides information from the pandemic period until the present.

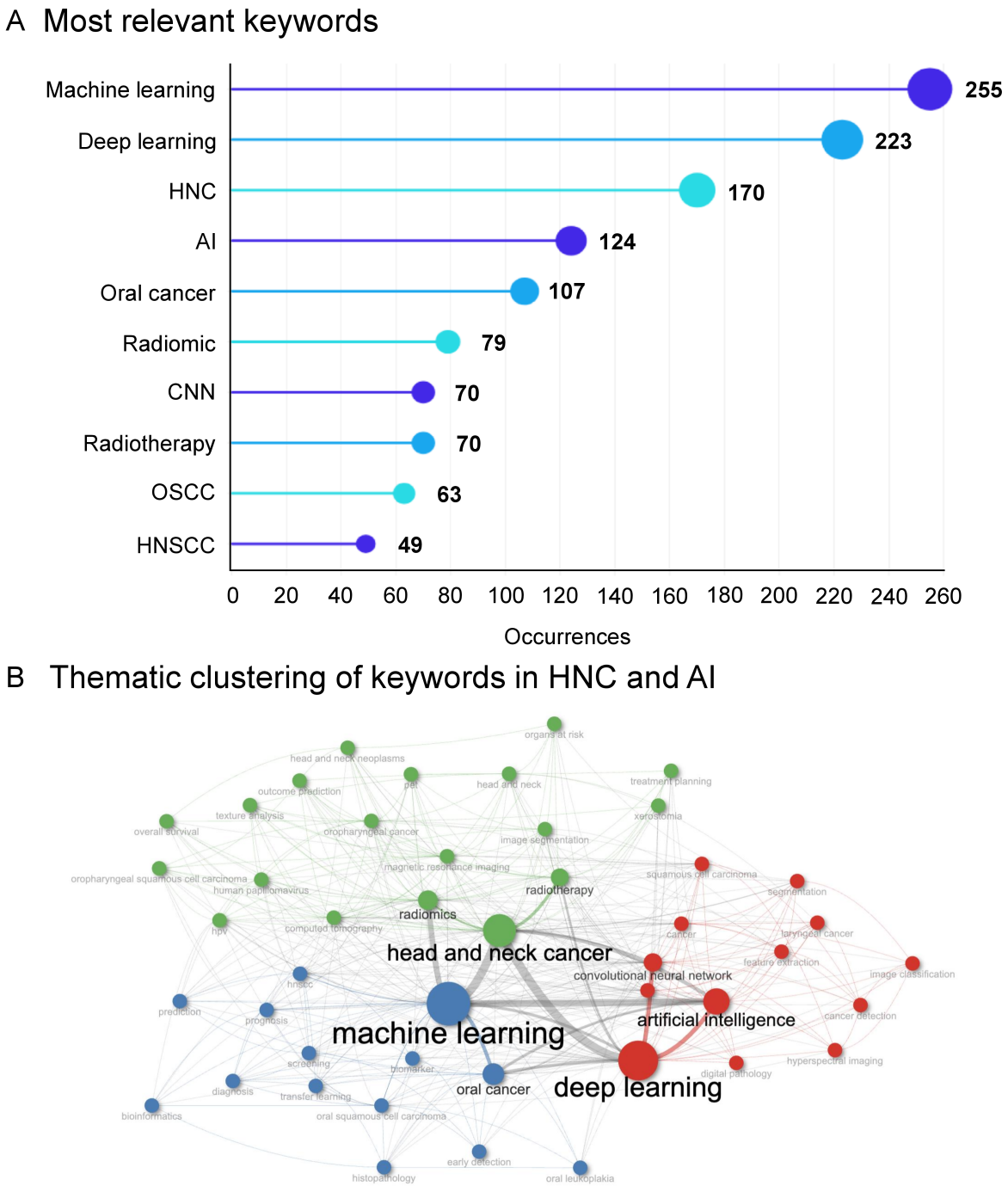


Figure 3. (A) Author's keyword analysis. The graphic displays the most frequently used keywords among the 46 terms that met the threshold of ten occurrences. Common terms include "machine learning," "deep learning," "artificial intelligence," "head and neck cancer," and "oral cancer," along with more specific terms like "radiomics," "radiotherapy," and "convolutional neural network". (B) Co-occurrence of author keywords. The figure illustrates the clustering of keywords into thematic groups. The green cluster represents terms related to radiomics and its applications in HNC, including radiotherapy and imaging techniques. The blue cluster focuses on machine learning applications in HNC, encompassing terms like prognosis and diagnosis. The red cluster includes AI-specific terms such as deep learning and CNN. Abbreviations: Artificial Intelligence (AI); Convolutional Neural Network (CNN); Head and Neck Cancer (HNC); Head and Neck Squamous Cell Cancer (HNSCC); Oral Squamous Cell Cancer (OSCC).

## DISCUSSION

This review maps the research landscape of AI in HNC through bibliometric analysis, spanning articles from 1995 to 2024. The results cover 29 years, revealing a recent exponential growth in interest in this topic. The significant increase, particularly starting from 2016, when the annual growth rate reached 94.4%, is not exclusive to HNC. In recent years, there has been a notable utilization of AI across the healthcare domain. A BA examining AI in healthcare revealed a significant increase in publications post-2014, closely aligning with the trends observed in this study [42]. This recent interest and growth, along with the increasing development of innovative technologies for AI tools, may explain why many publications are original research articles, with only 7.6% being review articles.

Despite the recent growth in interest and research in AI, especially for health-related applications, the concept of AI is not new. The term was first used during a summer project held by Dartmouth College (USA) in 1956. At that time, an attempt was made to explore how machines could use language, form abstractions and concepts, solve problems typically reserved for humans, and improve themselves [43]. Over the past 70 years, AI has not always lived up to its expectations, experiencing periods referred to as 'AI winters'. However, AI technology has become increasingly convincing, with its impact being felt across various fields and disciplines, including society, economics, healthcare, and politics [44]. One reason for the recent improvements in AI is the advancement in computational power, particularly with the development of Graphics Processing Unit (GPU) and Tensor Processing Unit (TPU), which allow for faster processing of complex algorithms.

Additionally, the availability of large datasets has enabled more effective training of AI models. Advances in machine learning techniques, such as deep learning, have also played a crucial role in enhancing AI capabilities. In HNC research, the first article identified in this BA was published in 1995. It evaluated the ability of a neural network to predict the likelihood of an individual having a malignant or potentially malignant oral lesion based on their risk habits. Even at that early stage, the study concluded that neural networks could be useful for screening at-risk patients [45]. This BA provides quantitative insights into scientific data from the WoSCC database. The metadata was

thoroughly analyzed, revealing key sources, research institutions, and countries based on the detailed results in section 3.

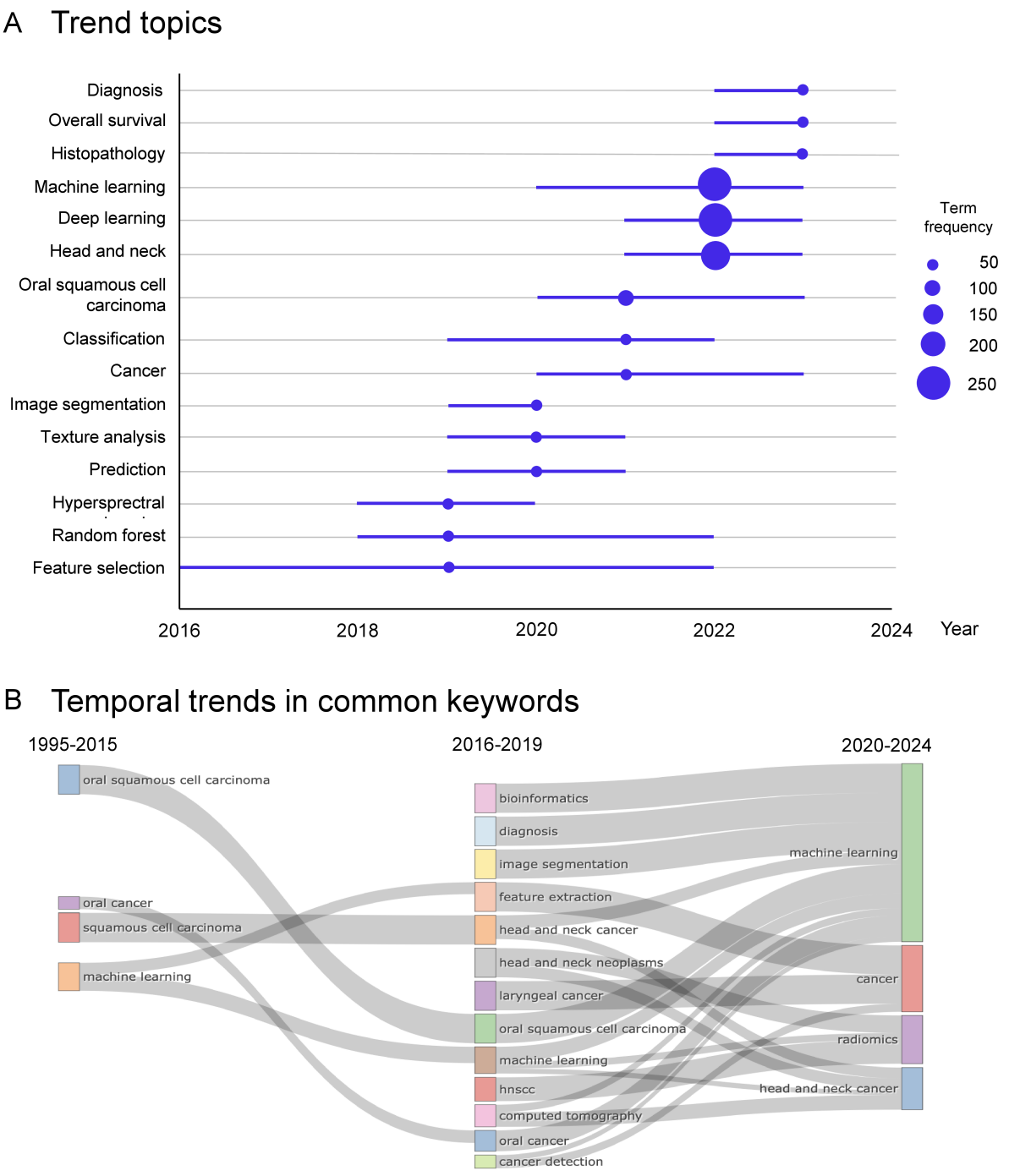


Figure 4. (A) Illustration of the most important keywords over the years. In 2023, the most used terms were "diagnosis" (21 occurrences), "overall survival" (10 occurrences) and "histopathology" (10 occurrences). (B) Temporal trends in common keywords. Demonstration of the progression of keywords used by authors in 3 distinct periods: 1995-2015 (before significant growth in publications), 2016-2019 (pre-COVID-19 era), and 2020-present (pandemic and current period). The figure highlights the changes in focus over time.

Thirteen sources contribute to one-third of all publications. Eight of them are dedicated to radiotherapy, oncology, or head and neck cancer, while the remaining encompass broader scientific or medical topics and computer research. Among these sources, three have an impact factor (IF) of 5 or higher, with the International Journal of Radiation Oncology Biology Physics having the highest IF. This concentration of high-impact publications in specialized journals highlights the significant focus and advancements in AI research within oncology and head and neck cancer.

The findings revealed a worldwide interest in this topic. However, a disparity between low-and-middle-income and high-income nations can be observed. All institutions ranked by the number of documents are from high-income countries, and their main collaboration patterns do not involve low-and-middle-income ones, despite China and India being listed among the top three producing countries. Among the 20 most productive countries, only six are low-and-middle-income economies, while 14 are high-income economies. It is important to emphasize that the general occurrence of HNC is on the rise in both, with an anticipated annual increase of 30% by 2030 [46]. Therefore, high-income countries, being at the forefront of research in this field, are more likely to develop and implement more effective strategies for HNC management. This research advantage may further reinforce existing disparities.

Disparities in AI research output between high- and low-income countries highlight the need for targeted resource allocation. High-income countries, leading in AI-driven HNC research, are more likely to develop and integrate advanced technologies into clinical practice, further widening the gap in healthcare accessibility. To mitigate these disparities, funding agencies and policymakers should improve the allocation of resources in underrepresented regions. Moreover, promoting collaboration in research between institutions in high- and low-resource settings can facilitate knowledge transfer, enhance access to high-quality datasets, and support the development of AI applications adapted to different healthcare settings. Addressing these gaps, AI has the potential to improve HNC diagnosis, treatment planning, and prognostic modeling globally. Moreover, it was observed that the United States leads in publications within this domain, likely due to its status as a technology development hub and its high incidence of HNC cases. Despite the high incidence, the mortality rate associated with this pathology remains comparatively low and continued to decline through 2021 (IARC/WHO, 2024). Several factors contributing to this decrease include

advancements in the timely identification of certain cancers and enhancements in treatment choices for both the adjuvant and metastatic stages [11]. The significant amount of research involving AI has the potential to contribute to the early detection and improved treatment of the disease. This reinforces the notion that advancements in this research field, including the development of prediction models for HNC, may be crucial for achieving lower incidence and death rates, and for predicting the occurrence of the disease. Therefore, there is a pressing need for the clinical application of AI tools based on these research advancements to fully realize their benefits in healthcare.

Both top-cited articles and keyword analysis revealed radiomics as a recurrent theme among articles. Radiomics emerged following the digitalization of radiology in the late 20th century and comprises algorithms that decompose input images into basic features used to classify or interpret the image, such as edges, gradients, shape, signal intensity, wavelength, and textures [47]. Radiomics can be applied to various imaging modalities, including PET, SPECT, MRI, and CT. The radiomic workflow begins with processing medical images in two, three, or four dimensions, containing quantitative data captured across various scales and machine variations. A region of interest (ROI) is defined to extract information, and features are extracted from this ROI. Various methods, including manual and automated segmentation, as well as deep learning architectures, can be employed [48].

In this BA, as expected, the term "radiomics" was often associated with imaging exam terms, radiotherapy, and organ segmentation among the studies, and the most cited articles primarily assessed prognosis and risk prediction. Our results are consistent with another BA published recently, which evaluated oropharyngeal cancer and HPV+. They reported quantitative imaging analysis as an emerging field in oncologic diseases, especially for diagnostic and prognostic purposes [49]. A recent systematic review revealed that AI-based radiomics in head and neck oncology encompasses both cancer diagnostics and prognosis. Radiomics-based diagnostics involve tumor staging, tumor grading, HPV status determination, and differentiating between malignant and benign tumors. Meanwhile, radiomics-based prognosis includes predicting metastasis, local and distant failures, treatment response, recurrence, and patient survival. In summary, radiomics enables the extraction of higher-level data that are currently under-utilized in routine clinical practice. Future studies may develop models that combine radiomics features with clinical data or other

omics approaches, including genomics, proteomics, or pathomics to advance personalized and precision oncology [12].

Assessing the 50 most cited publications, the analysis of specialties revealed that radiology was the predominant field, underscoring the critical role of medical imaging in this domain. In terms of methodological rigor, the reporting of EQUATOR guidelines was inconsistent. While few studies explicitly adhered to established guidelines, a significant number did not specify compliance, highlighting a gap in standardization in AI research. A diverse array of AI algorithms was employed across the studies. Deep learning models, particularly U-Net variants, were frequently used for image segmentation, demonstrating their potential to automate diagnostic workflows. These models consistently outperformed traditional techniques in segmentation accuracy and efficiency, reinforcing their suitability for medical image analysis. Traditional machine learning techniques, including SVM, decision trees, discriminant analysis, and MARS, were also widely utilized, showcasing their versatility in predictive modeling. Ensemble learning approaches, such as bagging, boosting, and random forests, further contributed to classification and prognostic tasks by integrating multiple models to enhance predictive performance. They demonstrated robustness across diverse datasets, although with heterogeneous outcomes influenced by algorithmic parameters and data variability.

Trending topics analysis has highlighted "diagnosis" and "histopathology" as prominent themes in recent evidence. In this context, a study developed a custom-made deep learning model to assist pathologists in detecting Oral Squamous Cell Carcinoma (OSCC) from histopathology images. The model, utilizing seven layers of convolutional operations, aimed to identify OSCC or control images among more than 2,000 images in the testing and training sets. The authors concluded that their deep learning model effectively diagnosed OSCC, improved diagnostic speed and accuracy, and reduced the workload of pathologists [7]. Another study evaluated deep learning in smartphone-based images of oral lesions for automatic detection of oral cancer. They proposed an approach for collecting centered-rule oral cavity images and created five categories of diseases. Their findings suggested it as a potential tool for early diagnosis and a great method to improve deep learning algorithm performance for cancer detection [50]. Moreover, a systematic review summarized the perspectives of AI for HNC diagnosis, supporting the potential applications of supervised machine learning

methods as aids in detecting and grading malignant lesions in the head and neck region. Despite the positive outlook in this area, the review noted limited evidence and a high risk of bias within the studies included for analysis [6]. Thus, the use of AI for diagnosis and histopathology analysis in HNC appears to be a promising and evolving field with areas yet to be explored.

Another notable focus among top-cited articles, co-cited references, and keyword analyses involves strategies for radiotherapy planning. Some of the most cited studies describe strategies employing convolutional deep learning frameworks for automatically delineating organs at risk from CT images. Additionally, they discuss 3D dose prediction and distribution algorithms based on patient-specific geometry and prescription dose. These advancements enable rapid and precise treatment planning for intensity-modulated radiation therapy (IMRT), which typically requires manual contouring of structures and a prominent level of expertise to produce personalized high-quality plans. Ongoing efforts aim to optimize these tools and address challenges such as inter-patient anatomical variation and low CT soft tissue contrast [25,26,29,30].

Among the top-cited articles in 2023, the primary focus was survival prediction. Various machine learning algorithms, including SVM, logistic regression, ANN, decision tree, and random forest, have been utilized in disease risk prediction models using unstructured data [51]. Furthermore, prediction models for oncologic outcomes, treatment toxicity, and pathological findings have already been developed [52]. Despite the benefits of health prediction, several challenges remain for their routine implementation. These challenges include inadequate technological infrastructure, limited access to diverse and well-annotated datasets, data standardization issues, interpretation of results by healthcare professionals, and regulatory barriers for AI usage. The absence of standardized policies for AI deployment in healthcare exacerbates these difficulties, making integration into clinical practice challenging [53].

Some AI-driven systems have been clinically tested to enhance diagnosis and treatment of HNC. In radiotherapy, AI-supported applications have demonstrated efficiency in organ-at-risk segmentation and dose optimization, potentially improving patients' quality of life and optimizing treatment workflows [54,55]. In diagnostic tasks, AI has shown significant potential in analyzing medical images, including radiological and histological exams, often surpassing human radiologists in accuracy. Additionally, AI-driven systems have been employed to automate histopathological analysis, aiding in

tumor grading and segmentation [56]. These advancements illustrate AI's practical transition from research to clinical application, enhancing segmentation accuracy, survival prediction, and early detection. However, further development is required to ensure these systems achieve the necessary robustness and generalizability for effective implementation across diverse HNC patient populations.

Our study stands out for its methodological rigor. Although not usually required for BA, it was registered on the OSF platform to ensure its integrity and reproducibility. This allowed for a critical assessment of its protocol and research planning before execution, thereby reducing potential biases. Additionally, the material and methods section of this article (section 2) was described following a recent and preliminary guideline for BA reporting [19], ensuring clear eligibility criteria (section 2.3) and meticulous data refinement (section 2.4), with authors assessing the studies blinded and cross-checking afterward.

Furthermore, an investigation of recently published health and medicine-related bibliometric studies reported some information that is often missing in some BAs. They revealed that data related to title clarity, description of database characteristics, date of search, eligibility criteria, and description of the collection process are frequently omitted from reports [57]. In this study, we provide all this information.

This study also has limitations that need to be considered. Firstly, BA is a secondary study involving a vast amount of data, some of which may be missing or inadequately described. In this study, an average of 6.2% of the data was unavailable, mainly concerning DOIs, abstracts, and keywords. Secondly, the dataset is obtained from WoSCC, although it is one of the most accessed databases worldwide, some important articles may only be available in other databases, potentially limiting the representativeness of the results. Finally, the assessment of citation metrics is time-dependent, meaning that recent articles are less cited than earlier ones. These limitations can impact the overall results but are unlikely to change the trends presented.

## CONCLUSION

The study identified an increase in the use of AI in HNC research since 2016 and indicated a notable disparity in publication quantity between low- and middle-income and high-income countries. Future efforts should focus on fostering international collaborations, standardizing methodologies, and expanding access to AI-driven tools to ensure equitable advancements in HNC research and care. Current research hotspots predominantly encompass radiomics, diagnosis, radiotherapy, image segmentation, and survival prediction, emphasizing radiology as the most explored specialty. Despite the promising advancements, the clinical adoption of AI-based systems for managing HNC patients encounters numerous obstacles, such as concerns over data security and the need for regulatory clearance. To complete, although most studies are original, further clinical trials and reviews are needed to enhance the accessibility of AI tools in HNC for healthcare professionals worldwide.

**REFERENCES**

1. Mahmood H, Shaban M, Rajpoot N, Khurram SA. Artificial Intelligence-based methods in head and neck cancer diagnosis: an overview. *Br J Cancer*. 2021;124(12):1934-1940. doi:10.1038/s41416-021-01386-x

2. Mäkitie AA, Alabi RO, Ng SP, et al. Artificial Intelligence in Head and Neck Cancer: A Systematic Review of Systematic Reviews. *Adv Ther*. 2023;40(8):3360-3380. doi:10.1007/s12325-023-02527-9

3. Sung H, Ferlay J, Siegel RL, et al. Global Cancer Statistics 2020: GLOBOCAN Estimates of Incidence and Mortality Worldwide for 36 Cancers in 185 Countries. *CA Cancer J Clin*. 2021;71(3):209-249. doi:10.3322/caac.21660

4. Sun A, Xing Z, Lv R, et al. Research progress of immunotherapy for advanced head and neck cancer. *Medical Oncology*. 2024;41(6). doi:10.1007/s12032-024-02375-9

5. Lander DP, Kallogjeri D, Piccirillo JF. Smoking, Drinking, and Dietary Risk Factors for Head and Neck Cancer in Prostate, Lung, Colorectal, and Ovarian Cancer Screening Trial Participants. *JAMA Otolaryngol Head Neck Surg*. 2024;150(3):249-256. doi:10.1001/jamaoto.2023.4551

6. Mahmood H, Shaban M, Indave BI, Santos-Silva AR, Rajpoot N, Khurram SA. Use of artificial intelligence in diagnosis of head and neck precancerous and cancerous lesions: A systematic review. *Oral Oncol*. 2020;110. doi:10.1016/j.oraloncology.2020.104885

7. Yang SY, Li SH, Liu JL, et al. Histopathology-Based Diagnosis of Oral Squamous Cell Carcinoma Using Deep Learning. *J Dent Res*. 2022;101(11):1321-1327. doi:10.1177/00220345221089858

8. Salmanpour MR, Rezaeijo SM, Hosseinzadeh M, Rahmim A. Deep versus Handcrafted Tensor Radiomics Features: Prediction of Survival in Head and Neck Cancer Using Machine Learning and Fusion Techniques. *Diagnostics*. 2023;13(10). doi:10.3390/diagnostics13101696

9. Bang C, Bernard G, Le WT, Lalonde A, Kadoury S, Bahig H. Artificial intelligence to predict outcomes of head and neck radiotherapy. *Clin Transl Radiat Oncol*. 2023;39. doi:10.1016/j.ctro.2023.100590

10. Kim DW, Lee S, Kwon S, Nam W, Cha IH, Kim HJ. Deep learning-based survival prediction of oral cancer patients. *Sci Rep*. 2019;9(1). doi:10.1038/s41598-019-43372-7

11. Siegel RL, Giaquinto AN, Jemal A. Cancer statistics, 2024. *CA Cancer J Clin*. Published online January 17, 2024. doi:10.3322/caac.21820

12. Alabi RO, Elmusrati M, Leivo I, Almangush A, Mäkitie AA. Artificial Intelligence-Driven Radiomics in Head and Neck Cancer: Current Status and Future Prospects. *Int J Med Inform*. 2024;188. doi:10.1016/j.ijmedinf.2024.105464

13. Meyer AND, Giardina TD, Spitzmueller C, Shahid U, Scott TMT, Singh H. Patient perspectives on the usefulness of an artificial intelligence-assisted symptom checker: Cross-sectional survey study. *J Med Internet Res*. 2020;22(1). doi:10.2196/14679

14. Araújo ALD, Moraes MC, Pérez-de-Oliveira ME, et al. Machine learning for the prediction of toxicities from head and neck cancer treatment: A systematic review with meta-analysis. *Oral Oncol*. 2023;140. doi:10.1016/j.oraloncology.2023.106386

15. Kourou K, Exarchos TP, Exarchos KP, Karamouzis M V., Fotiadis DI. Machine learning applications in cancer prognosis and prediction. *Comput Struct Biotechnol J*. 2015;13:8-17. doi:10.1016/j.csbj.2014.11.005

16. Wu X, Li W, Tu H. Big data and artificial intelligence in cancer research. *Trends Cancer*. 2024;10(2):147-160. doi:10.1016/j.trecan.2023.10.006

17. Donthu N, Kumar S, Mukherjee D, Pandey N, Lim WM. How to conduct a bibliometric analysis: An overview and guidelines. *J Bus Res*. 2021;133:285-296. doi:10.1016/j.jbusres.2021.04.070

18. Hassan W, Duarte AE. Bibliometric analysis: A few suggestions. *Curr Probl Cardiol*. 2024;49(8). doi:10.1016/j.cpcardiol.2024.102640

19. Montazeri A, Mohammadi S, M.Hesari P, Ghaemi M, Riazi H, Sheikhi-Mobarakeh Z. Preliminary guideline for reporting bibliometric reviews of the biomedical literature (BIBLIO): a minimum requirements. *Syst Rev*. 2023;12(1). doi:10.1186/s13643-023-02410-2

20. Ouzzani M, Hammady H, Fedorowicz Z, Elmagarmid A. Rayyan-a web and mobile app for systematic reviews. *Syst Rev*. 2016;5(1). doi:10.1186/s13643-016-0384-4

21. Öztürk O, Kocaman R, Kanbach DK. How to design bibliometric research: an overview and a framework proposal. *Review of Managerial Science*. Published online 2024. doi:10.1007/s11846-024-00738-0

22. van Eck NJ, Waltman L. Software survey: VOSviewer, a computer program for bibliometric mapping. *Scientometrics*. 2010;84(2):523-538. doi:10.1007/s11192-009-0146-3

23. Aria M, Cuccurullo C. bibliometrix: An R-tool for comprehensive science mapping analysis. *J Informetr*. 2017;11(4):959-975. doi:10.1016/j.joi.2017.08.007

24. Gerds TA, Cai T, Schumacher M. The performance of risk prediction models. *Biometrical Journal*. 2008;50(4):457-479. doi:10.1002/bimj.200810443

25. Zhu W, Huang Y, Zeng L, et al. AnatomyNet: Deep Learning for Fast and Fully Automated Whole-volume Segmentation of Head and Neck Anatomy. Published online August 15, 2018. doi:10.1002/mp.13300

26. Tong N, Gou S, Yang S, Ruan D, Sheng K. Fully automatic multi-organ segmentation for head and neck cancer radiotherapy using shape representation model constrained fully convolutional neural networks. *Med Phys*. 2018;45(10):4558-4567. doi:10.1002/mp.13147

27. Leger S, Zwanenburg A, Pilz K, et al. A comparative study of machine learning methods for time-To-event survival data for radiomics risk modelling. *Sci Rep*. 2017;7(1). doi:10.1038/s41598-017-13448-3

28. Parmar C, Grossmann P, Rietveld D, Rietbergen MM, Lambin P, Aerts HJWL. Radiomic machine-learning classifiers for prognostic biomarkers of head and neck cancer. *Front Oncol*. 2015;5(DEC). doi:10.3389/fonc.2015.00272

29. Fan J, Wang J, Chen Z, Hu C, Zhang Z, Hu W. Automatic treatment planning based on three-dimensional dose distribution predicted from deep learning technique. *Med Phys*. 2019;46(1):370-381. doi:10.1002/mp.13271

30. Nguyen D, Jia X, Sher D, et al. 3D radiotherapy dose prediction on head and neck cancer patients with a hierarchically densely connected U-net deep learning architecture. *Phys Med Biol*. 2019;64(6). doi:10.1088/1361-6560/ab039b

31. Le QT, Sutphin PD, Raychaudhuri S, et al. *Identification of Osteopontin as a Prognostic Plasma Marker for Head and Neck Squamous Cell Carcinomas 1*. http://aacrjournals.org/clincancerres/article-pdf/9/1/59/2085004/df0103000059.pdf

32. Lajer CB, Nielsen FC, Friis-Hansen L, et al. Different miRNA signatures of oral and pharyngeal squamous cell carcinomas: A prospective translational study. *Br J Cancer*. 2011;104(5):830-840. doi:10.1038/bjc.2011.29

33. Salmanpour MR, Hosseinzadeh M, Rezaeijo SM, Rahmim A. Fusion-based tensor radiomics using reproducible features: Application to survival prediction in head and neck cancer. *Comput Methods Programs Biomed*. 2023;240. doi:10.1016/j.cmpb.2023.107714

34. Ziober AF, Patel KR, Alawi F, et al. Identification of a gene signature for rapid screening of oral squamous cell carcinoma. *Clinical Cancer Research*. 2006;12(20 PART 1):5960-5971. doi:10.1158/1078-0432.CCR-06-0535

35. Onken MD, Winkler AE, Kanchi KL, et al. A surprising cross-species conservation in the genomic landscape of mouse and human oral cancer identifies a transcriptional signature predicting metastatic disease. *Clinical Cancer Research*. 2014;20(11):2873-2884. doi:10.1158/1078-0432.CCR-14-0205

36. Jurmeister P, Bockmayr M, Seegerer P, et al. *Machine Learning Analysis of DNA Methylation Profiles Distinguishes Primary Lung Squamous Cell Carcinomas from Head and Neck Metastases*. Vol 11.; 2019. http://stm.sciencemag.org/

37. Das N, Hussain E, Mahanta LB. Automated classification of cells into multiple classes in epithelial tissue of oral squamous cell carcinoma using transfer learning and convolutional neural network. *Neural Networks*. 2020;128:47-60. doi:10.1016/j.neunet.2020.05.003

38. Shaban M, Khurram SA, Fraz MM, et al. A Novel Digital Score for Abundance of Tumour Infiltrating Lymphocytes Predicts Disease Free Survival in Oral Squamous Cell Carcinoma. *Sci Rep*. 2019;9(1). doi:10.1038/s41598-019-49710-z

39. Jemal A, Bray F, Center MM, Ferlay J, Ward E, Forman D. Global cancer statistics. *CA Cancer J Clin*. 2011;61(2):69-90. doi:10.3322/caac.20107

40. Ronneberger O, Fischer P, Brox T. U-net: Convolutional networks for biomedical image segmentation. In: *Lecture Notes in Computer Science (Including Subseries Lecture Notes in Artificial Intelligence and Lecture Notes in Bioinformatics)*. Vol 9351. Springer Verlag; 2015:234-241. doi:10.1007/978-3-319-24574-4_28

41. Aerts HJWL, Velazquez ER, Leijenaar RTH, et al. Decoding tumour phenotype by noninvasive imaging using a quantitative radiomics approach. *Nat Commun*. 2014;5. doi:10.1038/ncomms5006

42. Guo Y, Hao Z, Zhao S, Gong J, Yang F. Artificial intelligence in health care: Bibliometric analysis. *J Med Internet Res*. 2020;22(7). doi:10.2196/18228

43. McCarthy J, Minsky ML, Rochester N, Shannon CE. *A Proposal for the Dartmouth Summer Research Project on Artificial Intelligence*.; 2006. doi:10.1609/aimag.v27i4.1904

44. Schwendicke F, Samek W, Krois J. Artificial Intelligence in Dentistry: Chances and Challenges. *J Dent Res*. 2020;99(7):769-774. doi:10.1177/0022034520915714

45. Speight P, Elliott A, Jullien J, Downer M, Zakzrewska J. The use of artificial intelligence to identify people at risk of oral cancer and precancer. *Br Dent J*. 1995;179:382-387. doi:10.1038/sj.bdj.4808932

46. Gormley M, Creaney G, Schache A, Ingarfield K, Conway DI. Reviewing the epidemiology of head and neck cancer: definitions, trends and risk factors. *Br Dent J*. 2022;233(9):780-786. doi:10.1038/s41415-022-5166-x

47. Leite AF, Vasconcelos K de F, Willems H, Jacobs R. Radiomics and Machine Learning in Oral Healthcare. *Proteomics Clin Appl*. 2020;14(3). doi:10.1002/prca.201900040

48. Rogers W, Seetha T, Refaee S, Lieverse TIY, Granzier RWY, Ibrahim R. *Radiomics: From Qualitative to Quantitative Imaging*. Vol 93.; 2020.

49. Ammirabile A, Mastroleo F, Marvaso G, et al. Mapping the research landscape of HPV-positive oropharyngeal cancer: a bibliometric analysis. *Crit Rev Oncol Hematol*. 2024;196. doi:10.1016/j.critrevonc.2024.104318

50. Lin H, Chen H, Weng L, Shao J, Lin J. Automatic detection of oral cancer in smartphone-based images using deep learning for early diagnosis. *J Biomed Opt*. 2021;26(08). doi:10.1117/1.jbo.26.8.086007

51. Uddin S, Khan A, Hossain ME, Moni MA. Comparing different supervised machine learning algorithms for disease prediction. *BMC Med Inform Decis Mak*. 2019;19(1). doi:10.1186/s12911-019-1004-8

52. Chinnery T, Arifin A, Tay KY, et al. Utilizing Artificial Intelligence for Head and Neck Cancer Outcomes Prediction From Imaging. *Canadian Association of Radiologists Journal*. 2021;72(1):73-85. doi:10.1177/0846537120942134

53. Bera K, Braman N, Gupta A, Velcheti V, Madabhushi A. Predicting cancer outcomes with radiomics and artificial intelligence in radiology. *Nat Rev Clin Oncol*. 2022;19(2):132-146. doi:10.1038/s41571-021-00560-7

54. Hoque SMH, Pirrone G, Matrone F, et al. Clinical Use of a Commercial Artificial Intelligence-Based Software for Autocontouring in Radiation Therapy: Geometric Performance and Dosimetric Impact. *Cancers (Basel)*. 2023;15(24). doi:10.3390/cancers15245735

55. Ahervo H, Korhonen J, Lim Wei Ming S, et al. Artificial intelligence-supported applications in head and neck cancer radiotherapy treatment planning and dose optimisation. *Radiography*. 2023;29(3):496-502. doi:10.1016/j.radi.2023.02.018

56. Broggi G, Maniaci A, Lentini M, et al. Artificial Intelligence in Head and Neck Cancer Diagnosis: A Comprehensive Review with Emphasis on Radiomics, Histopathological, and Molecular Applications. *Cancers (Basel)*. 2024;16(21). doi:10.3390/cancers16213623

57. Koo M, Lin SC. An analysis of reporting practices in the top 100 cited health and medicine-related bibliometric studies from 2019 to 2021 based on a proposed guidelines. *Heliyon*. 2023;9(6). doi:10.1016/j.heliyon.2023.e16780

## TABLES

Table I – Top 10 countries, affiliations, sources, and authors by number of documents.

| Rank | Country | ND | Affiliation | ND | Source | ND | Author | ND | TC |
|---|---|---|---|---|---|---|---|---|---|
| 1 | **USA** | 352 | **Helmholtz Association** (Germany) | 131 | **Medical Physics** (IF: 3.8) | 54 | **Wang, Y** | 28 | 73 |
| 2 | **China** | 188 | **Univ Texas System** (USA) | 114 | **Cancers** (IF: 5.2) | 46 | **Fuller, C** | 27 | 88 |
| 3 | **India** | 112 | **Emory University** (USA) | 90 | **Radiotherapy and Oncology** (IF: 5.7) | 36 | **Mohamed, A** | 25 | 73 |
| 4 | **England** | 77 | **German Cancer Research Center** (Germany) | 82 | **Frontiers in Oncology** (IF: 4.7) | 32 | **Wang, X** | 24 | 118 |
| 5 | **Netherlands** | 70 | **University of Texas Southwestern Medical Center Dallas** (USA) | 67 | **International Journal of Radiation Oncology Biology Physics** (IF: 7.0) | 30 | **Wang, J** | 20 | 56 |
| 6 | **Germany** | 67 | **University of Toronto** (Canada) | 67 | **Scientific Reports** (IF: 4.6) | 28 | **Li, J** | 19 | 32 |
| 7 | **Canada** | 65 | **Dresden University of Technology** (Germany) | 63 | **Oral Oncology** (IF: 4.8) | 24 | **Li, Y** | 17 | 32 |
| 8 | **Italy** | 55 | **University of Helsinki** (Finland) | 59 | **Head and Neck-Journal for the Sciences and Specialties of the Head and Neck** (IF: 2.9) | 20 | **Liu, Y** | 17 | 76 |
| 9 | **Japan** | 46 | **Harvard University** (USA) | 58 | **Physics in Medicine and Biology** (IF: 3.5) | 19 | **Wang, H** | 17 | 61 |
| 10 | **South Korea** | 44 | **UTMD Anderson Cancer Center** (USA) | 57 | **Diagnostics** (IF: 3.6) | 17 | **Fei, B** | 16 | 85 |

IF: Impact Factor; ND: Number of Documents; TC: Total Citations.

Table II – The 10 most cited documents.

| Rank | Author, Year | Title | Source | Nationality of the corresponding author | Study type | TC | TC per year |
|---|---|---|---|---|---|---|---|
| 1 | Zhu et al., 2018 | **AnatomyNet: Deep learning for fast and fully automated whole-volume segmentation of head and neck anatomy** | Medical Physics (IF: 3.8) | USA | Article | 309 | 51.50 |
| 2 | Parmar et al., 2015 | **Radiomic Machine-Learning Classifiers for Prognostic Biomarkers of Head and Neck Cancer** | Frontiers in Oncology (IF: 4.7) | USA | Article | 260 | 26.00 |
| 3 | Fan et al., 2019 | **Automatic treatment planning based on three-dimensional dose distribution predicted from deep learning technique** | Medical Physics (IF: 3.8) | China | Article | 204 | 34.00 |
| 4 | Gerds et al., 2008 | **The Performance of Risk Prediction Models** | Biometrical Journal (IF: 1.7) | Denmark | Review | 197 | 11.59 |
| 5 | Nguyen et al., 2019 | **3D radiotherapy dose prediction on head and neck cancer patients with a hierarchically densely connected U-net deep learning architecture** | Physics in Medicine and Biology (IF:3.5) | USA | Article | 178 | 29.67 |
| 6 | Le et al., 2003 | **Identification of osteopontin as a prognostic plasma marker for head and neck squamous cell carcinomas** | Clinical Cancer Research (IF: 11.5) | USA | Article | 178 | 8.09 |
| 7 | Kim et al., 2019 | **Deep learning-based survival prediction of oral cancer patients** | Scientific Reports (IF: 4.6) | South Korea | Article | 172 | 28.67 |
| 8 | Tong et al., 2018 | **Fully automatic multi-organ segmentation for head and neck cancer radiotherapy using shape representation model constrained fully convolutional neural networks** | Medical Physics (IF: 3.8) | USA | Article | 151 | 21.57 |
| 9 | Lajer et al., 2011 | **Different miRNA signatures of oral and pharyngeal squamous cell carcinomas: a prospective translational study** | British Journal of Cancer (IF: 8.8) | Denmark | Article | 149 | 10.64 |

| | | | | | | | |
|---|---|---|---|---|---|---|---|
| 10 | Leger et al., 2017 | **A comparative study of machine learning methods for time-to-event survival data for radiomics risk modelling** | Scientific Reports (IF: 4.6) | Germany | Article | 148 | 18.50 |

IF: Impact Factor; TC: Total Citations.

# APPENDIX

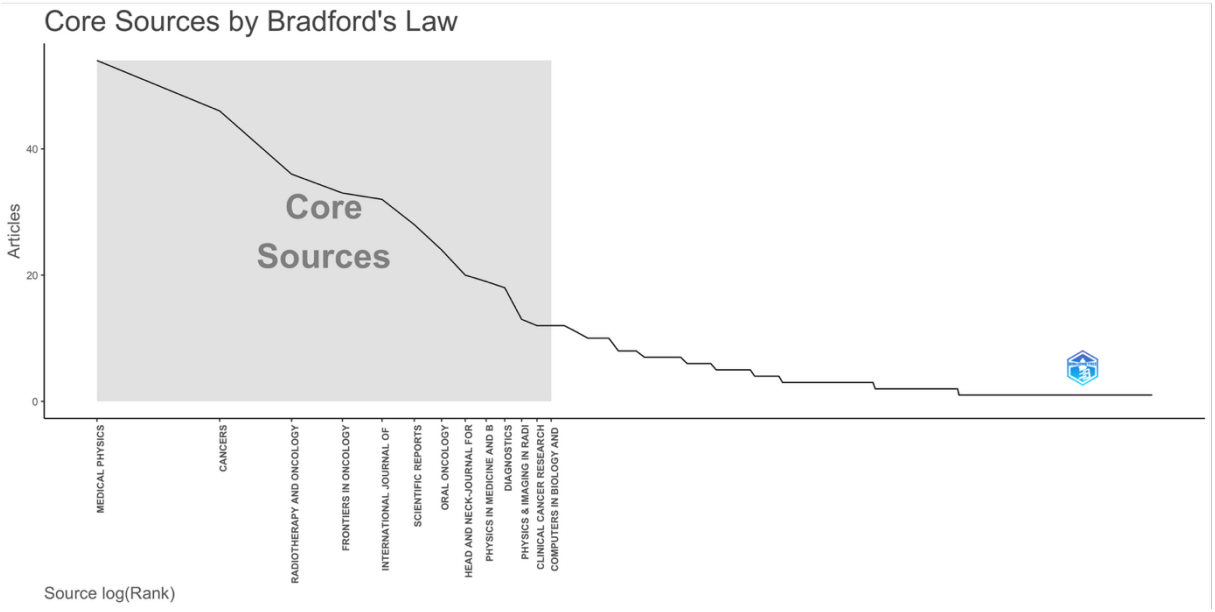


Supplementary Figure 1. Core sources by Bradford's Law

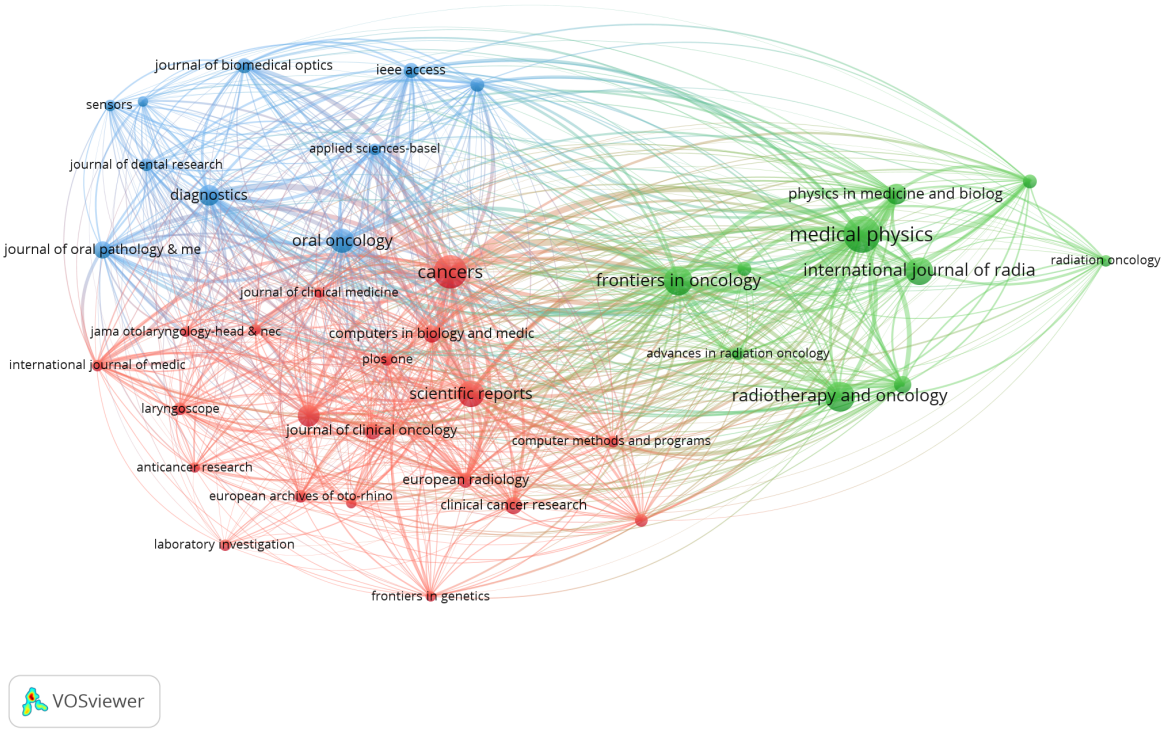


Supplementary Figure 2. Bibliographic coupling of sources. A minimum of five published documents were stablished. Of 387 terms, 40 met the threshold.

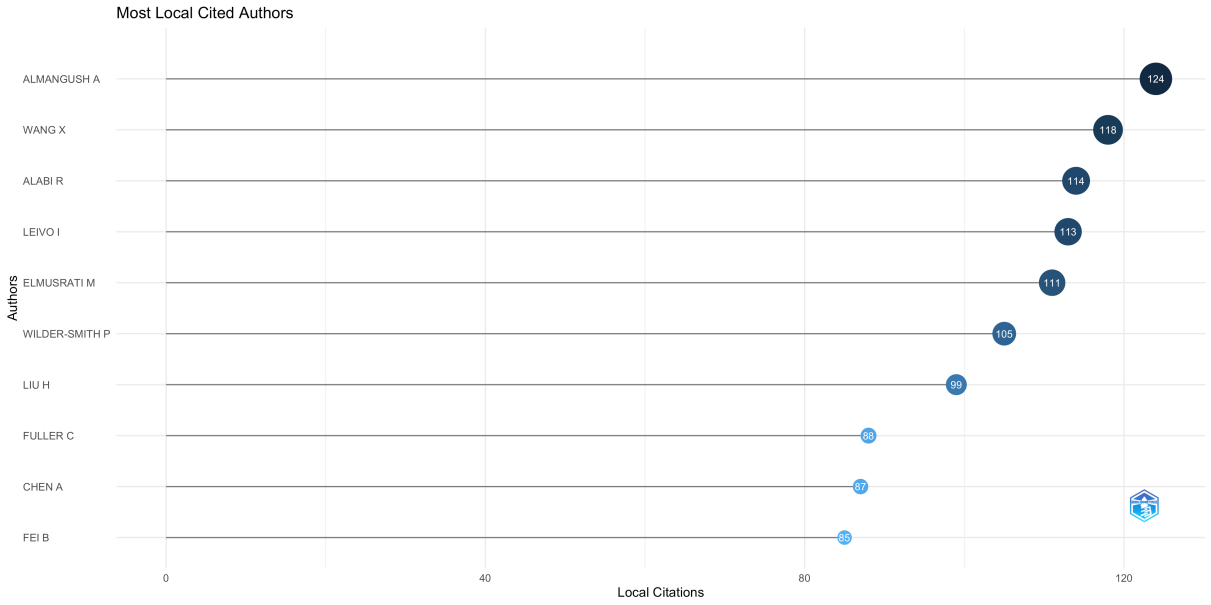


Supplementary Figure 3. The most cited authors.

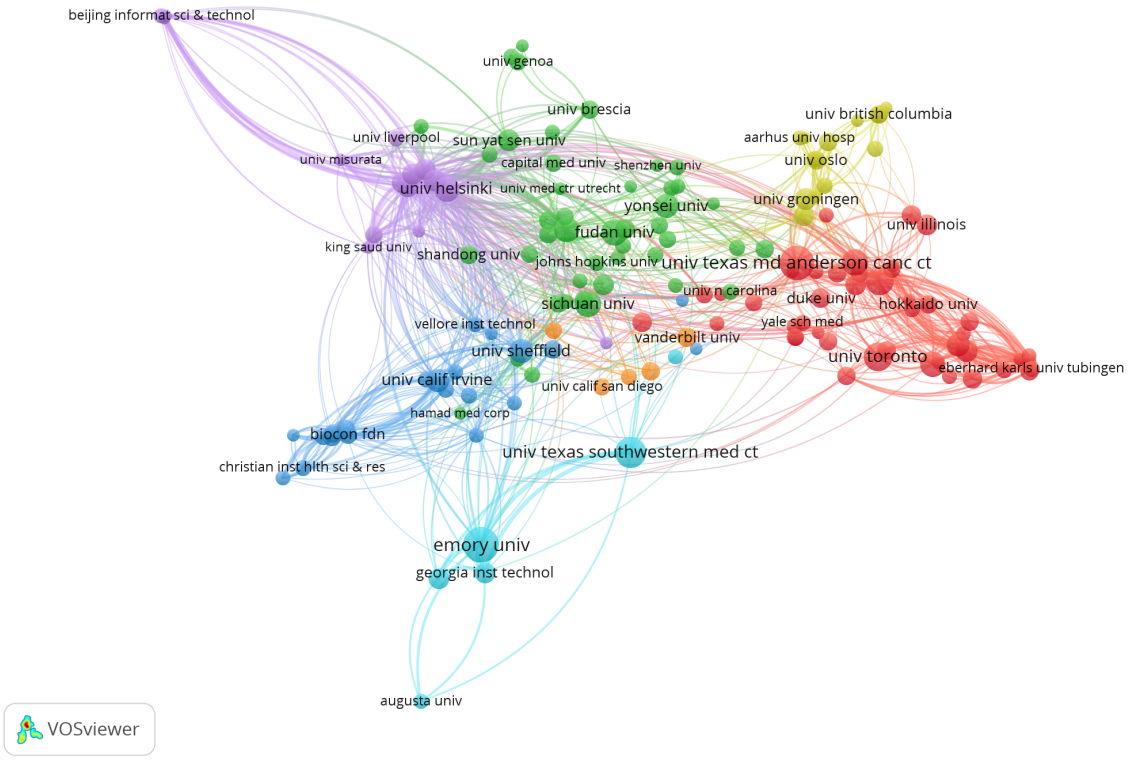


Supplementary Figure 4. Co-authorship of affiliations. Out of 1,505 affiliations, 51 published at least 20 articles.

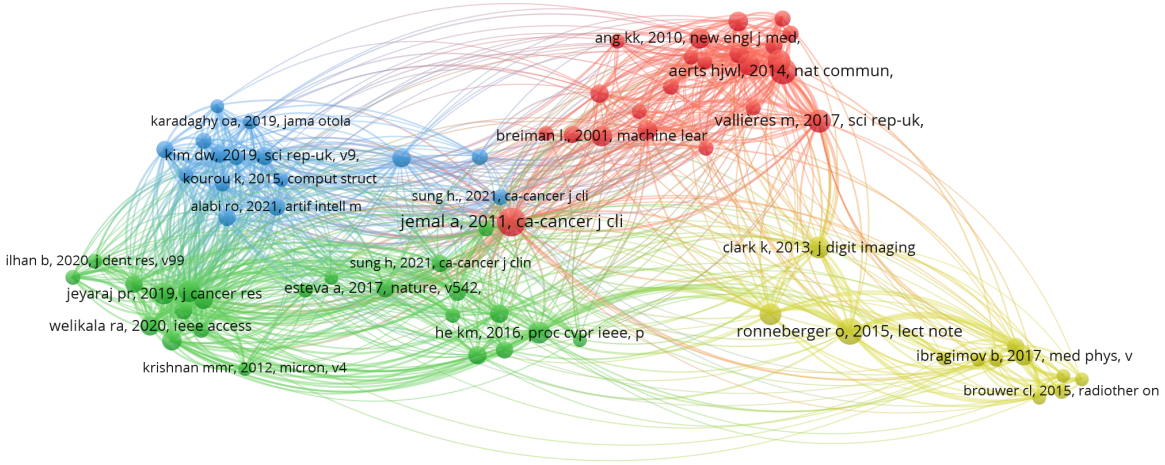


Supplementary Figure 5. Co-citation analysis of cited references. Out of 24,285 references, 25 were cited at least 35 times.

Supplementary Table 1 – The 50 most cited studies.

| Rank | Author/Year/Country | Specialty | EQUATOR Guidelines | Algorithm | Algorithm Application | Performance |
|---|---|---|---|---|---|---|
| 1 | Zhu et al., 2018 USA | Radiology | - | AnatomyNet | Automatic segmentation of organs-at-risk | The model can improve segmentation accuracy and simplify the auto segmentation pipeline |
| 2 | Parmar et al., 2015 USA | Radiology | - | BAG, BY, BST, DT, DA, GLM, MARS, NN, Nnet, PLSR, RF, SVM | Prediction of overall survival | Three feature selection methods minimum redundancy maximum relevance (AUC = 0.69, Stability = 0.66), mutual information feature selection (AUC = 0.66, Stability = 0.69), and conditional infomax feature extraction (AUC = 0.68, Stability = 0.7) had high prognostic performance and stability. The three classifiers BY (AUC = 0.67, RSD = 11.28), RF (AUC = 0.61, RSD = 7.36), and NN (AUC = 0.62, RSD = 10.52) also showed high prognostic performance and stability |
| 3 | Fan et al., 2019 China | Radiology | - | Residual Network (deep learning model) | Prediction of dose distribution in radiotherapy | Agreement between predictive plans and clinical plans, measured using clinical dose indices (D95%, Dmean, Dmax) and dose-volume histograms. |

| | | | | | | |
|---|---|---|---|---|---|---|
| | | | | | | Absolute differences between the predictive and manually optimized plans were insignificant for most clinical indices |
| 4 | Gerds et al., 2008<br>Germany | Statistics | - | LRM, CART, RF | Risk prediction models for medical decision-making and patient information | ROC AUC: RF 99.76%, LRM(4) 95.43%. Brier Score: RF 3.00, LRM(4) 8.28. Bootstrap Cross-Validation: RF AUC 91.68%, Brier Score 11.02, indicating optimistic apparent performance |
| 5 | Nguyen et al., 2019<br>USA | Oncology | - | HD U-net (deep learning-based, which combines the U-net and DenseNet architectures) | Prediction of dose distribution in radiotherapy | The proposed model achieved an average error of 6.3% for the maximum dose to organs at risk, an average error of 5.1% for the mean dose to organs at risk, 12 times fewer trainable parameters than the standard U-net model, dose prediction 4 times faster than the DenseNet model |
| 6 | Le et al., 2003<br>USA | Pathology | - | LDA | Identification of gene profiles associated with tumor hypoxia and prognosis | LDA model Accuracy: 81.6% |

| | | | | | | |
|---|---|---|---|---|---|---|
| 7 | Kim et al., 2019<br>South Korea | Oncology | - | DeepSurv (deep learning-based model, RSF, CPH | Prediction of overall survival | DeepSurv: Best performance with a C-index of 0.810 (training) and 0.781 (testing); RSF: C-index of 0.770 (training) and 0.764 (testing); CPH: C-index of 0.756 (training) and 0.694 (testing) |
| 8 | Tong et al., 2018<br>USA | Radiology | - | FCNN (based on the U-Net architecture), SRM | Automatic segmentation of organs-at-risk | Dice Similarity Coefficient: Brainstem (86.97%), Mandible (93.60%), Left Parotid (83.87%), among others. Positive Predictive Value and Sensitivity: Varied results but generally superior to FCNN without SRM |
| 9 | Lajer et al., 2011<br>Denmark | Pathology | - | SVM | Generation a diagnostic microRNA signature for OSCC and pharyngeal squamous cell carcinoma | Accuracy Rate: 93% in external validation; Sensitivity: 100%; Specificity: 86% |
| 10 | Leger et al., 2017<br>Germany | Radiology | - | The Cox model, the NET-Cox method with LASSO and elastic-net regularization; models based on BT: BT-Cox, BT-CIndex; BGLM: | Prediction of loco-regional tumor control and overall survival | Local-Regional Tumor Control: MSR-RF with Spearman feature selection (C-index: 0.71; 95% CI: [0.62–0.83]);<br>BT-CIndex (C-index: 0.71) and BT- |

| | | | | | | |
|---|---|---|---|---|---|---|
| | | | | BGLM-Cox, BGLM-CIndex; RF: RSF, MSR-RF; SR and models based on the Weibull distribution: BT- and BGLM-Weibull | | Weibull (C-index: 0.70); OS: BGLM-CIndex and BGLM-Weibull, both with a C-index of 0.64 |
| 11 | Almangush et al., 2020<br>Finland | Pathology | - | The article is a narrative review, discussing the application of machine learning and deep learning, but it does not test any algorithms | - | - |
| 12 | Jeyaraj and Samuel Nadar, 2019<br>India | Radiology | - | Regression-based deep CNN | Oral cancer detection | For the classification between malignant and benign tumors, accuracy: 91.4%, specificity: 94%, sensitivity: 91%; for the classification between malignant tumors and normal tissues: accuracy: 94.5%, specificity: 98%, sensitivity: 94% |
| 13 | Aubreville et al., 2017<br>Germany | Pathology/Radiology | - | CNN: PPF and TF | OSCC detection | PPF (CNN/ppf@0.5x): accuracy: 88.3%, sensitivity: 86.6%, specificity: 90.0%, AUC: 0.955; PPF (CNN/ppf@1.0x): accuracy: 88.3%, sensitivity: 86.6%, specificity: 90.0%, area Under the Curve (AUC): 0.96; TF (CNN/TF@0.55x): accuracy: 87.02%, sensitivity: |

| | | | | | | |
|---|---|---|---|---|---|---|
| | | | | | | 90.71%, specificity: 83.80%, AUC: 0.948 |
| 14 | Halicek et al., 2017 USA | Pathology/Radiology | - | CNN: TensorFlow | Application of deep learning for automatic tissue labeling in surgical specimens using hyperspectral imaging | Sensitivity 81%, specificity 78%, accuracy 80% |
| 15 | Diamant et al., 2019 Canada | Radiology | - | CNN | Prediction of treatment outcomes | When compared to a traditional radiomic framework: AUC of 0.88 in predicting distant metastasis. When combining the previous model: AUC of 0.92 |
| 16 | Carnielli et al., 2018 Brazil | Pathology | - | Not specified | Identification of peptide signatures in saliva predicting lymph node metastasis | Saliva-based prognostic signatures were evaluated to distinguish OSCC patients with (N+) and without (N0) lymph node metastasis. Best-performing peptide-level signature (S2): Accuracy: 82.8%, AUC: 82.8%. Best protein-level signature (S4): AUC: 73.9% |
| 17 | Da-ano et al., 2020 France | Radiology | - | Modified versions of the ComBat: M-ComBat, B- | Harmonization of radiomic features | For locally advanced cervical cancer: RF with BM-ComBat achieved 89% |

| | | | | | | |
|---|---|---|---|---|---|---|
| | | | | ComBat, BM-ComBat. Multivariate Regression with LASSO, RF, SVM | across multicenter datasets to improve the predictive power of clinical outcome models | balanced accuracy and MCC of 0.89; for locally advanced laryngeal cancer: RF with BM-ComBat reached 86% balanced accuracy and MCC of 0.59 |
| 18 | Kann et al., 2018 USA | Radiology | - | DLNN; Architecture variations tested: BoxNet, SmallNet, DualNet | Identification of nodal metastasis and tumor extranodal extension | Extranodal Extension Detection: AUC: 0.91 (95% CI: 0.85–0.97), accuracy: 85.7%, sensitivity: 88%, specificity: 85%, PPV: 66%, NPV: 95%; Nodal Metastasis Detection: AUC: 0.91 (95% CI: 0.86–0.96), accuracy: 85.5%, sensitivity: 84%, specificity: 87%, PPV: 88%, NPV: 82% |
| 19 | Shaban et al., 2019 United Kingdom | Pathology | - | CNN: ResNet50, DenseNet, Inception-v3, Xception, and MobileNet | Objective quantification of tumor infiltrating lymphocytes | Tissue Classification (TRC-5, MobileNet): accuracy: 96.31%, sensitivity: 92.66%, specificity: 97.55%, F1-Score: 92.62%, AUC: 98.91% |
| 20 | Zhang et al., 2019 China | Pathology | - | CNN: ResNet34 | Automated diagnosis of laryngeal squamous cell carcinoma | 100% accuracy, AUC: 0.95, Validation accuracy: 95.9% (5-fold cross-validation), Cohen's kappa > 0.90 |

| | | | | | | |
|---|---|---|---|---|---|---|
| 21 | Cardenas et al., 2018<br>USA | Radiology | - | Deep Auto-Encoders (A deep learning model) | Automated delineation of clinical target volumes | DSC: Median DSC of 0.81 (range: 0.62–0.90) compared with physician-delineated volumes. MSD: Median value of 2.8 mm (range: 1.6–5.5 mm) |
| 22 | Winck et al., 2015<br>Brazil | Pathology | - | SVM | Proteomics-based classification of OSCC using salivary proteome analysis | Precision: 92.5%, recall (Sensitivity): 90%, AUC: 92.9%, Kappa Value: 0.78 |
| 23 | Luo et al., 2020<br>USA | Immunology | - | FARDEEP | Profiling HPV16 E7-induced immune evasion mechanisms via STING pathway | FARDEEP proved robust against outliers in RNA-Seq datasets and enabled the quantification of various immune cell types in the tumor microenvironment |
| 24 | Ariji et al., 2019<br>Japan | Radiology | - | CNN: AlexNet | Diagnosis of lymph node metastasis | Accuracy: 78.2%, sensitivity: 75.4%, specificity: 81.0%, PPV: 79.9%, NPV: 77.1%, AUC: 0.80 |
| 25 | Gabryś et al., 2018<br>Germany | Radiology | - | LRM (L1, L2, and Elastic Net penalties), SVM, kNN, ET, GTB | Xerostomia risk assessment | Generalization AUCs:<br>Early xerostomia (0–6 months): best performance by kNN (AUC: 0.65); late xerostomia: best performance by GTB (AUC: 0.65) long-term xerostomia: best performance by ET (AUC: 0.88). |

| | | | | | | |
|---|---|---|---|---|---|---|
| | | | | | | Longitudinal models: best performance by GTB (AUC: 0.63) |
| 26 | Chakravarthy et al., 2016<br>United Kingdom | Pathology | - | k-NN and RF | Prediction of HPV in HNC | Gene Expression Classifiers: RF: Kappa value = 0.96; k-NN: Kappa value = 0.94. Methylation Classifiers: RF: Kappa value = 0.92, k-NN: Kappa value = 0.93 |
| 27 | Chang et al., 2013<br>Malaysia | Pathology | - | ANFIS, ANN, SVM and LRM | Prediction of oral cancer prognosis | Best Model: ReliefF-GA-ANFIS using 3 input features: Drink, Invasion, and p63 (accuracy: 93.81%, AUC: 0.90). Second best: ReliefF-GA-ANN model (84.62% accuracy, AUC: 0.83) |
| 28 | Zlotogorski-Hurvitz et al., 2019<br>Israel | Pathology | - | PCA–LDA and SVM | To determine the Fourier-transform infrared spectra of salivary exosomes from oral cancer patients and healthy individuals and to assess its diagnostic potential using computational-aided models | PCA–LDA: 100% sensitivity, 89% specificity, 95% accuracy; SVM: 100% training accuracy, 89% cross-validation accuracy |

| | | | | | | |
|---|---|---|---|---|---|---|
| 29 | Fei et al., 2017 USA | Surgical Oncology | - | ELDA | Cancer diagnosis | Oral Cavity Tissue: 90% ± 8% accuracy, 89% ± 9% sensitivity, 91% ± 6% specificity; Thyroid Tissue: 94% ± 6% accuracy, 94% ± 6% sensitivity, 95% ± 6% specificity |
| 30 | Ziober et al., 2006 USA | Pathology | - | SVM | Cancer diagnosis | Cross-validation accuracy: 96% using the 25-gene predictor set; Independent validation sets: Penn dataset: 87% accuracy; RO dataset: 86% accuracy; GSE1722 dataset: 89% accuracy. The predictor demonstrated 100% specificity only to oral tumors |
| 31 | D'Souza et al., 2010 USA | Epidemiology | - | DT and SVM | Prediction of HPV in HNC | For demographic data only: PPV: 75%, NPV: 68%; for all HNSCC, PPV: 79–83%, NPV: 74–85%. For oropharyngeal cancer, PPV: 59–60%., NPV: 71–77% |
| 32 | Song et al., 2020 China | Pathology | REMARK | LASSO | Real-time diagnosis of OSCC using saliva metabolomics and conductive polymer | Training set: 95.3% accuracy. Validation set (external): 86.7% accuracy. AUC for classifications: OSCC vs. premalignant lesions: 0.917; OSCC vs. healthy controls: 0.992 |

| | | | | | | |
|---|---|---|---|---|---|---|
| | | | | | spray ionization mass spectrometry. | |
| 33 | Kann et al., 2019 USA | Radiology | TRIPOD | 3D CNN: DualNet | Identification of extranodal extension on pretreatment imaging for HNC | For the Mount Sinai Validation Dataset, AUC of 0.84, accuracy of 83.1%, sensitivity of 71%, and specificity of 85%. For The Cancer Genome Atlas Validation Dataset, AUC of 0.90, accuracy of 88.6%, sensitivity of 82%, and specificity of 91% |
| 34 | Vrtovec et al., 2020 Slovenia | Radiology | - | U-Net, DeepMedic and variants for 3D CNN-based segmentation | Identification of target volumes and organs at risk in head and neck radiotherapy | The review highlights various deep learning architectures applied to organ-at-risk auto-segmentation |
| 35 | Lu et al., 2017 USA | Radiology | - | ELDA, SVM and RF | Cancer diagnosis | Hyperspectral Imaging for distinguishing tumor vs. normal tissue: for oral cavity, accuracy: 89%, sensitivity: 90%, specificity: 90%, AUC: 0.95; for larynx and pharynx, accuracy: 94%, sensitivity: 95%, specificity: 90%, AUC: 0.97; for thyroid, accuracy: 92%, sensitivity: 92%, specificity: 94%, AUC: 0.96 |

| | | | | | | |
|---|---|---|---|---|---|---|
| 36 | Giraud et al., 2019 France | Radiology | PRISMA | SVM, RF, ANN and LRM | Prediction of treatment outcomes | - |
| 37 | Onken et al., 2014 USA | Genomics | - | NGS, Weighted Voting Classifier, GSEA, SVM | Identification of metastasis-associated signatures in oral squamous cell carcinoma | SVM-Based Clinical Assay: 93.5% accuracy |
| 38 | Bur et al., 2019 USA | Pathology | - | Decision Forest, GBM, Kernel SVM and LRM | Prediction of occult nodal metastasis | Decision Forest: AUC = 0.840, Sensitivity = 91.7%, Specificity = 57.6%; GBM: AUC = 0.798; Kernel SVM: AUC = 0.776. Tumor DOI Model: AUC = 0.657, Sensitivity = 75%, Specificity = 45.8% |
| 39 | Kosmin et al., 2019 United Kingdom | Radiology | - | AnatomyNet and CNN | Automatic segmentation of organs-at-risk | The study reviews the transition from atlas-based auto-segmentation to deep learning-based models |
| 40 | Welikala et al., 2020 United Kingdom | Radiology | - | ResNet-101 and Faster R-CNN | Automated detection and classification of oral lesions for the early detection of oral cancer | Image classification achieved an F1 score of 87.07% for identification of images that contained lesions and 78.30% for the identification of images that required referral. Object detection achieved an F1 score of 41.18% for |

| | | | | | | |
|---|---|---|---|---|---|---|
| | | | | | | the detection of lesions that required referral |
| 41 | (Li et al., 2019) China | Oncology | - | Poisson LASSO Regression Model and RF | Prediction and classification of quality assurance results for volumetric modulated arc therapy plans | Using 90% as the action limit at 3%/2 mm gamma criteria, Poisson LASSO: Specificity: 97.5%, Sensitivity: 31.6%; RF: Specificity: 87.7%, Sensitivity: 100% |
| 42 | Jurmeister et al., 2019 Germany | Pathology | - | ANN, SVM and RF | Differentiation between pulmonary metastases and primary lung cancers | For validation cohort, ANN (Accuracy = 96.4%, AUC = 0.9934), SVM (Accuracy = 95.7%, AUC = 0.9915), RF (Accuracy = 87.8%, AUC = 0.9708); for independent clinical cohort, ANN (Accuracy = 98.0%, AUC = 1.0), SVM (Accuracy = 96.1%, AUC = 1.0), RF (Accuracy = 84.3%, AUC = 0.976) |
| 43 | Babier et al., 2020 Canada | Radiology | - | GAN | Development of a knowledge-based automated planning pipeline for predicting treatment plans | The best performing knowledge-based automated planning plans were generated using predictions from the 3D GAN model that were multiplicatively scaled. These plans satisfied 77% of all clinical criteria, |

| | | | | | | |
|---|---|---|---|---|---|---|
| | | | | | | compared to the clinical plans, which satisfied 67% of all criteria |
| 44 | van der Veen et al., 2019<br>Belgium | Radiology | - | 3D CNN | Automatic segmentation of organs-at-risk | The network achieved an accuracy of 90% and 84% DSC averaged over all organs at risk for radiation oncologists 1 and 2 respectively, with an average symmetric surface distance of 0.7 and 1.5 mm, which was in 93% and 73% of the cases lower than the interobserver variability |
| 45 | Fu et al., 2020<br>China | Pathology | STROBE | CNN | OSCC detection from photographic images | On the clinical validation dataset, the algorithm achieved comparable performance to that of the average oral cancer expert in terms of accuracy (92.3% vs 92.4%, sensitivity (91.0% vs 91.7%), and specificity (93.5% vs 93.1%) |
| 46 | Jethanandani et al., 2018<br>USA | Radiology | PRISMA | SVM, LDA, LASSO Regression and RF | - | - |
| 47 | M. D. Anderson Cancer Center Head and Neck Quantitative Imaging Working Group, 2018 | Radiology | - | DT-Based Classifier and Multivariable Cox Proportional Hazards Model | Radiomic signatures for local recurrence using | Radiomic Signature Composition derived from Intensity Direct Local Range Max and Neighbor Intensity Difference 2.5 Complexity. Kaplan- |

| | | | | | | |
|---|---|---|---|---|---|---|
| | USA | | | | primary tumor texture analysis | Meier Analysis: Patients with favorable radiomic signatures had a 5-year local control rate of 94%; those with unfavorable signatures had 5-year local control rate between 62% and 80% |
| 48 | Forghani et al., 2019 Canada | Pathology | - | RF | Prediction of cervical lymph node metastasis | Multi-energy texture analysis models: accuracy: up to 88%; sensitivity: 100%; specificity: 67%, PPV: 83%, NPV: 100%; single-energy (65 keV) texture analysis: accuracy of 60-63% |
| 49 | Song et al., 2018 USA | Oncology | - | CNN | Automatic classification of smartphone-based oral dysplasia and malignancy images | Accuracy: 86.9%; sensitivity: 85.0%; specificity: 88.7% |
| 50 | Das et al., 2020 India | Pathology | - | CNN (AlexNet, VGG-16, VGG-19 and ResNet-50) and proposed custom CNN Model | Multi-class grading of OSCC from biopsy images | Pre-trained Models: ResNet-50: Accuracy = 92.15%; VGG-19: Accuracy = 84.67%; VGG-16: Accuracy = 77.89%; AlexNet: Accuracy = 72.17%; for the proposed CNN Model, the accuracy was 97.5%, precision was 97.14% and recall 93.67% |

AUC – area under the curve; BAG – bagging; BGLM – boosting gradient linear models; BT – boosting trees; BY – Bayesian; CART – classification and regression trees; CPH – Cox proportional hazard; CNN – convolutional neural networks; DA – discriminant analysis; DSC – Dice similarity coefficient; DLNN – deep learning neural networks; DT – decision trees; ELDA – ensemble linear discriminant analysis; ET – extra trees; FARDEEP – fast and robust deconvolution of tumor-infiltrating lymphocytes; FCNN – fully convolutional neural networks; GA – genetic algorithm; GAN – generative adversarial network; GBM – gradient boosting machine; GLM – generalized linear models; GSEA – gene set enrichment analysis; GTB – gradient tree boosting; HD U-Net – hierarchically densely connected U-Net; kNN – k-nearest neighbors; LASSO – least absolute shrinkage and selection operator; LDA – linear discriminant analysis; LRM – logistic regression models; MCC – Matthews correlation coefficient; MARS – multiple adaptive regression splines; MSD – mean surface distance; MSR-RF – random forest using maximally selected rank statistics; NGS – next-generation sequencing; NN – nearest neighbors; Nnet – neural networks; NPV – negative predictive value; OS – overall survival; OSCC – oral squamous cell carcinoma; PCA-LDA – principal component analysis / linear discriminant analysis; PLSR – principal component regression; PPF – patch-probability fusion; PPV – positive predictive value; PRISMA – Preferred Reporting Items for Systematic Reviews and Meta-Analyses; REMARK – Reporting Recommendations for Tumor Marker Prognostic Studies; ResNet – residual network; RF – random forests; ROC – receiver operating characteristic; RSD – relative standard deviation; RSF – random survival forest; SR – survival regression; SRM – shape representation model; STROBE – Strengthening the Reporting of Observational Studies in Epidemiology; SVM – support vector machines; TF – transfer learning; TRIPOD – Transparent Reporting of a Multivariable Prediction Model for Individual Prognosis or Diagnosis.

Supplementary Table 2 – Ranking of studies that reported accuracy in the 50 most cited papers for cancer diagnostic (N=9 studies) and cancer metastasis outcomes (N=4 studies).

| **Outcome** | | **Diagnosis** | | | **Metastasis** | |
|---|---|---|---|---|---|---|
| **Rank** | **Study** | **Algorithm** | **Accuracy (%)** | **Study** | **Algorithm** | **Accuracy (%)** |
| 1 | Ziober et al., 2006 USA | SVM | 96 | Onken et al., 2014 USA | NGS, Weighted Voting Classifier, GSEA, SVM | 93.5 |
| 2 | Zhang et al., 2019 China | CNN: ResNet34 | 95.9 | Kann et al., 2018 USA | DLNN | 85.7 |
| 3 | Lu et al., 2017 USA | ELDA | 94 | Carnielli et al., 2018 Brazil | Not specified | 82.8 |
| 4 | Fu et al., 2020 China | CNN | 92.4 | Ariji et al., 2019 Japan | CNN: AlexNet | 78.2 |
| 5 | Jeyaraj and Nadar et al., 2019 | Regression-based deep CNN | 91.4 | | | |

| | | | |
|---|---|---|---|
| | India | | |
| 6 | Fei et al., 2017<br>USA | ELDA | 90 |
| 7 | Aubreville et al., 2017<br>Germany | CNN: PPF | 88.3 |
| 8 | Song et al., 2018<br>USA | CNN: VGG-CNN-M | 86.9 |
| 9 | Song et al., 2020<br>China | LASSO Regression | 86.7 |

CNN – convolutional neural networks; DLNN – deep learning neural networks; ELDA – ensemble linear discriminant analysis; GSEA – gene set enrichment analysis; LASSO – least absolute shrinkage and selection operator; NGS – next-generation sequencing; PPF – patch-probability fusion; SVM – support vector machine.

Supplementary Table 3 – Ranking of the algorithm performances reported by accuracy in the 50 most cited papers.

| Rank | Study | Algorithm | Application | Accuracy (%) |
|---|---|---|---|---|
| 1 | Jurmeister et al., 2019<br>Germany | ANN | Differentiation between pulmonary metastases and primary lung cancers | 98 |
| 2 | Das et al., 2020<br>India | Proposed Custom CNN Model | Multi-class grading of OSCC from biopsy images | 97.5 |
| 3 | Shaban et al., 2019<br>United Kingdom | CNN: MobileNet | Objective quantification of tumor infiltrating lymphocytes | 96.31 |
| 4 | Ziober et al., 2006<br>USA | SVM | Cancer diagnosis | 96 |

| | | | | |
|---|---|---|---|---|
| 5 | Zhang et al., 2019 China | CNN: ResNet34 | Automated diagnosis of laryngeal squamous cell carcinoma | 95.9 |
| 6 | ZlotogorskiHurvitz et al., 2019 Israel | PCA–LDA | To determine the Fourier-transform infrared spectra of salivary exosomes from oral cancer patients and healthy individuals and to assess its diagnostic potential using computational-aided models | 95 |
| 7 | Lu et al., 2017 USA | ELDA | For larynx and pharynx cancer diagnosis | 94 |
| 8 | Chang et al., 2013 Malaysia | ReliefF-GA | Prediction of oral cancer prognosis | 93.81 |
| 9 | Onken et al., 2014 USA | SVM | Identification of metastasis-associated signatures in OSCC | 93.5 |
| 10 | Lajer et al., 2011 Denmark | SVM | Generation a diagnostic microRNA signature for OSCC and pharyngeal squamous cell carcinoma | 93 |
| 11 | Fu et al., 2020 China | Cascaded CNN | OSCC detection from photographic images | 92.4 |
| 12 | Jeyaraj and Nadar et al., 2019 India | Regression-based deep CNN | Oral cancer detection | 91.4 |
| 13 | Fei et al., 2017 USA | ELDA | Cancer diagnosis | 90 |
| 14 | Van der Veen et al., 2019 Belgium | 3D CNN | Automatic segmentation of organs-at-risk | 90 |
| 15 | Da-ano et al., 2020 | RF | Harmonization of radiomic features across multicenter | 89 |

| | | | | |
|---|---|---|---|---|
| | France | | datasets to improve the predictive power of clinical outcome models | |
| 16 | Kann et al., 2019 USA | CNN: DualNet | Identification of extranodal extension on pretreatment imaging for HNC | 88.6 |
| 17 | Aubreville et al., 2017 Germany | CNN: PPF | OSCC detection | 88.3 |
| 18 | Forghani et al., 2019 Canada | RF | Prediction of cervical lymph node metastasis | 88 |
| 19 | Song et al., 2018 USA | CNN: VGG-CNN-M | Automatic classification of smartphone-based oral dysplasia and malignancy images | 86.9 |
| 20 | Song et al., 2020 China | LASSO Regression | Real-time diagnosis of OSCC using saliva metabolomics and conductive polymer spray ionization mass spectrometry. | 86.7 |
| 21 | Kann et al., 2018 USA | DLNN | Identifcation of nodal metastasis and tumor extranodal extension | 85.7 |
| 22 | Carnielli et al., 2018 Brazil | Not specified | Identification of peptide signatures in saliva predicting lymph node metastasis | 82.8 |
| 23 | Le et al., 2003 USA | LDA | Identification of gene profiles associated with tumor hypoxia and prognosis | 81.6 |

| | | | | |
|---|---|---|---|---|
| 24 | Halicek et al., 2017 USA | CNN: TensorFlow | Application of deep learning for automatic tissue labeling in surgical specimens using hyperspectral imaging | 80 |

ANN – artificial neural networks; CNN – convolutional neural networks; DLNN – deep learning neural networks; ELDA – ensemble linear discriminant analysis; GA – genetic algorithm; LASSO – least absolute shrinkage and selection operator; LDA – linear discriminant analysis; OSCC – oral squamous cell carcinoma; PCA-LDA – principal component analysis – linear discriminant analysis; PPF – patch-probability fusion; RF – random forest; SVM – support vector machine.

## CAPÍTULO 2

Intended submission: Dentomaxillofacial Radiology (IF: 4.1)

https://academic.oup.com/dmfr

### Fractal and radiomorphometric analysis in CBCT scans of post-radiotherapy head and neck cancer patients

## ABSTRACT

**Introduction:** Head and neck cancer often requires radiotherapy (RT), which can induce bone alterations and osteoradionecrosis. Fractal dimension (FD) analysis and radiomorphometric indices provide quantitative assessment of mandibular bone microarchitecture. This study aimed to evaluate cortical and trabecular mandibular bone in post-RT patients compared with matched non-irradiated controls. **Methods:** Cone-Beam Computed Tomography scans of the mandible were analyzed to obtain the Computed Tomography Mandibular Index (CTMI), the Computed Tomography Cortical Index (CTCI), and FD values. Measurements were performed in predefined regions of interest that captured both trabecular and cortical compartments. Statistical analyses included ICC for reliability, t-tests, Mann–Whitney tests, Chi-square, ANOVA, and Kruskal–Wallis tests ($p<0.05$). **Results:** No significant differences were observed between post-RT and control groups for FD, CTMI, or CTCI ($p > 0.05$). Mean trabecular FD was 1.26 ± 0.14 in the post-RT group and 1.24 ± 0.11 in controls, while cortical FD was 0.92 ± 0.10 in both groups. Mean CTMI values were 3.68 ± 0.93 (post-RT) and 3.92 ± 0.83 (controls), and CTCI distribution did not differ between groups. Higher trabecular FD was observed in patients with laryngeal tumors compared with other sites (1.21 ± 0.16 vs. 1.33 ± 0.05; $p = 0.003$). **Conclusion:** While CBCT-based FD and radiomorphometric indices did not differ significantly between irradiated and control patients, variations related to tumor site and post-RT interval suggest heterogeneous bone responses. Individualized management and further research using volumetric and advanced imaging analyses are recommended for predicting RT-related bone complications. Therefore, a personalized approach to risk prediction and intervention should be adopted for each patient before dental procedures. **Advances in Knowledge:** To the best of our knowledge, this is the first study to combine FD analysis and radiomorphometric indices using CBCT scans to evaluate both cortical and trabecular mandibular bone in patients who underwent head and neck RT. The results highlight the potential of CBCT-based quantitative assessments for early detection of radiation-induced bone changes.

## KEYWORDS

Head and neck cancer; radiotherapy; cone-beam computed tomography; fractal dimension; radiomorphometric indices.

## INTRODUCTION

Head and neck cancer (HNC) comprises a heterogeneous group of malignancies, predominantly represented by squamous cell carcinoma [1–3]. It can affect the lip, oral cavity, larynx, nasopharynx, oropharynx, hypopharynx, and salivary glands, accounting for approximately 950,000 new cases and over 480,000 deaths annually worldwide [4]. Radiotherapy (RT) plays a central role in treatment, being used in approximately 75% of cases, either alone or in combination with chemotherapy and surgical procedures [5,6].

RT aims to destroy rapidly dividing cells, resulting in tumor reduction, and can be employed as either a curative or palliative treatment modality [7]. Advances in irradiation have improved significantly in recent years, enabling more individualized treatment and more precise targeting of the tumor region through technologies such as Image-Guided Radiotherapy (IGRT) and Intensity-Modulated Radiotherapy (IMRT) [8]. However, due to the small, irregular anatomy of the head and neck region and the presence of numerous organs at risk (OAR), this treatment is still associated with several adverse effects, including xerostomia, dysphagia, mucositis, radiodermatitis, candidiasis, rampant dental caries, trismus, fatigue, osteoradionecrosis and others [8–11].

In bone tissue, radiation primarily affects the vascular supply, leading to a rapid reduction in osteoblasts and an increase in osteoclastic activity, resulting in decreased bone density, trabecular remodeling, and the replacement of active red marrow with yellow marrow [12,13]. Cortical and trabecular bone exhibit distinct biological and structural characteristics that may result in different responses to ionizing radiation. Trabecular bone is highly vascularized and metabolically active, with a greater surface area and higher bone turnover rate, making it potentially more sensitive to early radiation-induced alterations. In contrast, cortical bone is denser, less vascularized, and undergoes slower remodeling, and radiation-related changes in this compartment may manifest later or be less pronounced in cross-sectional imaging. These differences suggest that cortical and trabecular bone should be evaluated separately when investigating radiation-induced mandibular changes. Consequently, the morphology, strength, and microarchitecture of the bone are altered in irradiated regions [14].

The main undesirable clinical outcome at the bone level following RT is osteoradionecrosis (ORN), an iatrogenic condition observed in cancer patients who undergo radiation therapy in the head and neck region [15,16]. Recently, Castro et al. reported that ORN was observed in 7% of cases (95% CI: 4−10%) [17]. ORN is associated with risk factors such as poor oral hygiene and tooth extractions after RT and can progress to morbid states characterized by a high symptom burden and poor quality of life due to tooth loss, impaired orofacial function, and pain [15,16]. Therefore, the early identification of radiation-induced bone alterations may help prevent such outcomes.

Fractal dimension (FD), a mathematical method by which irregular and complex body structures may be evaluated, can be applied to assess such structures in dental images, allowing for the quantification of bone microarchitecture complexity [18]. These methods are frequently employed to identify bone alterations in patients with systemic disorders, serving as important tools for screening and enabling the early diagnosis of conditions that affect bone morphology [19–21].

Radiomorphometric indices are qualitative and quantitative image analysis methods widely used for the evaluation of imaging exams, such as panoramic radiographs [20]. Examples of these indices, such as Computed Tomography Cortical Index (CTCI) and Computed Tomography Mental Index (CTMI), which have been adapted for assessment using cone-beam computed tomography (CBCT), have proven to be useful tools for identifying bone alterations [22], particularly in the mandibular cortical region, a site potentially affected by RT [23].

Based on the known biological effects of ionizing radiation on bone tissue, we hypothesized that patients treated with head and neck radiotherapy would exhibit measurable alterations in mandibular cortical and trabecular bone when compared with matched non-irradiated controls. Specifically, we hypothesized that fractal dimension and radiomorphometric indices derived from CBCT images would differ between irradiated and control patients. Additionally, we hypothesized that these quantitative bone parameters would be influenced by tumor location, radiation dose delivered to the mandible, and the time elapsed since completion of radiotherapy.

Accordingly, this study aimed to assess mandibular cortical and trabecular bone in irradiated patients using CBCT-based fractal dimension and radiomorphometric indices and to compare the results with matched non-irradiated controls.

## METHODS

This study was approved by the Ethics Committee of the Faculty of Health Sciences, University of Brasília (protocol number 72787723.4.0000.0030). Informed consent was obtained from all participants. Recruited patients received a printed pamphlet containing all relevant information about the study and were given access to the research team for further contact in case additional clarification was needed.

### Study population - post-RT patients and matched-control group:

Post-RT patients were recruited from the High-Complexity Oncology Care Center at the University Hospital of Brasília. They underwent RT between 2019 and 2024. All patients received CBCT imaging at the Oral Care Center of the same hospital after completing their RT treatment. Data on tumor site, histopathologic diagnosis, smoking status, treatment, radiation therapy technique, time from RT to CBCT scan, and radiation dose were collected. These patients were matched with control individuals whose CBCT scans were available in the hospital database.

Patients were divided into two groups. Group 1 consisted of CBCT scans from post-RT patients who had completed treatment and showed no recurrent lesions at the time of examination. Group 2 consisted of non-oncologic patients without metabolic bone diseases and with noncontributory medical histories. Groups 1 and 2 were matched by nationality, sex, and age.

Patients in Group 1 received external beam irradiation performed using a medical linear accelerator (Clinac CX, Varian Medical Systems, Palo Alto, CA, USA), employing the three-dimensional conformal radiotherapy (3D-CRT) technique. RT planning was conducted using the Eclipse Planning System, version 13.6 (Varian Medical Systems, Palo Alto, CA, USA). The anterior region of the mandible was also segmented in this program to estimate the radiation dose delivered to the areas in

which the analyses were performed, which are described in detail subsequently. Fig. 1 illustrates the RT treatment planning, presenting heat-map dose distributions and a representative dose–volume histogram.

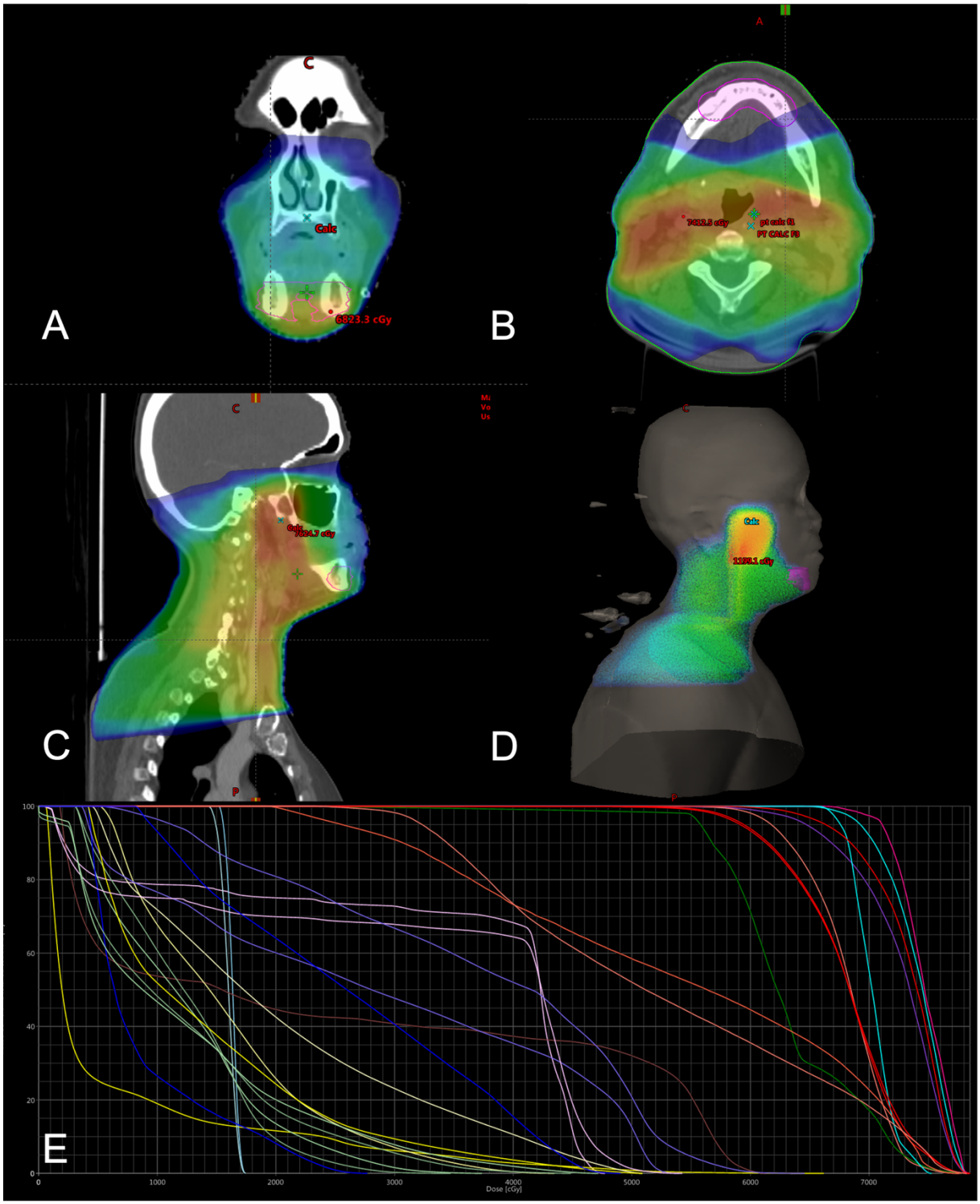


Figure 1. Heat-map dose distribution and a representative dose–volume histogram. (A) coronal computed tomography (CT) view; (B) axial CT view; (C) sagittal CT view; (D) three-dimensional reconstruction; and (E) dose–volume histogram.

CBCT scans were acquired using the i-CAT Classic system (Imaging Sciences International, Inc., PA, USA) by two calibrated dentists from the same institution, trained by the same oral and maxillofacial radiologist, following a standardized protocol. Images were obtained at 120 kVp and 37.07 mAs, with a voxel size of 0.2 mm and a typical exposure time of 26.9 seconds. Scans were excluded from the analysis if they presented artifacts, improper patient positioning, bone alterations in the regions of interest, absence of the target areas, or motion blur due to patient movement during acquisition.

For training purposes, two evaluators performed the measurements independently at two different time points, with a one-week washout interval, following a computer-generated randomized list of 10 CBCT scans. Both evaluators were blinded to the patients' case or control status, and anonymization was performed using the Clinical Trials Processor (CTP), provided by the Radiological Society of North America (RSNA) at http://mirc.rsna.org. After the training phase, one evaluator conducted the final measurements for all patients using the same computer (Lenovo 15.6″ Intel Core i5-7200U 8 GB RAM 1 TB HDD Windows 10 LED HD resolution 1366 × 768).

**The fractal dimension analysis – FD**

FD analysis was performed separately in trabecular and cortical regions of the mandible to capture potential compartment-specific responses to radiotherapy, reflecting differences in vascularization, metabolic activity, and remodeling dynamics between these bone types. Fig. 2 illustrates the Regions of Interest (ROIs) for bilateral mandibular trabecular (ROIs 1 and 2) and cortical (ROIs 3 and 4) FD analysis. The trabecular ROI was standardized as a 20×20-pixel square, while the cortical ROI was a 15×15-pixel square. To define the analysis area, the CBCT scans were loaded into the free and open-source software 3D Slicer (version 5.5.0) and displayed using multiplanar reconstruction (MPR), with axial, coronal, and sagittal views.

In the axial plane, the mental foramen was identified, and a line was drawn along the outer cortical surface of the mandible, tangent to the foramen. A perpendicular slice to this line was then selected. The corresponding images from the coronal view window, after slice preparation, were exported to the Fiji image processing package,

bundled with 64-bit Java for Windows (ImageJ v1.52n; National Institutes of Health, Bethesda, MD), along with the BoneJ plugin, which was used to calculate FD values using the box-counting method.

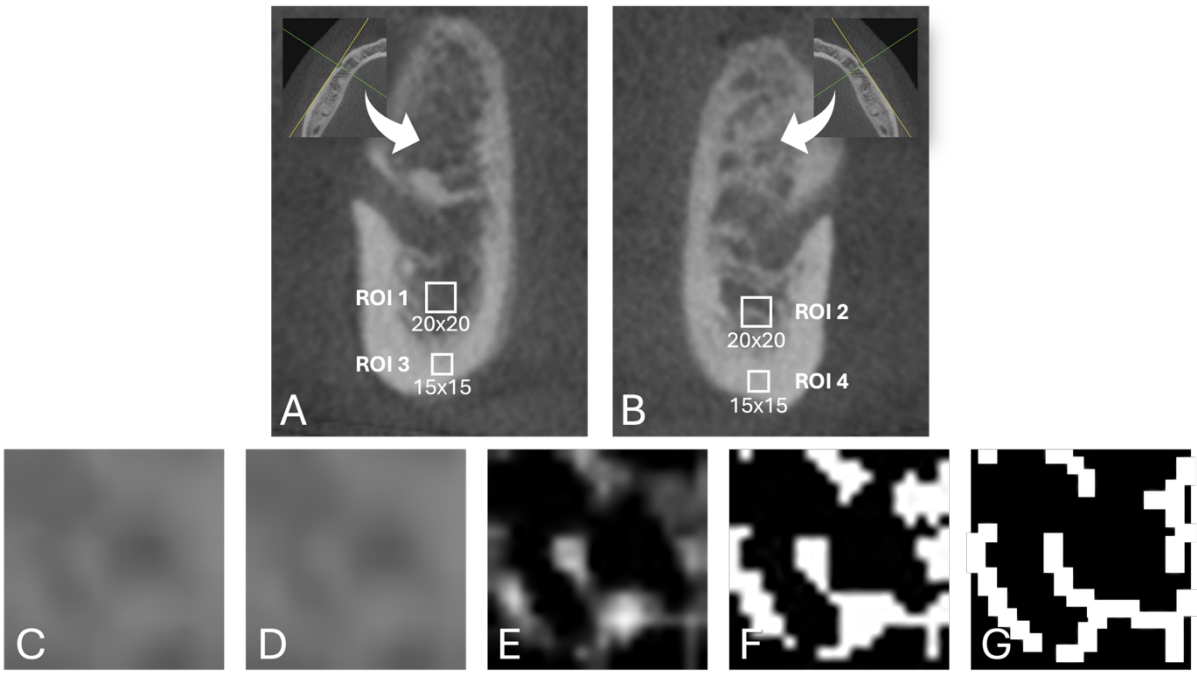


Figure 2. FD analysis. (A) right side analysis with ROI 1 (trabecular) and ROI 3 (cortical); (B) left side analysis with ROI 2 (trabecular) and ROI 4 (cortical); (C) crop; (D) gaussian Blur; (E) math; (F) threshold; (G) binary.

Image processing (Fig. 2) followed a methodology validated in previous studies, particularly those conducted by the same research group and based on the steps proposed by White and Rudolph [24].

**Computed Tomography Mental Index – CTMI**

CTMI was defined by Koh and Kim [22] according to Ledgerton et al. [25] as the thickness of the mandibular cortex in the region below the mental foramen, measured as the distance between the inner and outer cortical borders along a line perpendicular to two parallel reference planes established in the axial view. The tomographic slice selected for CTMI measurement was taken from the coronal view after the slice preparation described above (Fig. 3).

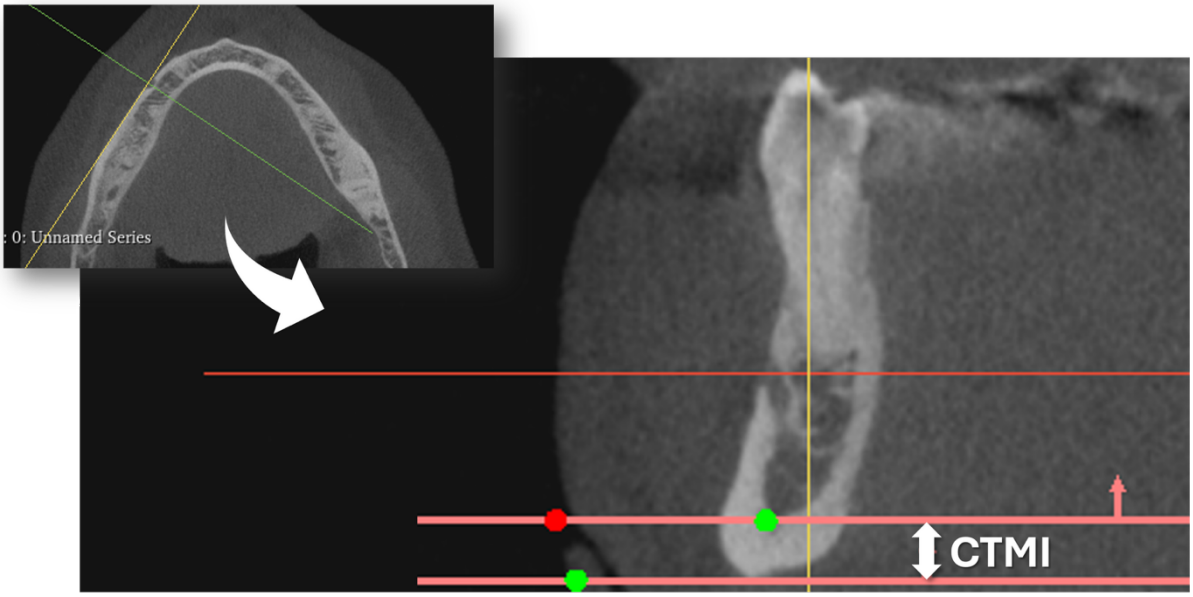


Figure 3. CTMI measurement procedure - distance between the inner and outer cortical borders at the mental foramen region.

**Computed Tomography Cortical Index - CTCI**

CTCI is an analysis by Koh and Kim [22] based on the Mandibular Cortical Index (MCI), in which the cortical bone in the region of the mental foramen, observed in the sagittal view, is classified according to the criteria proposed by Klemetti et al. [26] (Fig. 4):

- Type 1: The endosteal margin is even and sharp on both sides;
- Type 2: Semilunar defects, lacunar resorption, and endosteal residues are observed on one or both sides;
- Type 3: The endosteal margin is thin and porous, with heavy endosteal residues.

**Group 1 analysis**

Patients in Group 1 were divided into subgroups for analysis. According to the tumor site, the specific locations of the primary tumors were considered (larynx, nasopharynx, parotid gland, oropharynx, oral cavity, maxillary sinus, and submandibular gland). They were also divided, based on tumor location, into two major subgroups: patients with tumors in the head region (nasopharynx, parotid gland,

oropharynx, oral cavity, maxillary sinus, and submandibular gland) and those with tumors in the neck region (larynx). According to the maximum radiation dose to the anterior region of the mandible, patients were categorized into those who received <30 Gy and >30 Gy in this region. Regarding the mean dose to the anterior region of the mandible, they were divided into three groups: <10 Gy, 10–30 Gy, and >30 Gy. Lastly, they were categorized according to the interval between RT and CBCT, distinguishing those evaluated at <30 months and >30 months. FD and radiomorphometric indices were assessed within these contexts for intragroup comparison.

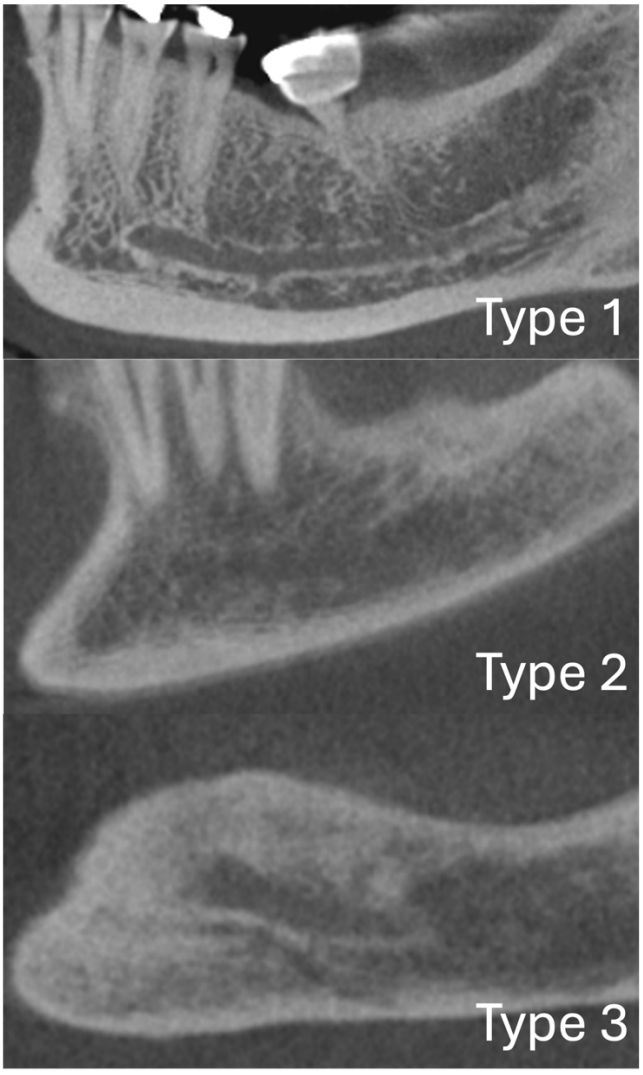


Figure 4. CTCI analysis. Type 1: The endosteal margin is even and sharp on both sides; type 2: Semilunar defects, lacunar resorption, and endosteal residues are observed on one or both sides; type 3: The endosteal margin is thin and porous, with heavy endosteal residues.

### Statistical analysis

A reliability test was conducted at two different time points for two evaluators, with a one-week washout interval during the training phase. The Intraclass Correlation Coefficient (ICC) was interpreted according to the guidelines of Portney and Watkins [27]. ROI outcomes were analyzed independently, and both left and right sides were assessed. Normality was assessed by the Shapiro–Wilk test. Age, CTMI and mean dose were compared between groups using the parametric Student's t-test. The number of teeth, FD values and maximum dose were compared between groups using the non-parametric Mann–Whitney U test. The Chi-square test was used to assess the distribution of CTCI classifications based on the observed and expected counts, assuming no association in the population. Tumor site groups and mean dose groups were evaluated for differences in CTMI and FD. One-way ANOVA was used for CTMI, while FD was analyzed with the Kruskal–Wallis test. A p-value $< 0.05$ was considered statistically significant. Statistical analyses were conducted using Jamovi software (version 2.6.44, The jamovi project, Sydney, Australia) and GraphPad Prism (version 10.6.1, GraphPad Software, San Diego, CA, USA).

## RESULTS

A total of 117 patients diagnosed with HNC who underwent RT between 2019 and 2024 were initially screened for eligibility. Several patients were excluded due to death, unavailability, relocation, refusal to participate, or inability to attend clinical appointments. Consequently, 26 patients consented to participate and underwent CBCT. Two participants were subsequently excluded due to the absence of target anatomical regions following surgical resection, resulting in a final study group of 24 irradiated patients (Group 1). For comparison, CBCT scans from 24 non-irradiated individuals were retrospectively selected from the institutional imaging database (Group 2). Therefore, the final analytical sample comprised 48 CBCT examinations. Fig. 5 illustrates the sample selection process.

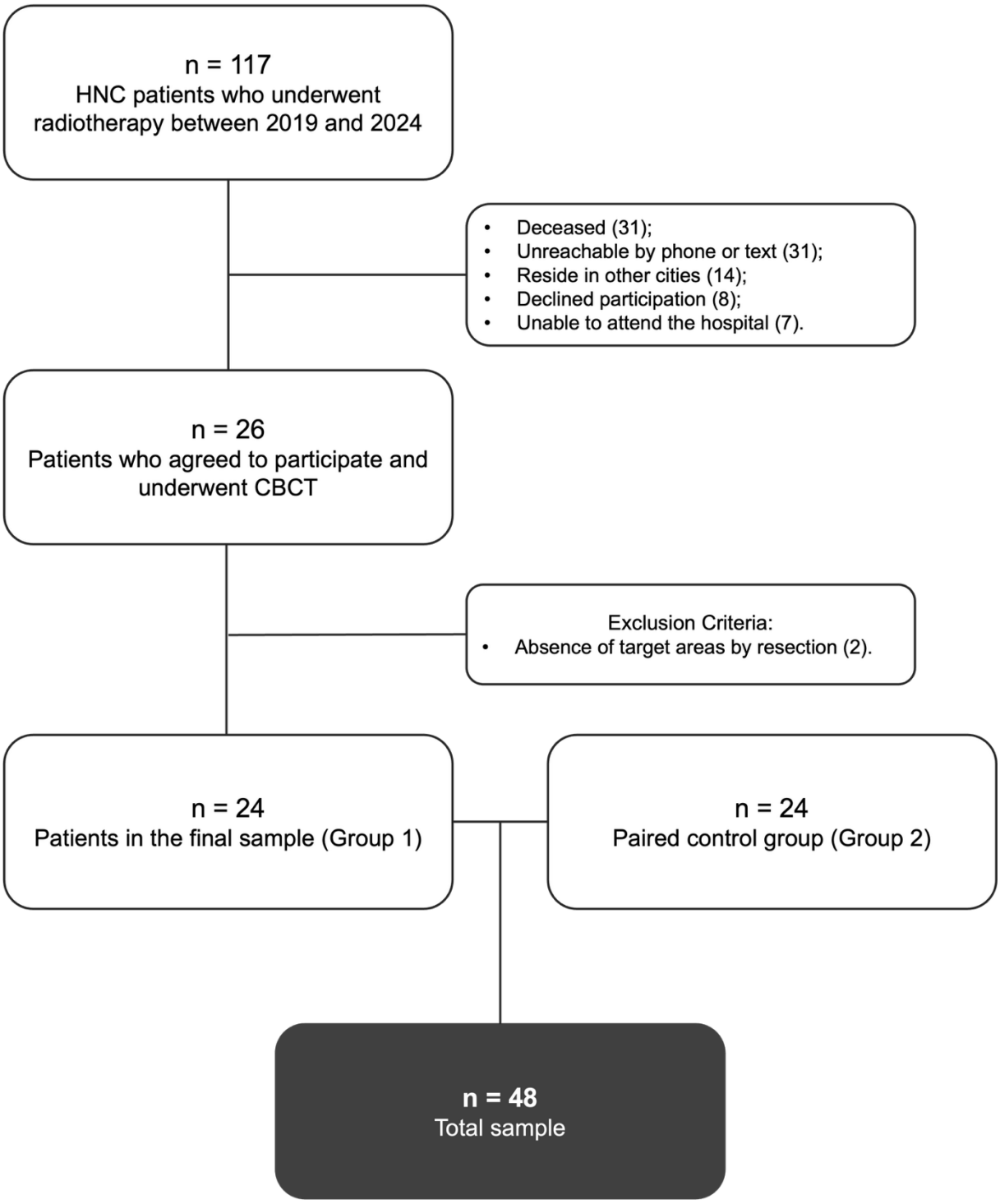


Figure 5. Study sample flowchart.

The sample consisted of 36 males (75%) and 12 females (25%). The mean age was 64.3 years (SD 10.9) in Group 1 and 62.6 years (SD 10.1) in Group 2, with no statistically significant difference between groups ($p = 0.576$). The number of teeth differed significantly between the two groups, with a mean of 4 teeth in Group 1 (SD

4.79) and 9 teeth in Group 2 (SD 5.14) (p = 0.002). Descriptive characteristics of the studied sample is presented by Supplementary Table S1

In group 1, the most prevalent tumor site was the larynx (41.6%), followed by the oral cavity (25%); the oropharynx, nasopharynx, and parotid gland (8.3% each); and, finally, the submandibular gland and maxillary sinus (4.1% each). Most histopathologic diagnoses were squamous cell carcinoma (83.3%). There were also two cases of adenoid cystic carcinoma (8.3%), one case of mucoepidermoid carcinoma (4.1%), and one case of malignant spindle cell neoplasm (4.1%). Twenty patients reported being smokers (83.3%) for a mean of 29.45 years (SD 14.66), eighteen of whom detailed their smoking frequency, with a mean of 15.11 cigarettes per day (SD 11.8). Only two patients reported not smoking, and two patients did not provide information regarding smoking habits. Regarding treatment, 16 patients underwent concomitant chemotherapy, and 6 had previously undergone surgery.

The mean total radiation dose received by the patients was 66.06 Gy (SD 5.93), ranging from 48 Gy to 70 Gy. The anterior mandibular region segmented had a mean volume of 17.23 $cm^3$ (SD 3.27) and received a mean maximum dose of 29.89 Gy (SD 24.37), ranging from 1 Gy to 70 Gy, and a mean dose of 14.1 Gy (SD 16.43), ranging from 0.5 Gy to 54 Gy. The mean interval between the last RT session and CBCT acquisition was 28.87 months (SD 19.11).

**Agreement and consistency**

During training, intra-rater reliability coefficients revealed good agreement for FD (ICC = 0.835; 95% CI: 0.714–0.907), excellent agreement for CTMI (ICC = 0.972; 95% CI: 0.933–0.989), and perfect agreement for CTCI (ICC = 1.0) for Evaluator 1. Similarly, Evaluator 2 demonstrated good agreement for FD (ICC = 0.886; 95% CI: 0.795–0.938), excellent agreement for CTMI (ICC = 0.990; 95% CI: 0.976–0.996), and perfect agreement for CTCI (ICC = 1.0).

Inter-rater reliability between the two evaluators was also classified as good for FD (ICC = 0.863; 95% CI: 0.757–0.925), excellent for CTMI (ICC = 0.959; 95% CI: 0.903–0.983), and perfect for CTCI (ICC = 1.0).

**Group 1 Analysis**

Regarding the tumor site, a significant difference was observed among the seven sites for trabecular FD analysis (ROI 1 + ROI 2) ($p = 0.021$) and for CTMI ($p < 0.001$). For cortical FD (ROI 3 + ROI 4), no significant differences were observed between the groups ($p = 0.068$). These data are presented in Supplementary Table S2.

Patients with tumors in the head region received higher maximum and mean radiation doses to the anterior region of the mandible compared to those diagnosed with tumors in the neck region ($p = 0.024$ and $p = 0.015$, respectively). Trabecular FD was higher in patients with neck tumors ($p = 0.003$), while no significant differences were observed for cortical FD, CTMI, or CTCI analyses ($p = 0.412$, $p = 0.573$, and $p = 0.158$, respectively). Data regarding these findings can be found in Tables 1 and 2, and Supplementary Figure S1.

No significant differences were observed between patients who received <30 Gy or >30 Gy in the anterior region of the mandible in terms of trabecular FD ($p = 0.310$), cortical FD ($p = 1.000$), CTMI ($p = 0.598$), or CTCI ($p = 0.708$). Similarly, regarding the mean dose received, no statistically significant differences were observed between the analyzed groups. Data on maximum and mean doses are presented in Supplementary Tables S3 and S4, and Supplementary Figure S2.

Concerning the interval between RT and CBCT acquisition, higher CTMI values were observed in the group evaluated after 30 months ($p = 0.034$). No differences between groups were observed for FD or CTCI analyses. Data can be found in Supplementary Table S5, and Supplementary Figure S3.

**Comparative analysis between groups**

Table 3 presents the results of FD analysis between groups for each ROI and for the sum of the ROIs corresponding to the mandibular trabecular and cortical regions. Mean FD values did not differ between groups for any of the evaluated ROIs or for the sum of the ROIs corresponding to the trabecular and cortical bone ($p > 0.05$) (Fig. 6).

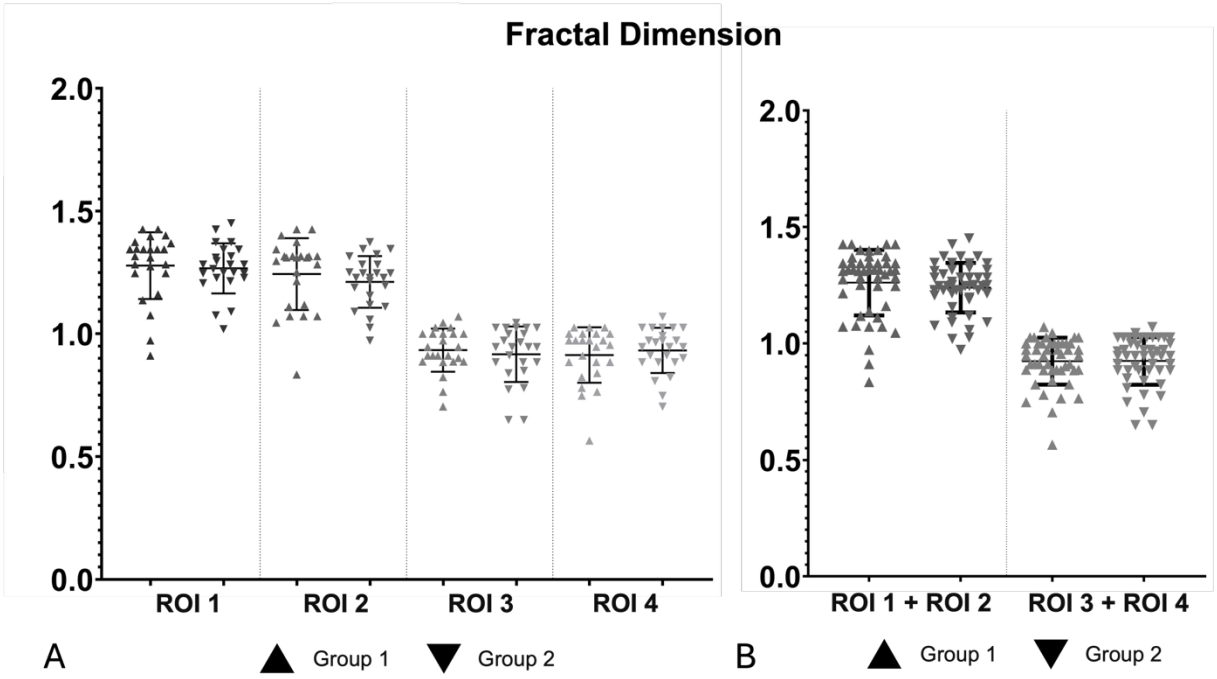


Figure 6. FD results between groups. (A) FD values for each ROI in Groups 1 (apex upward) and 2 (apex downward). ROI 1: right trabecular; ROI 2: left trabecular; ROI 3: right cortical; ROI 4: left cortical. (B) FD values grouped for trabecular (ROI 1 + ROI 2) and cortical (ROI 3 + ROI 4) analyses, with the same triangle notation for groups. No statistically significant differences were observed between groups in any analysis ($p > 0.05$).

Regarding CTMI, Group 1 exhibited mean values of 3.91 for the right side (SD 0.972) and 3.45 for the left side (SD 0.854). In Group 2, the means were 3.99 for the right side (SD 0.883) and 3.85 for the left side (SD 0.775), with no significant differences observed between groups for either side ($p = 0.763$; $p = 0.096$). CTMI data are presented in Table 4.

Evaluation of CTCI revealed that, among patients in Group 1, 14 patients were classified as type 1 cortical (58.3%), followed by 7 patients as type 2 (29.2%) and 3 patients as type 3 (12.5%). In Group 2, 19 patients were classified as type 1 (79.2%), 3 as type 2 (12.5%), and 2 as type 3 (8.3%). No significant differences were observed between groups ($p = 0.278$). CTCI data between groups are presented in Table 5. Fig. 7 presents the graphical comparison of CTMI and CTCI values between groups.

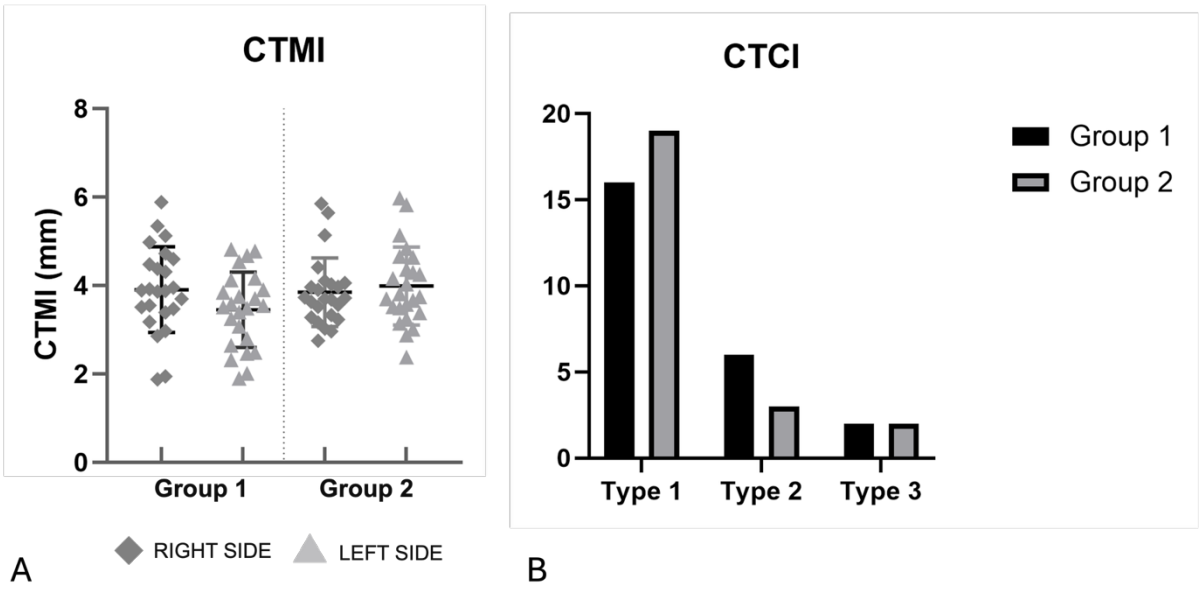


Figure 7. Radiomorphometric indices results between groups. (A) CTMI values for Groups 1 and 2. (B) CTCI values for Groups 1 and 2. No statistically significant differences were observed between the groups for either index ($p > 0.05$).

## DISCUSSION

This study provides novel evidence on the mandibular bone response to head and neck RT by jointly assessing FD and radiomorphometric indices on CBCT images. By comparing post-RT patients with matched non-irradiated controls, we demonstrated that CBCT-based FD, CTMI, and CTCI measurements do not differ significantly between groups, while revealing site- and time-dependent variations, particularly lower trabecular FD in patients with head tumors and higher CTMI values at longer post-treatment intervals. These findings add to the existing literature by showing that CBCT-derived radiomorphometric indices and FD remain largely unchanged after RT, while revealing site- and time-dependent variability in mandibular bone response [28,29].

Several studies have employed radiomorphometric analysis and FD in various dental imaging modalities, including panoramic radiography, CBCT, micro-CT, periapical radiography, sialography, bitewing radiography, ultrasound, and lateral cephalometric radiography [18]. These techniques have been used as tools for the identification, screening, and diagnostic support of both local and systemic conditions affecting bone structure, such as osteoporosis, bruxism, chronic kidney disease, familial adenomatous polyposis, endocrine disorders, and osteogenesis imperfecta [19–

[21,30–32]. To the best of our knowledge, this is the first study to evaluate radiomorphometric indices and FD in CBCT scans from post-RT patients, comparing them with a matched control group.

The radiomorphometric indices used in this study were proposed for CBCT evaluation as adaptations of indices originally developed for panoramic radiographs [25,26]. This adaptation enabled assessment within three-dimensional image sections. In the study by Koh and Kim, for example, this approach allowed the differentiation of female patients diagnosed with osteoporosis from control subjects using the CTCI [22]. A previous study also reported a significant correlation between the radiomorphometric indices investigated in this study and FD in CBCT images [33]. Considering this, our study evaluated these indices jointly with FD to investigate possible alterations in the mandibular cortical and trabecular bone associated with RT treatment, given that bone microarchitecture is modified in irradiated regions [14].

A previous study analyzed FD and radiomorphometric indices in patients who underwent RT for nasopharyngeal carcinoma, reporting a reduction in trabecular FD among irradiated patients compared with the control group, with no differences observed over time up to three years [28]. These findings partially align with those of the present study, as lower trabecular FD values were observed in patients with tumors in the head region compared with those with tumors in the neck region, without changes across the evaluated time intervals. However, unlike the findings of that study, no statistically significant differences were found when comparing irradiated patients with the paired control group in the present analysis. This discrepancy may be explained by the fact that, while the previous study included only patients diagnosed with nasopharyngeal carcinoma, our sample comprised a heterogeneous group of head and neck tumors in the comparison with controls. In addition, the different imaging modalities used may account for the divergent results, as distortions inherent to panoramic radiographs may influence FD analysis [28]. In our study, assessments were performed in three-dimensional image sections, allowing isolation of the trabecular region without superimposition of the cortical bone or other structures, and CBCT imaging introduces fewer distortions compared with panoramic radiography.

Previous studies have established that RT alters the structure and increases the fragility of cortical bone [34,35]. A study evaluated cortical bone after RT in rabbit tibiae using micro-computed tomography, reporting a significant increase in cortical

thickness and a reduction in porosity at the first assessment, followed by a subsequent increase in porosity later point [23]. The same study did not observe significant changes in FD values. These findings are comparable to those of the present study, in which higher CTMI values were observed in patients evaluated less than 30 months after RT, without changes in cortical FD over time. However, the results differ regarding the qualitative assessment of cortical bone: in our study, no changes in the CTCI were observed, whereas the cited study reported an increase in intracortical porosity over time [23]. It should be noted that the assessments were performed using different methodologies [23].

Authors observed in a systematic literature review that both high doses (30 Gy) and low doses (1–2 Gy) can induce bone deterioration, with immediate and late effects, although these are more pronounced at later stages [14]. They reported that low doses affect mesenchymal progenitor cells and increase osteoclastic activity shortly after exposure, while high doses lead to loss of bone density, increased porosity, and a higher risk of fracture [14]. In our study, the anterior region of the mandible in patients was exposed to doses ranging from 1 Gy to 70 Gy; however, cellular-level changes were not investigated. No differences were found between patients who received <30 Gy or >30 Gy as the maximum dose, nor among the categories of mean dose. Nevertheless, patients with tumors in the head region received higher maximum and mean radiation doses and exhibited lower trabecular FD values compared with patients with tumors in the neck (larynx) region. Additionally, the greater metabolic activity and regenerative capacity of trabecular bone compared with cortical bone [28] may explain why these alterations were observed in trabecular FD in relation to tumor site, whereas no changes in cortical bone were detected through this analysis.

A recent study evaluated how RT alters the morphology and spatial organization of cortical mandibular canals in 23 patients who underwent RT with doses ranging from 60 to 76 Gy, with follow-up assessments for up to eight years [29]. This study found no significant differences between patients and control groups in FD analysis, a finding consistent with the results of the present work. The authors suggested that RT modifies the shape and size of the canals (changes related to compromised vascularization) but does not affect their spatial distribution over time [29].

In recent years, significant advances have been made in the definition and management of ORN in patients undergoing head and neck RT. Peterson et al.

consolidated recommendations, emphasizing pre- and post-RT dental care, judicious use of antibiotics, and the combination of pentoxifylline and tocopherol (PENTO) in mild to moderate cases, while highlighting surgery as the primary treatment for advanced cases and moving away from routine hyperbaric oxygen therapy [16]. Concurrently, Moreno et al. developed an international consensus to establish a standardized definition of ORN and classification criteria, including non-exposed cases, as well as nine essential data points for standardization in research and clinical practice [15]. This consensus is crucial for reducing underdiagnosis, standardizing data collection, enabling comparisons between studies, aligning with previously described clinical management recommendations, and providing a foundation for future predictive strategies and artificial intelligence model development in this field [15]. In our study, given the sample size and protocol employed, no bone alterations were observed between irradiated patients and paired controls that could objectively indicate factors associated with a higher risk of developing complications such as ORN based on CBCT evaluation.

The findings of this study suggest the need to manage head and neck cancer patients treated with RT on an individual basis regarding the risk of developing toxicities. So that the patients exhibit a highly heterogeneous profile in terms of diagnosis, tumor location, treatment received, radiation doses delivered to different OARs, and time since treatment completion. Consultation with the professional responsible for RT planning prior to clinical or surgical interventions in these patients is important to determine risk assessment. Future research investigating variables capable of predicting patients at higher risk of developing complications is warranted. Recent studies using radiomics and machine learning have opened a new path toward personalized RT for head and neck cancer and ORN prediction, revealing these strategies as promising tools in this process [11,36]. Therefore, due to heterogeneous bone responses, personalized risk stratification and patient-specific interventions are recommended prior procedures.

This study also has some limitations. Considering our sample, the number of subgroup comparisons performed, analyses involving tumor site, radiation dose categories, and post-radiotherapy interval were considered exploratory. Therefore, these results should be interpreted with caution and primarily as hypothesis-generating. The lack of standardized protocols for FD analysis in CBCT and the need

to adapt existing protocols, originally developed for radiographs, for image processing may introduce bias, although the different groups and subgroups were evaluated using the same parameters. Sample attrition is another important limitation, given that head and neck cancer is associated with high morbidity and mortality. Establishing protocols for three-dimensional FD analysis using volumes of interest could increase the amount of information obtained from the analyzed region and function as a “virtual biopsy.”

## CONCLUSION

In conclusion, CBCT-based assessment of mandibular cortical and trabecular bone using fractal dimension and radiomorphometric indices did not reveal significant differences between irradiated patients and matched controls. However, site-specific and time-related variations suggest heterogeneous bone responses following head and neck radiotherapy. These findings highlight the complexity of radiation-induced bone alterations and underscore the need for individualized patient assessment and for future studies employing larger samples and advanced three-dimensional quantitative approaches. Therefore, a personalized approach to risk prediction and intervention should be adopted for each patient before dental procedures.

## REFERENCES

1. Mahmood H, Shaban M, Rajpoot N, Khurram SA. Artificial Intelligence-based methods in head and neck cancer diagnosis: an overview. Br J Cancer. 2021 Jun 8;124(12):1934–40.

2. Mäkitie AA, Alabi RO, Ng SP, Takes RP, Robbins KT, Ronen O, et al. Artificial Intelligence in Head and Neck Cancer: A Systematic Review of Systematic Reviews. Vol. 40, Advances in Therapy. Adis; 2023. p. 3360–80.

3. Silvestre-Barbosa Y, oria Tavares Castro V, Di Carvalho Melo L, Elaine Diniz Reis P, Ferreira Leite A, Barros Ferreira E, et al. Worldwide research trends on artificial intelligence in head and neck cancer: a bibliometric analysis. Oral Surg Oral Med Oral Pathol Oral Radiol [Internet]. 2025;140:64–78. Available from: https://doi.org/10.1016/j.oooo.2025.02.014

4. Bray F, Laversanne M, Sung H, Ferlay J, Siegel RL, Soerjomataram I, et al. Global cancer statistics 2022: GLOBOCAN estimates of incidence and mortality worldwide for 36 cancers in 185 countries. CA Cancer J Clin. 2024 May;74(3):229–63.

5. Bang C, Bernard G, Le WT, Lalonde A, Kadoury S, Bahig H. Artificial intelligence to predict outcomes of head and neck radiotherapy. Clin Transl Radiat Oncol. 2023 Mar 1;39.

6. Atun R, Jaffray DA, Barton MB, Bray F, Baumann M, Vikram B, Hanna TP, Knaul FM, Lievens Y, Lui TY, Milosevic M, O'Sullivan B, Rodin DL, Rosenblatt E, Van Dyk J, Yap ML, Zubizarreta E, Gospodarowicz M. Expanding global access to radiotherapy. Lancet Oncol. 2015;16(10):1153-86.

7. Chaput G, Regnier L. Radiotherapy: clinical pearls for primary care. Can Fam Physician. 2021;67(10):753-7.

8. Ahervo H, Korhonen J, Lim Wei Ming S, Guan Yunqing F, Soini M, Lian Pei Ling C, et al. Artificial intelligence-supported applications in head and neck cancer radiotherapy treatment planning and dose optimisation. Vol. 29, Radiography. W.B. Saunders Ltd; 2023. p. 496–502.

9. Li CX, Sun JL, Gong ZC, Liu H, Ding MC, Zhao HR. An umbrella review exploring the effect of radiotherapy for head and neck cancer patients on the frequency of jaws osteoradionecrosis. Vol. 27, Cancer/Radiotherapie. Elsevier Masson s.r.l.; 2023. p. 434–46.

10. Leong WC, Manan HA, Hsien CCM, Wong YF, Yahya N. Fatigue following head and neck cancer radiotherapy: a systematic review of dose correlates. Vol. 32, Supportive Care in Cancer. Springer Science and Business Media Deutschland GmbH; 2024.

11. Araújo ALD, Moraes MC, Pérez-de-Oliveira ME, Silva VM da, Saldivia-Siracusa C, Pedroso CM, et al. Machine learning for the prediction of toxicities from head and neck cancer treatment: A systematic review with meta-analysis. Vol. 140, Oral Oncology. Elsevier Ltd; 2023.

12. Pacheco R, Stock H. Effects of radiation on bone. Curr Osteoporos Rep. 2013 Dec;11(4):299–304.

13. Soares PBF, Soares CJ, Limirio PHJO, de Jesus RNR, Dechichi P, Spin-Neto R, et al. Effect of ionizing radiation after-therapy interval on bone: histomorphometric and biomechanical characteristics. Clin Oral Investig. 2019 Jun 1;23(6):2785–93.

14. Bakar AAA, Mohamad NS, Mahmud MH, Razak HRA, Sudin AELT, Shuib S. Systematic Review on Multilevel Analysis of Radiation Effects on Bone Microarchitecture. Vol. 2022, BioMed Research International. Hindawi Limited; 2022.

15. Moreno AC, Watson EE, Humbert-Vidan L, Peterson DE, van Dijk L V., Urbano TG, et al. International Expert-Based Consensus Definition, Classification Criteria, and Minimum Data Elements for Osteoradionecrosis of the Jaw: An Interdisciplinary Modified Delphi Study. Int J Radiat Oncol Biol Phys. 2025 Jun 1;122(2):341–54.

16. Peterson DE, Koyfman SA, Yarom N, Lynggaard CD, Ismaila N, Forner LE, et al. Prevention and Management of Osteoradionecrosis in Patients With Head and Neck Cancer Treated With Radiation Therapy: ISOO-MASCC-ASCO Guideline. Journal of Clinical Oncology. 2024 Jun 1;42(16):1975–96.

17. Castro VT, Di Carvalho Melo L, Silvestre-Barbosa Y, Ferreira EB, Reis PED, Almeida FT, et al. Imaging-based maxillomandibular changes after head and neck radiotherapy: A systematic review and meta-analysis. Vol. 126, Journal of Stomatology, Oral and Maxillofacial Surgery. Elsevier Masson s.r.l.; 2025.

18. Kato CN, Barra SG, Tavares NP, Amaral TM, Brasileiro CB, Mesquita RA, et al. Use of fractal analysis in dental images: a systematic review. Dentomaxillofacial Radiology. 2019;20180457.

19. Pacheco-Pereira C, Silvestre-Barbosa Y, Almeida FT, Geha H, Leite AF, Guerra ENS. Trabecular and cortical mandibular bone investigation in familial adenomatous polyposis patients. Sci Rep. 2021 Dec 1;11(1).

20. Ersu N, Şirin Sarıbal G, Tanyeri FZ, Amuk M. Evaluation of chronic renal failure with cone beam computed tomography radiomorphometric indices and fractal analysis in the mandible. Oral Radiol. 2023 Jan 1;39(1):133–42.

21. Sindeaux R, Tadeu P, Figueiredo DS, Santos N, Melo D, Tereza A, et al. Fractal dimension and mandibular cortical width in normal and osteoporotic men and women. Maturitas [Internet]. 2014;77(2):142–8. Available from: http://dx.doi.org/10.1016/j.maturitas.2013.10.011

22. Koh KJ, Kim KA. Utility of the computed tomography indices on cone beam computed tomography images in the diagnosis of osteoporosis in women. Imaging Sci Dent. 2011 Sep;41(3):101–6.

23. Borges JS, Rabelo GD, Irie MS, Paz JLC, Spin-Neto R, Soares PBF. Cortical bone modifications after radiotherapy: Cortex porosity and osteonal changes evaluated over time. Braz Dent J. 2021 Jan 1;32(1):9–15.

24. White SC, Rudolph DJ. Alterations of the trabecular pattern of the jaws in patients with osteoporosis. Oral Surg Oral Med Oral Pathol Oral Radiol Endod. 1999;88(5):628–35.

25. Ledgerton D, Horner K, Devlin H, Worthington H. Radiomorphometric indices of the mandible in a British female population [Internet]. 1999. Available from: http://www.stockton-press.co.uk/dmfr

26. Klemetti E, Kolmakov S, Pantomography KH. Pantomography in assessment of the osteoporosis risk group. 1994;(10).

27. Portney, L. G. & Watkins, M. P. Foundations of Clinical Research: Applications to Practice 3rd edn. (Pearson/Prentice Hall, 2009).

28. Tepe RD, Toraman KO, Kayhan KB, Ozcan I, Karabas HC. Fractal Analysis of Mandible in Panoramic Radiographs of Patients Received Radiotherapy for Nasopharyngeal Carcinoma. Journal of Clinical Densitometry. 2025 Jan 1;28(1).

29. Tomazelli KB, Bianco BC, de Castro BR, Ramos I, Zimmer VR, Soares PBF, et al. Morphology and spatial distribution of cortical bone canals: Evaluation of shape parameters, lacunarity, and fractal dimension in the human irradiated mandible. Bone. 2025 Mar 1;192.

30. Çitir M, Karslioglu H, Uzun C. Evaluation of mandibular trabecular and cortical bone by fractal analysis and radiomorphometric indices in bruxist and non-bruxist patients. BMC Oral Health. 2023 Dec 1;23(1).

31. Prado HV, Debossan SAT, Loayza KS, Abreu LG, Brasileiro CB, Borges-Oliveira AC. Radiomorphometric indices and fractal dimension of the mandible in individuals with osteogenesis imperfecta: a matched cross-sectional study. Oral Surg Oral Med Oral Pathol Oral Radiol. 2023 Jul 1;136(1):102–11.

32. Yıldızer E, Sari SK, Peker F, Erdogan AR, Sancak K, Ertem SY. Assessment of Mandibular Bone Architecture in Patients with Endocrine Disorders Using Fractal Dimension and Histogram Analysis. Tomography. 2025 Jun 1;11(6).

33. Nursari EM, Kiswanjaya B, Wijanarko AP, Priaminiarti M, Bachtiar-Iskandar HH, Yoshihara A. The relationship between radiomorphometric indices and fractal dimension analysis: a cone-beam computed tomography study. Sci Rep. 2024 Dec 1;14(1).

34. Soares PBF, Soares CJ, Limirio PHJO, de Jesus RNR, Dechichi P, Spin-Neto R, et al. Effect of ionizing radiation after-therapy interval on bone: histomorphometric and biomechanical characteristics. Clin Oral Investig. 2019 Jun 1;23(6):2785–93.

35. Limirio PHJO, Soares PBF, Emi ETP, Lopes CDCA, Rocha FS, Batista JD, et al. Ionizing radiation and bone quality: Time-dependent effects. Radiation Oncology. 2019 Jan 22;14(1).

36. Urbano G, Humbert-vidan L, Patel V, Oral Surg M, Oksuz I, Peter King A, et al. Comparison of machine learning methods for prediction of osteoradionecrosis incidence in patients with head and neck cancer 1,2. 2021.

## TABLES

Table 1 – Analysis according tumor site, grouped as head or neck.

| | Head (n=14) | | Neck (n=10) | | |
|---|---|---|---|---|---|
| | Mean | SD | Mean | SD | p value |
| Maximum dose (Gy) | 39.7 | 23.1 | 17.14 | 20.48 | 0.024* |
| Mean dose (Gy) | 20.3 | 18.6 | 6 | 8.33 | 0.015* |
| Trabecular FD | 1.212 | 0.164 | 1.330 | 0.045 | 0.003* |
| Cortical FD | 0.935 | 0.092 | 0.908 | 0.111 | 0.412 |
| CTMI | 3.612 | 0.907 | 3.768 | 0.986 | 0.573 |

SD: standard deviation; *: $p<0.05$. Mann-Whitney U test: maximum dose, trabecular FD and cortical FD; T-test: mean dose and CTMI.

Table 2 – CTCI according to tumor site, grouped as head or neck.

| | CTCI | | | |
|---|---|---|---|---|
| | Type 1 | Type 2 | Type 3 | p value |
| Head (n=14) | 11 | 3 | 0 | 0.158 |
| Neck (n=10) | 5 | 3 | 2 | |

Chi-square test.

Table 3 – FD means in both groups.

| | Group 1 (n = 24) | | Group 2 (n = 24) | | |
|---|---|---|---|---|---|
| | Mean | SD | Mean | SD | p value |
| ROI 1 | 1.28 | 0.136 | 1.27 | 0.102 | 0.273 |
| ROI 2 | 1.24 | 0.146 | 1.21 | 0.105 | 0.170 |
| ROI 3 | 0.93 | 0.087 | 0.92 | 0.113 | 0.804 |
| ROI 4 | 0.91 | 0.113 | 0.93 | 0.092 | 0.764 |
| ROI 1 + ROI 2 | 1.26 | 0.141 | 1.24 | 0.106 | 0.069 |
| ROI 3 + ROI 4 | 0.92 | 0.101 | 0.92 | 0.102 | 0.944 |

ROI: Region of Interest; ROI 1: right trabecular; ROI 2: left trabecular; ROI 3: right cortical; ROI 4: left cortical; ROI 1 + ROI 2: trabecular, both sides; ROI 3 + ROI 4: cortical, both sides; SD: standard deviation. All comparisons were performed using the Mann–Whitney U test.

Table 4 – CTMI in both groups.

| | Group 1 (n = 24) | | Group 2 (n = 24) | | |
|---|---|---|---|---|---|
| | Mean | SD | Mean | SD | p value |
| CTMI (R) | 3.91 | 0.972 | 3.99 | 0.883 | 0.763 |
| CTMI (L) | 3.45 | 0.854 | 3.85 | 0.775 | 0.096 |
| CTMI (total) | 3.68 | 0.934 | 3.92 | 0.825 | 0.185 |

CTMI (R): Computed Tomography Mental Index right side; CTMI (L): Computed Tomography Mental Index left side; SD: standard deviation. All comparisons were performed using T-test.

Table 5 – CTCI in both groups.

| CTCI | Group | | p value |
|---|---|---|---|
| | 1 | 2 | |
| Type 1 | 14 | 19 | 0.278 |
| Type 2 | 7 | 3 | |
| Type 3 | 3 | 2 | |

Chi-square test.

## APPENDIX

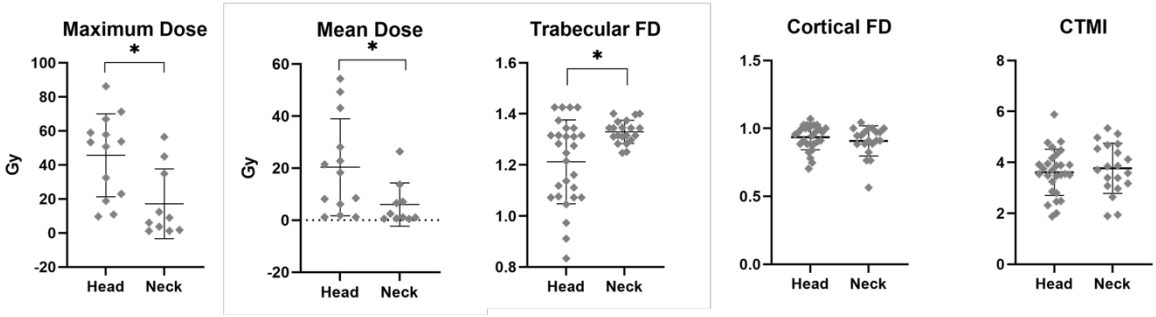


Supplementary Figure S1. Significant differences were observed for maximum dose (p = 0.024), mean dose (p = 0.015), and trabecular FD (p = 0.003). No significant differences were found for cortical FD (p = 0.412) or CTMI (p = 0.573).

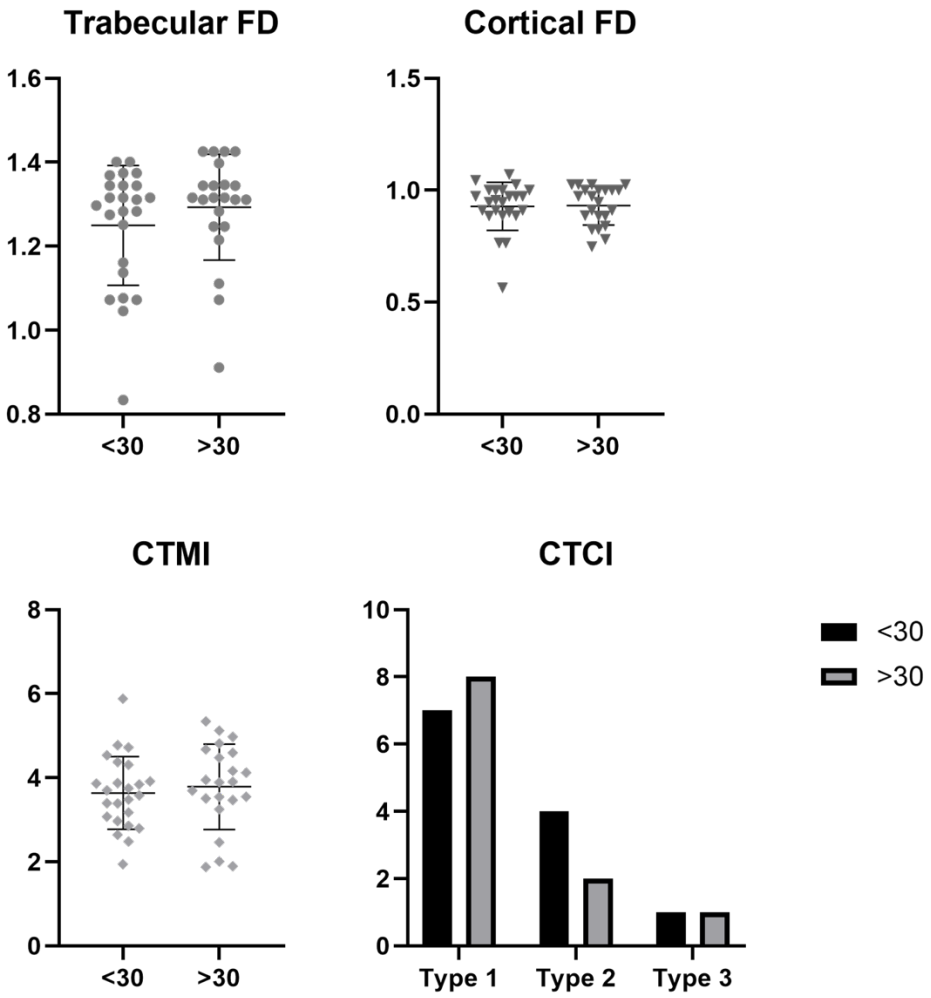


Supplementary Figure S2. FD and radiomorphometric indices according to maximum dose. No significant differences were observed between patients who received <30 Gy or >30 Gy in the anterior region of the mandible in terms of trabecular FD (p = 0.310), cortical FD (p = 1.000), CTMI (p = 0.598), or CTCI (p = 0.708).

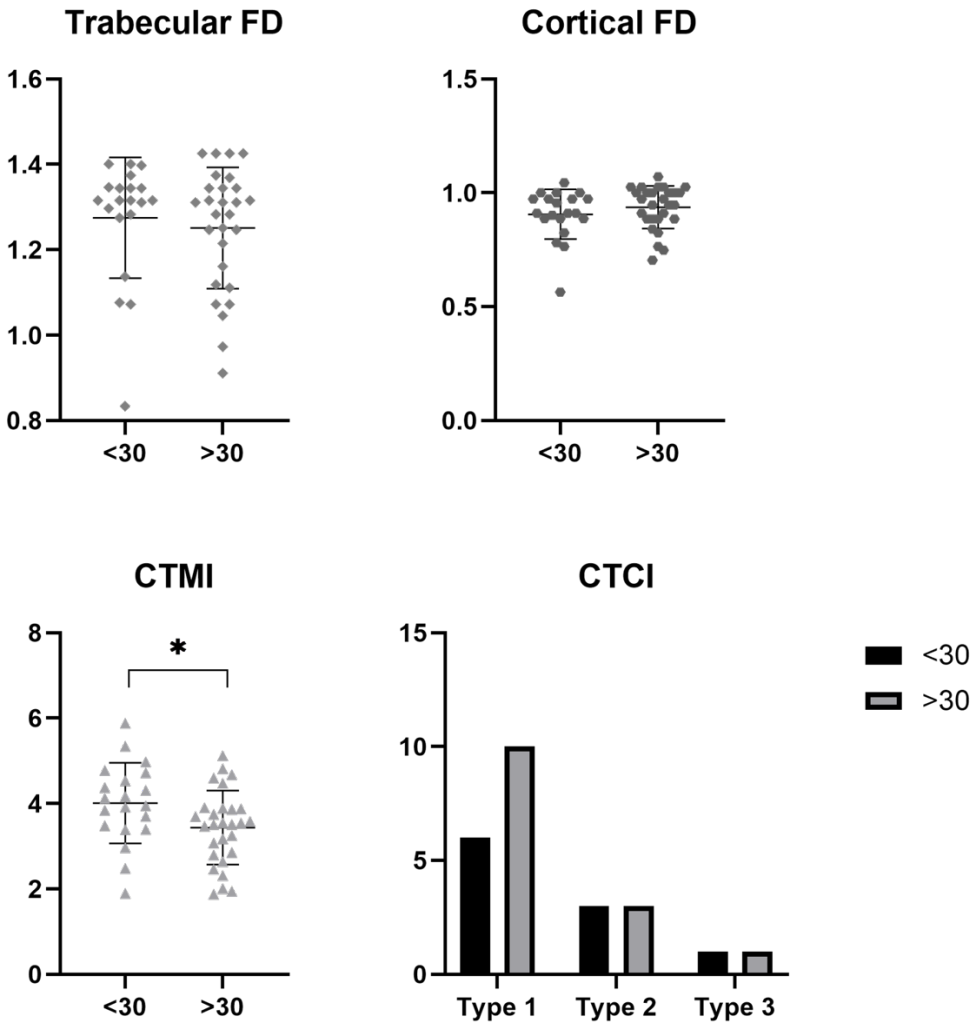


Supplementary Figure S3. FD and radiomorphometric indices according to time between RT and CBCT. Higher CTMI values were observed in the group evaluated after 30 months (p = 0.034). No differences between groups were observed for FD or CTCI analyses.

Supplementary Table S1 – Descriptive characteristics of the studied sample.

| | Group 1 (n = 24) | Group 2 (n = 24) | p value |
|---|---|---|---|
| Sex | 18 (M) 6 (F) | 18 (M) 6 (F) | - |
| Age | 64.3 (SD 10.9) | 62.6 SD (10.1) | 0.576 |
| Nationality | Brazilian | Brazilian | - |
| Number of teeth | 4 (SD 4.9) | 9 (SD 5.14) | 0.002* |

F: female; M: male; SD: standard deviation; *: p<0.05

Supplementary Table S2 – Comparison of FD and CTMI values according to tumor site.

| | Site of tumor | Mean | SD | p value |
|---|---|---|---|---|
| Trabecular FD | Larynx | 1.330 | 0.045 | 0.021* |
| | Nasopharynx | 1.048 | 0.103 | |
| | Parotid gland | 1.202 | 0.148 | |
| | Oropharynx | 1.299 | 0.134 | |
| | Oral cavity | 1.267 | 0.162 | |
| | Maxillary sinus | 1.223 | 0.213 | |
| | Submandibular gland | 1.046 | 0.102 | |
| Cortical FD | Larynx | 0.908 | 0.111 | 0.068 |
| | Nasopharynx | 0.996 | 0.079 | |
| | Parotid gland | 0.903 | 0.091 | |
| | Oropharynx | 1.006 | 0.025 | |
| | Oral cavity | 0.917 | 0.084 | |
| | Maxillary sinus | 0.986 | 0.055 | |
| | Submandibular gland | 0.794 | 0.128 | |
| CTMI | Larynx | 3.768 | 0.986 | <0.001* |
| | Nasopharynx | 3.681 | 0.161 | |
| | Parotid gland | 4.300 | 0.351 | |
| | Oropharynx | 3.679 | 0.544 | |
| | Oral cavity | 3.585 | 1.207 | |
| | Maxillary sinus | 2.824 | 0.042 | |
| | Submandibular gland | 2.912 | 0.842 | |

SD: standard deviation; *: p<0.05

Supplementary Table S3 – FD and radiomorphometric indices according to maximum dose.

| **Maximum dose** | **Trabecular FD** | | | **Cortical FD** | | | **CTMI** | | | **CTCI** | | | |
|---|---|---|---|---|---|---|---|---|---|---|---|---|---|
| | Mean | SD | p value | Mean | SD | p value | Mean | SD | p value | Type1 | Type2 | Type3 | p value |
| <30Gy | 1.250 | 0.143 | 0.310 | 0.928 | 0.108 | 1.000 | 3.640 | 0.865 | 0.598 | 7 | 4 | 1 | 0.708 |
| >30Gy | 1.293 | 0.126 | | 0.931 | 0.086 | | 3.787 | 1.014 | | 8 | 2 | 1 | |

SD: standard deviation

Supplementary Table S4 – FD and CTMI according to mean dose.

| | Mean Dose (Gy) | Mean | SD | p value |
|---|---|---|---|---|
| Trabecular FD | 0-10 | 1.261 | 0.136 | 0.389 |
| | 10-30 | 1.255 | 0.146 | |
| | >30 | 1.348 | 0.091 | |
| Cortical FD | 0-10 | 0.936 | 0.102 | 0.704 |
| | 10-30 | 0.922 | 0.097 | |
| | >30 | 0.914 | 0.082 | |
| CTMI | 0-10 | 3.710 | 0.871 | 0.845 |
| | 10-30 | 3.619 | 1.161 | |
| | >30 | 3.894 | 0.828 | |

SD: standard deviation

Supplementary Table S5 – FD and radiomorphometric indices according to time between RT and CBCT.

| **Time RT-CBCT** | **Trabecular FD** | | | **Cortical FD** | | | **CTMI** | | | **CTCI** | | | |
|---|---|---|---|---|---|---|---|---|---|---|---|---|---|
| | Mean | SD | p value | Mean | SD | p value | Mean | SD | p value | Type1 | Type2 | Type3 | p value |
| <30mo | 1.275 | 0.141 | 0.390 | 0.906 | 0.109 | 0.328 | 4.013 | 0.943 | 0.034* | 6 | 3 | 1 | 0.842 |
| >30mo | 1.251 | 0.142 | | 0.937 | 0.094 | | 3.437 | 0.866 | | 10 | 3 | 1 | |

mo: months; SD: standard deviation; *: p<0.0

## CONSIDERAÇÕES FINAIS

As evidências apresentadas nesta dissertação reforçam a complexidade do CCP, destacando tanto as oportunidades proporcionadas pelo uso de métodos computacionais, quanto os desafios clínicos das suas aplicações. A análise bibliométrica evidenciou o crescimento da aplicação da IA na pesquisa sobre o CCP, sobretudo em radiologia, RT, diagnóstico e predição de sobrevida. Houve um aumento no uso de IA na pesquisa de câncer de cabeça e pescoço desde 2016, porém indicou uma disparidade notável na quantidade de publicações entre países de alta renda e países de baixa/média renda. Sobre a carência de estudos com IA em países mais pobres, esse fator pode gerar viés sistêmico, bem como a ausência de diversidade étnica causaria um viés de representação. Porém, a heterogeneidade metodológica, a falta de padronização e a limitada validação externa ainda restringem a adoção dos métodos computacionais de forma mais ampla e confiável.

Por outro lado, o estudo primário demonstrou que a avaliação da morfologia óssea mandibular por índices radiomorfométricos e DF em pacientes irradiados não revelou diferenças significativas em comparação a controles, embora variações relacionadas à localização do tumor e à dose de radiação tenham sido observadas. Esses achados enfatizam a necessidade de abordagens individualizadas antes dos procedimentos odontológicos, como a estratificação de risco personalizada e intervenções específicas para cada paciente no acompanhamento pós-RT, considerando a heterogeneidade dos pacientes e dos protocolos de tratamento. Em conjunto, os resultados destacam o potencial das tecnologias computacionais, incluindo a análise radiômica e aprendizado de máquina, como ferramentas promissoras para a detecção precoce de alterações ósseas, predição de radiotoxicidades e suporte à decisão clínica personalizada, contribuindo para o avanço do manejo do CCP e para a melhoria da qualidade de vida dos pacientes.

## REFERÊNCIAS

ADOGA, A. A.; KOKONG, D. D.; MA'AN, N. D.; MUGU, J. G.; MGBACHI, C. J.; DAUDA, A. M. The predictive factors of primary head and neck cancer stage at presentation and survival in a developing nation's tertiary hospital. SAGE Open Medicine, v. 6, 1 ago. 2018.

AHERVO, H.; KORHONEN, J.; LIM WEI MING, S.; GUAN YUNQING, F.; SOINI, M.; LIAN PEI LING, C.; METSÄLÄ, E. Artificial intelligence-supported applications in head and neck cancer radiotherapy treatment planning and dose optimization Radiography W.B. Saunders Ltd, 1 maio 2023.

ALABI, R. O.; ELMUSRATI, M.; LEIVO, I.; ALMANGUSH, A.; MÄKITIE, A. A. Artificial Intelligence-Driven Radiomics in Head and Neck Cancer: Current Status and Future Prospects International Journal of Medical Informatics Elsevier Ireland Ltd, 1 ago. 2024.

ARAÚJO, A. L. D. *et al.* Machine learning for the prediction of toxicities from head and neck cancer treatment: A systematic review with meta-analysis Oral Oncology Elsevier Ltd, 1 maio 2023.

ATUN, Rifat; A JAFFRAY, David; BARTON, Michael B; BRAY, Freddie; BAUMANN, Michael; VIKRAM, Bhadrasain; HANNA, Timothy P; KNAUL, Felicia M; LIEVENS, Yolande; LUI, Tracey y M. Expanding global access to radiotherapy. The Lancet Oncology, [S.L.], v. 16, n. 10, p. 1153-1186, set. 2015

BAKAR, A. A. A.; MOHAMAD, N. S.; MAHMUD, M. H.; RAZAK, H. R. A.; SUDIN, A. E. L. T.; SHUIB, S. Systematic Review on Multilevel Analysis of Radiation Effects on Bone Microarchitecture BioMed Research International Hindawi Limited, 2022.

BANG, C.; BERNARD, G.; LE, W. T.; LALONDE, A.; KADOURY, S.; BAHIG, H. Artificial intelligence to predict outcomes of head and neck radiotherapy. Clinical and Translational Radiation Oncology, v. 39, 1 mar. 2023.

BORGES, J. S.; RABELO, G. D.; IRIE, M. S.; PAZ, J. L. C.; SPIN-NETO, R.; SOARES, P. B. F. Cortical bone modifications after radiotherapy: Cortex porosity and osteonal changes evaluated over time. Brazilian Dental Journal, v. 32, n. 1, p. 9–15, 1 jan. 2021.

BRAY, F.; LAVERSANNE, M.; SUNG, H.; FERLAY, J.; SIEGEL, R. L.; SOERJOMATARAM, I.; JEMAL, A. Global cancer statistics 2022: GLOBOCAN estimates of incidence and mortality worldwide for 36 cancers in 185 countries. CA: A Cancer Journal for Clinicians, v. 74, n. 3, p. 229–263, maio 2024.

CHAPUT, Genevieve; REGNIER, Laura. Radiotherapy: clinical pearls for primary care. Canadian Family Physician, [S.L.], v. 67, n. 10, p. 753-757, out. 2021. The College of Family Physicians of Canada.

ERSU, N.; ŞIRIN SARIBAL, G.; TANYERI, F. Z.; AMUK, M. Evaluation of chronic renal failure with cone beam computed tomography radiomorphometric indices and fractal analysis in the mandible. Oral Radiology, v. 39, n. 1, p. 133–142, 1 jan. 2023.

KATO, C. N. A. O.; BARRA, S. G.; TAVARES, N. P. K.; AMARAL, T. M. P.; BRASILEIRO, C. B.; MESQUITA, R. A.; ABREU, L. G. Use of fractal analysis in dental images: A systematic review Dentomaxillofacial Radiology British Institute of Radiology, 2020.

KOH, K. J.; KIM, K. A. Utility of the computed tomography indices on cone beam computed tomography images in the diagnosis of osteoporosis in women. Imaging Science in Dentistry, v. 41, n. 3, p. 101–106, set. 2011.

KOUROU, K.; EXARCHOS, T. P.; EXARCHOS, K. P.; KARAMOUZIS, M. V.; FOTIADIS, D. I. Machine learning applications in cancer prognosis and prediction Computational and Structural Biotechnology Journal Elsevier B.V., 2015.

LANDER, D. P.; KALLOGJERI, D.; PICCIRILLO, J. F. Smoking, Drinking, and Dietary Risk Factors for Head and Neck Cancer in Prostate, Lung, Colorectal, and Ovarian Cancer Screening Trial Participants. JAMA Otolaryngology - Head and Neck Surgery, v. 150, n. 3, p. 249–256, 14 mar. 2024.

LEITE, A. F.; VASCONCELOS, K. DE F.; WILLEMS, H.; JACOBS, R. Radiomics and Machine Learning in Oral Healthcare Proteomics - Clinical Applications Wiley-VCH Verlag, 1 maio 2020.

LEONG, W. C.; MANAN, H. A.; HSIEN, C. C. M.; WONG, Y. F.; YAHYA, N. Fatigue following head and neck cancer radiotherapy: a systematic review of dose correlates Supportive Care in Cancer Springer Science and Business Media Deutschland GmbH, , 1 jul. 2024.

LI, C. X.; SUN, J. L.; GONG, Z. C.; LIU, H.; DING, M. C.; ZHAO, H. R. An umbrella review exploring the effect of radiotherapy for head and neck cancer patients on the frequency of jaws osteoradionecrosis Cancer/Radiotherapie Elsevier Masson s.r.l., 1 set. 2023.

LINS, L. S. DA S.; BEZERRA, N. V. F.; FREIRE, A. R.; ALMEIDA, L. DE F. D. DE; LUCENA, E. H. G. DE; CAVALCANTI, Y. W. Socio-demographic characteristics are related to the advanced clinical stage of oral cancer. Medicina Oral Patologia Oral y Cirugia Bucal, v. 24, n. 6, p. e759–e763, 1 nov. 2019.

MAHMOOD, H.; SHABAN, M.; INDAVE, B. I.; SANTOS-SILVA, A. R.; RAJPOOT, N.; KHURRAM, S. A. Use of artificial intelligence in diagnosis of head and neck precancerous and cancerous lesions: A systematic review Oral Oncology Elsevier Ltd, 1 nov. 2020.

MAHMOOD, H.; SHABAN, M.; RAJPOOT, N.; KHURRAM, S. A. Artificial Intelligence-based methods in head and neck cancer diagnosis: an overview. British Journal of Cancer, v. 124, n. 12, p. 1934–1940, 8 jun. 2021.

MÄKITIE, A. A. *et al.* Artificial Intelligence in Head and Neck Cancer: A Systematic Review of Systematic Reviews Advances in Therapy Adis, 1 ago. 2023.

MEYER, A. N. D.; GIARDINA, T. D.; SPITZMUELLER, C.; SHAHID, U.; SCOTT, T. M. T.; SINGH, H. Patient perspectives on the usefulness of an artificial intelligence-assisted symptom checker: Cross-sectional survey study. Journal of Medical Internet Research, v. 22, n. 1, 1 jan. 2020.

MORENO, A. C. *et al.* International Expert-Based Consensus Definition, Classification Criteria, and Minimum Data Elements for Osteoradionecrosis of the Jaw: An Interdisciplinary Modified Delphi Study. International Journal of Radiation Oncology Biology Physics, v. 122, n. 2, p. 341–354, 1 jun. 2025.

NASCIMENTO DE CARVALHO, F.; CAMARGO CANCELA, M. DE; MESENTIER DA COSTA, L.; LEITE MARTINS, L. F.; DIAS, F. L.; BEZERRA DE SOUZA, D. L.; RIBEIRO PINTO, L. F. Disparities in stage at diagnosis of head and neck tumours in Brazil: a comprehensive analysis of hospital-based cancer registries. The Lancet Regional Health - Americas, v. 42, 1 fev. 2025.

PACHECO, R.; STOCK, H. Effects of radiation on bone. Current Osteoporosis Reports, v. 11, n. 4, p. 299–304, dez. 2013.

PACHECO-PEREIRA, C.; SILVESTRE-BARBOSA, Y.; ALMEIDA, F. T.; GEHA, H.; LEITE, A. F.; GUERRA, E. N. S. Trabecular and cortical mandibular bone investigation in familial adenomatous polyposis patients. Scientific Reports, v. 11, n. 1, 1 dez. 2021.

PETERSON, D. E. *et al.* Prevention and Management of Osteoradionecrosis in Patients With Head and Neck Cancer Treated With Radiation Therapy: ISOO-MASCC-ASCO Guideline. Journal of Clinical Oncology, v. 42, n. 16, p. 1975–1996, 1 jun. 2024.

RUMGAY, H. *et al.* Global burden of oral cancer in 2022 attributable to smokeless tobacco and areca nut consumption: a population attributable fraction analysis. The Lancet Oncology, v. 25, n. 11, p. 1413–1423, 1 nov. 2024.

SALMANPOUR, M. R.; REZAEIJO, S. M.; HOSSEINZADEH, M.; RAHMIM, A. Deep versus Handcrafted Tensor Radiomics Features: Prediction of Survival in Head and Neck Cancer Using Machine Learning and Fusion Techniques. Diagnostics, v. 13, n. 10, 1 maio 2023.

SANTOS, MO; LIMA, FCS; MARTINS, LFF; OLIVEIRA, JFP; ALMEIDA, LM; CANCELA, MC. Estimativa de Incidência de Câncer no Brasil, 2023-2025. Revista Brasileira de Cancerologia, [S.L.], v. 69, n. 1, p. 1-11, 6 fev. 2023. Revista Brasileira De Cancerologia (RBC). http://dx.doi.org/10.32635/2176-9745.rbc.2023v69n1.3700

SINDEAUX, R. *et al.* Fractal dimension and mandibular cortical width in normal and osteoporotic men and women. Maturitas, v. 77, n. 2, p. 142–148, 2014.

SILVESTRE-BARBOSA, Y.; CASTRO, V.T.; MELO, L.D.C.; REIS, P.E.D.; LEITE, A.F.; FERREIRA, E.B.; GUERRA, E.N.S. Worldwide research trends on artificial intelligence in head and neck cancer: a bibliometric analysis. Oral Surgery, Oral Medicine, Oral Pathology And Oral Radiology, [S.L.], v. 140, n. 1, p. 64-78, jul. 2025. Elsevier BV

SOARES, P. B. F.; SOARES, C. J.; LIMIRIO, P. H. J. O.; JESUS, R. N. R. DE; DECHICHI, P.; SPIN-NETO, R.; ZANETTA-BARBOSA, D. Effect of ionizing radiation after-therapy interval on bone: histomorphometric and biomechanical characteristics. Clinical Oral Investigations, v. 23, n. 6, p. 2785–2793, 1 jun. 2019.

TEPE, R. D.; TORAMAN, K. O.; KAYHAN, K. B.; OZCAN, I.; KARABAS, H. C. Fractal Analysis of Mandible in Panoramic Radiographs of Patients Received Radiotherapy for Nasopharyngeal Carcinoma. Journal of Clinical Densitometry, v. 28, n. 1, 1 jan. 2025.

TOMAZELLI, K. B.; BIANCO, B. C.; CASTRO, B. R. DE; RAMOS, I.; ZIMMER, V. R.; SOARES, P. B. F.; GRANDO, L. J.; RABELO, G. D. Morphology and spatial distribution of cortical bone canals: Evaluation of shape parameters, lacunarity, and fractal dimension in the human irradiated mandible. Bone, v. 192, 1 mar. 2025.

WU, X.; LI, W.; TU, H. Big data and artificial intelligence in cancer research Trends in Cancer Cell Press, , 1 fev. 2024.

YANG, S. Y.; LI, S. H.; LIU, J. L.; SUN, X. Q.; CEN, Y. Y.; REN, R. Y.; YING, S. C.; CHEN, Y.; ZHAO, Z. H.; LIAO, W. Histopathology-Based Diagnosis of Oral Squamous Cell Carcinoma Using Deep Learning. Journal of Dental Research, v. 101, n. 11, p. 1321–1327, 1 out. 2022.

## ANEXOS

Parecer Consubstanciado do Conselho de Ética em Pesquisa – Faculdade de Ciências da Saude da Universidade de Brasília.

FACULDADE DE CIÊNCIAS DA SAÚDE DA UNIVERSIDADE DE BRASÍLIA - UNB

**PARECER CONSUBSTANCIADO DO CEP**

**DADOS DA EMENDA**

**Título da Pesquisa:** Novas abordagens sobre os efeitos adversos da radioterapia na região de cabeça e pescoço: estudo de imagem craniofacial

**Pesquisador:** Vitória Tavares de Castro

**Área Temática:**

**Versão:** 4

**CAAE:** 72787723.4.0000.0030

**Instituição Proponente:** DEPARTAMENTO DE ODONTOLOGIA DA UNIVERSIDADE DE BRASILIA

**Patrocinador Principal:** Financiamento Próprio

**DADOS DO PARECER**

**Número do Parecer:** 6.933.030

**Apresentação do Projeto:**

Conforme documento "PB_INFORMAÇÕES_BÁSICAS_2325196_E1.pdf", postado em 05/06/2024:

"Resumo:

Introdução: A radioterapia é amplamente utilizada como tratamento para neoplasias malignas de cabeça e pescoço, no entanto, existem efeitos adversos potenciais a longo prazo. As alterações ósseas e das vias aéreas após radioterapia não estão completamente elucidadas na literatura, apesar dos tecidos da região craniofacial serem inevitavelmente afetados pela radioterapia. Objetivos: O objetivo desse estudo é avaliar as alterações induzidas pela radioterapia na região de cabeça e pescoço por meio de análises de imagem. Materiais e Métodos: Este trabalho será composto por três partes. Parte I: Elaboração de uma revisão sistemática objetivando esclarecer se exames de imagem são capazes de detectar precocemente complicações causadas no complexo maxilomandibular após a radioterapia na região cabeça e pescoço. Parte II: Estudo experimental prospectivo, no qual serão avaliadas radiografias panorâmicas e tomografias computadorizadas de feixe cônico realizadas como exame de rotina assistencial composto por 2 grupos: um grupo de pessoas que realizaram o tratamento de radioterapia de cabeça e pescoço e um grupo controle sem radioterapia, pareados em idade e sexo. Nessa etapa serão analisados os seguintes parâmetros: dimensão fractal, análise por índices radiomorfométricos, reabsorção óssea, área luminal das vias aéreas,

**Endereço:** Faculdade de Ciências da Saúde, Universidade de Brasília - Campus Darcy Ribeiro
**Bairro:** Asa Norte **CEP:** 70.910-900
**UF:** DF **Município:** BRASILIA
**Telefone:** (61)3107-1947 **E-mail:** cepfsunb@gmail.com